

UC Berkeley

UC Berkeley Electronic Theses and Dissertations

Title

Managing disease-related amphibian declines using genomics

Permalink

<https://escholarship.org/uc/item/3k14v8ps>

Author

Rothstein, Andrew P

Publication Date

2020

Peer reviewed|Thesis/dissertation

Managing disease-related amphibian declines using genomics

By

Andrew P. Rothstein

A dissertation submitted in partial satisfaction of the

requirements for the degree of

Doctor of Philosophy

in

Environmental Science, Policy, and Management

in the

Graduate Division

of the

University of California, Berkeley

Committee in charge:

Professor Erica Bree Rosenblum, Chair

Professor Britt Koskella

Professor Ian Wang

Fall 2020

Abstract

Managing disease-related amphibian declines using genomics

by

Andrew P. Rothstein

Doctor of Philosophy in Environmental Science, Policy, and Management

University of California, Berkeley

Professor Erica Bree Rosenblum, Chair

Rates of emerging infectious diseases are increasing globally. Impacts of emerging diseases on wildlife populations have been identified as major drivers to species declines and extinctions. Disease-related species loss has necessitated prioritizing mitigation and management in wild populations. In particular, amphibians have been disproportionately affected by the disease, chytridomycosis, caused by a fungal pathogen *Batrachochytrium dendrobatidis* (Bd). Decades of amphibian species being on the brink of extinction has accelerated the need to interrogate amphibian-Bd interactions. In this dissertation, I focus on an emblematic example of amphibian-Bd dynamics. The mountain yellow-legged frog (*Rana muscosa/sierrae*), a high alpine species of the Sierra Nevada of California, have declined across more than 90% of their historical range with Bd being a major driver to their decline. While many populations have been lost, there are some remaining frog populations persisting even with Bd present. This devastating loss of a species juxtaposed to potential hope for recovery presents an excellent opportunity to investigate host-pathogen dynamics as well as refining conservation strategies to bolster remaining populations. Thus, I explore this host-pathogen system by integrating a genomic perspective to both species and disease management. For Chapter 2, I focus on a region of the frog species range that is under intensive conservation efforts and used genetic samples from both extant and extirpated populations to inform management actions. In Chapter 3, I take a pathogen perspective and use similar genetic tools in a comparative approach to investigate underlying evolutionary histories of Bd in the Sierra Nevada of California and Central Panama. In Chapter 4, I expand our genomic efforts to the entire mountain yellow-legged frog species range to create an explicit framework for species recovery and management. Together, my work weaves topics of conservation genetics, disease ecology, and evolutionary biology to highlight the use of genomics for applied conservation and builds novel frameworks for addressing species declines in the face of persistent threats.

TABLE OF CONTENTS

Acknowledgements	iii
Chapter 1 Introduction	1
Chapter 2 Stepping into the past to conserve the future: archived skin swabs from extant and extirpated populations inform genetic management of an endangered amphibian	3
2.1 Abstract.....	3
2.2 Introduction.....	4
2.3 Materials and Methods	5
2.4 Results.....	8
2.5 Discussion	9
2.6 Figures	14
2.7 Tables.....	23
Chapter 3 Divergent evolutionary histories of pathogen <i>Batrachochytrium dendrobatidis</i> between two regions with emblematic patterns of amphibian decline	29
3.1 Abstract.....	29
3.2 Introduction.....	30
3.3 Materials and Methods	31
3.4 Results.....	34
3.5 Discussion	35
3.6 Figures	39
Chapter 4 Rangewide conservation genomics using amplicon-based sequencing for the mountain yellow-legged frog species complex (<i>Rana muscosa/sierrae</i>)	47
4.1 Abstract.....	47
4.2 Introduction.....	48
4.3 Materials and Methods	49
4.4 Results.....	51
4.5 Discussion	52
4.6 Figures	55
Chapter 5 Conclusions	61
References	62

ACKNOWLEDGEMENTS

First, thank you to my advisor Bree Rosenblum. Bree provided me an opportunity to reach intellectual, scientific, and personal heights I only dreamed of. I thank her for insightful and genuine conversations exploring how to find true happiness in work and life. I thank her for invaluable perspectives, encouragement, generosity, and guidance. And for always and unrelentingly supporting my life goals, wherever they may take me. I am grateful to have Bree not only as a mentor but also as friend.

Thank you to my peers. The RoLab graduate students current (Clay Noss, Allie Byrne, Maggie Grundler) and past (Maddie Girard, Karina Klonoski, Alex Krohn, and Tom Poorten) who helped make this whole graduate journey worthwhile. Thanks to the postdocs that provided countless mentoring moments coupled with friendships (Molly Womack, Obed Hernández-Gómez, Max Lambert, Tommy Jenkinson, Alex Gunderson, and Gideon Bradburd). “I would follow any one of you to battle.” I built lifelong relationships with this group and my most memorable Berkeley moments are surely with those above. Thank you to my fellow cohort mates Tyler Anthony and Nick Goedeking. Thank you to Hannah Kania whose dedication, enthusiasm, and wonder for science has kept me inspired to mentor.

Gratitude to the many faculty and collaborators who helped cultivate my imaginative and creative scientific pursuits. Specifically, thank you to my wonderful committee Britt Koskella and Ian Wang for support, enthusiasm, and genuine interest in my work. Thank you to Roland Knapp for long conversations about ecology, conservation, and making sense of nature. I appreciate his mentorship, dedication, and the unconditional hope that comes with this work. Thank you to Lydia Smith for unparalleled patience, knowledge, and support to get my work across the finish line. Also, thank you to collaborators for which none of my work would be possible including Danny Boiano, Cherie Briggs, Adam Backlin, Robert Fisher, Thomas Smith, and SNARL field crews over the years.

Thank you to the incredibly stimulating communities I had the privilege of being a part of including Department of Environmental Science, Policy, & Management, Berkeley EEID group, and the Museum of Vertebrate Zoology.

Thank you to my family who always supported my career pursuits. My dad, Jay Rothstein, for not only being a mentor in science and but also in my life. Thank you to Terry Goletz for your love, compassion, and perspectives on science. To my mom, Madeline Danny, for always pushing me to strive for the best and, while being thousands of miles away, being close to my heart and supporting my passions.

Lastly, to my partner Anne. She took a chance to join me on this journey and grow our life together. She helps me be a better and whole person. I look up to her. I love you and am excited for our next chapter.

CHAPTER 1 INTRODUCTION

Rates of emerging infectious diseases are increasing globally [1]. Impacts of emerging infectious disease on wildlife populations have been identified as major drivers to species declines forcing conservation efforts to prioritize mitigating disease [1–3]. However, active management of wildlife populations amidst ongoing epizootics can be challenging due to lack of existing knowledge and diagnostic resources. Therefore, triaging enigmatic declines requires a comprehensive investigation on processes influencing both host and infecting pathogen populations [4–7].

Amphibians have been dramatically affected by emerging infectious diseases. One of the most imperiled taxonomic group in the world, an estimated 30% of amphibian species are in decline due to persistent threats with disease being a primary driver in many cases [8–12]. Chytridiomycosis, the disease caused by the pathogen *Batrachochytrium dendrobatidis* (Bd), has been identified as significant threat to amphibian species worldwide [9,13–17]. Bd, predominantly an aquatic fungus of the chytridiomycota lineage, infects keratinized skin cells of amphibians. Subsequent infections become lethal if pathogen load reaches high intensity [18,19]. Rapidly infecting susceptible individuals, Bd can wipe out entire populations and, in some cases, extirpate species from the landscape [17,20,21]. Such dramatic declines require immediate on the ground conservation action to potentially recover species.

My dissertation research focuses on an emblematic example of amphibian-Bd dynamics - the precipitous decline of mountain yellow-legged frog species (*Rana muscosa/sierrae*). *Rana muscosa/sierrae*, that inhabit high alpine lakes and streams of the Sierra Nevada of California, have vanished from more than 90% of their range with Bd being a significant factor influencing their decline [22]. While many populations have been lost, there are some remaining frog populations persisting even with Bd present [23]. Devastating loss coupled with potential hope for recovery presents an excellent opportunity to explore host-pathogen dynamics and inform strategies to recover extant frog populations. Advancements in next-generation sequencing and decreased costs of genomic technologies have made it increasingly possible to address these complex host-pathogen interactions [24–27]. By generating data from many samples at hundreds and thousands of independent locations on both the host and pathogen genomes, my research taps into evolutionary processes that guide host and pathogen dynamics and ultimately inform conservation efforts [27–29].

In Chapter 2, I focus on the landscape of California’s Sequoia and Kings Canyon National Parks where *Rana muscosa/sierrae* populations have been significantly impacted by invasive fish and disease [17,30–32]. Recovery efforts for these frog populations use translocations and reintroductions as management actions. Limited fine-scale genetic information [33] has impacted long-term recovery efforts and therefore a comprehensive genetic assessment could guide management efforts among these populations. Our study uses hundreds of archived skin swabs from both extirpated and extant frog populations to build a complete genetic assessment within park boundaries. Using our robust amplicon based genetic data set we find that samples clustered into three distinct groups, largely matching watershed boundaries. We also find evidence of historical gene flow between watershed boundaries with a pattern of north to south migration. Our results show that genetic diversity does not differ between disease status of frog populations. The fine-scale genetic assessment provides important management recommendations and highlighted the power of minimally invasive sampling for robust recovery of endangered species.

Shifting to a Bd perspective, Chapter 3 focuses on incorporating similar fine scale genetic methods in Chapter 2 to study pathogen population genetics. Investigations of novel wildlife pathogens sometimes only rely on epizootological data to inform hypotheses about disease emergence. However, integrating genetic information with epizootological data can uncover gaps in our *a priori* assumptions and build a more complete picture of pathogen history [34–39]. In Chapter 3, we use an amplicon-based method to challenge key assumptions about the devastating zoonotic disease impacting amphibians globally. Previous work surmised that in both regions the hypervirulent Global Panzootic Lineage of Bd (BdGPL) was a novel and recently introduced with subsequent wave-like spread across amphibian communities. Focusing on two emblematic systems, the Sierra Nevada of California and Central Panama, we retrospectively compare and explore genetic signatures of Bd. By integrating genetic data at similar temporal and spatial scales we demonstrate that BdGPL outbreaks with analogous epizootic signatures had substantially different evolutionary histories. In Central Panama we observe Bd genetic signatures largely match the hypothesis of recent and rapid spread across the landscape. Conversely, in the Sierra Nevada we find significant spatial genetic structure, increased levels of genetic diversity, and older inferred history using time-dated phylogenetics. Contrasting genetic histories in these two regions highlight the important value of integrating field observed disease declines with pathogen genetic data to build a complete picture of disease emergence and spread.

In my last chapter, I expand sampling from Chapter 2 building a complete genetic picture across the range of *Rana muscosa/sierrae*. Conservation genomics is an integral part of endangered species recovery plans [27,29,40]. Despite the value of this information, some taxa, such as amphibians, have not fully benefitted from genomic technologies. Large and complex genomes of amphibians have typically hindered ease and implementation of genomic applications [41–43]. Furthermore, amphibian declines necessitate conservation interventions to recover population [26,44]. *Rana muscosa/sierrae* are a prime example of the need for genomic assessments coupled with methodological limitations. Currently, rangewide conservation plans for *Rana muscosa/sierrae* are based on a single mitochondrial gene [33]. *Rana muscosa/sierrae* complex genomes have precluded more extensive genomic sampling and therefore limited the genomic resolution across the species complex. Compiling hundreds of archived skin swabs from frog populations across the range, we sought to investigate rangewide genetic structure and diversity to inform conservation efforts for this imperiled species. Using similar methods in Chapter 2, our results identify eight major genetic clusters across *Rana muscosa/sierrae* populations. Although we find distinct genetic clusters, we also observe admixture across cluster boundaries. We find that genetic diversity is similar between clusters with some exceptions, especially from populations in Yosemite National Parks. Results of this comprehensive genomic assessment could have immediate impacts for species recovery. We explore how our results can explicitly inform management units across *Rana muscosa/sierrae* range and managing disease related amphibian declines.

Threats to biodiversity, like disease, are complex and require integrating the best available tools to combat species declines. Continued advancements in genomic technologies will accelerate opportunities for integration into active wildlife management. However, what is the best way to use genomics, in the most pressing of scenarios, to inform current recovery actions? My dissertation chapters showcase the power of genomics, amidst a backdrop of the devastating effects of persistent threats, to directly inform conservation management.

CHAPTER 2 STEPPING INTO THE PAST TO CONSERVE THE FUTURE: ARCHIVED SKIN SWABS FROM EXTANT AND EXTIRPATED POPULATIONS INFORM GENETIC MANAGEMENT OF AN ENDANGERED AMPHIBIAN

Andrew P. Rothstein, Roland A. Knapp, Gideon Bradburd, Daniel M. Boiano, Cheryl J. Briggs, Erica Bree Rosenblum

Originally published in *Molecular Ecology* (2020; **29**,14) and reproduced here with the permission of Roland A. Knapp, Gideon Bradburd, Daniel M. Boiano, Cheryl J. Briggs, Erica Bree Rosenblum

2.1 ABSTRACT

Moving animals on a landscape through translocations and reintroductions is an important management tool used in the recovery of endangered species, particularly for the maintenance of population genetic diversity and structure. Management of imperiled amphibian species rely heavily on translocations and reintroductions, especially for species that have been brought to the brink of extinction by habitat loss, introduced species, and disease. One striking example of amphibian declines and associated management efforts is in California's Sequoia and Kings Canyon National Parks with the mountain yellow-legged frog species complex (*Rana sierrae/muscosa*). Mountain yellow-legged frogs have been extirpated from more than 93% of their historic range, and limited knowledge of their population genetics has made long-term conservation planning difficult. To address this, we used 598 archived skin swabs from both extant and extirpated populations across 48 lake basins to generate a robust Illumina-based nuclear amplicon dataset. We found that samples grouped into three main genetic clusters, concordant with watershed boundaries. We also found evidence for historical gene flow across watershed boundaries with a north-to-south axis of migration. Finally, our results indicate that genetic diversity is not significantly different between populations with different disease histories. Our study offers specific management recommendations for imperiled mountain yellow-legged frogs and, more broadly, provides a population genetic framework for leveraging minimally invasive samples for the conservation of threatened species.

2.2 INTRODUCTION

Translocations and reintroductions are fundamental management actions used in the recovery of threatened and endangered species [45–48]. While translocations and reintroductions have been successful for some animal populations [49–51], they also present major challenges, especially in certain taxonomic groups, such as amphibians [48,49,51]. Amphibians are one of the most imperiled lineages worldwide, with greater than 30% of known species currently threatened with extinction [52]. Translocations and reintroductions are an important tool in amphibian conservation given local extirpations in many species around the world [53,54]. However, these approaches to combat amphibian declines have had variable success [55–57]. Amphibian translocation and reintroduction programs can be hindered by many factors such as complex life histories [48], limited dispersal paired with high site fidelity [58], insufficient natural history information [48,54], and continued presence of unmitigated threats at release sites [51,53,56]. Even in the face of these challenges, translocations and reintroductions may be the only conservation tool available to restore many amphibian populations.

An emblematic example of amphibian declines and associated recovery efforts is the mountain yellow-legged frog (MYLF) species complex. The mountain yellow-legged frog (*Rana muscosa*) was split into the Sierra Nevada yellow-legged frog (*Rana sierrae*) and southern mountain yellow-legged frog (*Rana muscosa*) based on genetic, morphologic, and acoustic data [33]. In the Sierra Nevada mountains of California, both species inhabit mid and high elevation lakes, ponds, and streams [59]. Once the most abundant amphibian in the Sierra Nevada [60], MYLFs have disappeared from >93% of their historical ranges despite the majority of their habitat being on federally protected lands [33]. Currently, both *R. sierrae* and *R. muscosa* are state and federally listed as threatened or endangered species [61,62]. Primary causes of these declines include the widespread introduction of non-native trout into previously fishless water bodies [22,63–66] and the spread of the amphibian chytrid fungus (*Batrachochytrium dendrobatidis*, hereinafter “Bd”) [17]. Bd is a recently emerged and highly virulent fungal pathogen that attacks amphibian skin, causes the disease chytridiomycosis, and can rapidly lead to mortality in susceptible species. Bd currently threatens hundreds of amphibians species worldwide [9,67], and MYLFs are particularly susceptible.

In response to the threat of MYLF extirpations in Sequoia and Kings Canyon National Parks (SEKI), populations in this jurisdiction are currently the focus of intensive conservation efforts. MYLFs historically occupied all major watersheds in SEKI but have declined precipitously over the past four decades [17,30,68,69], often due to the arrival of Bd. These Bd-caused declines have left over half of historically occupied lake basins empty of MYLFs (see all historical lakes once occupied by frogs in Fig 2.1A). However, some MYLF populations remain in SEKI, many of which are naïve to Bd and a few that are persisting or even recovering despite ongoing Bd infection. Persisting populations are important sources of frogs for restoring the species complex across its native range [70]. Bd-naïve populations are likely highly susceptible to imminent infections and are therefore not currently used in translocations or reintroductions. With few conservation tools left for managers to pursue other than non-native trout eradication, MYLF conservation actions across SEKI have focused on using translocations and reintroductions to bolster extant populations or recover extirpated populations.

One of the main limitations in SEKI recovery and management efforts is designating effective conservation management units. Our current understanding of genetic variation in MYLFs is based on a 13-year old study that used a single mitochondrial marker to describe genetic

structure across the entire species range with 91 total individuals and limited sampling from SEKI (n=39) [33]. This study identified a species-level split (between *R. muscosa* and *R. sierrae*) within SEKI park boundaries. The 2007 assessment has served as an important guide to MYLF conservation for over a decade, but a finer-scale study of spatial genetic variation in SEKI is urgently needed to better inform conservation efforts. Specifically, higher resolution genetic data can help with species delimitation, identifying management units, and aid in maintaining historical genetic structure in the face of ongoing threats.

To address the need for higher resolution genetic data, our study combines a minimally invasive sampling methodology and robust nuclear amplicon sequencing to create a population genetic framework for future MYLF translocation and reintroduction efforts. Notably, our study includes skin swab samples from both extant and extirpated populations across both species, providing a critical understanding of historical and contemporary genetic variation in these endangered species. Our study addresses the following three questions: 1) What are the key MYLF genetic groups that can serve as management units in SEKI? 2) How much gene flow is observed within and across major watershed boundaries in SEKI? and 3) Does genetic diversity differ among populations that are Bd-naïve, and either declining, extirpated, or persisting following Bd outbreaks? Our results provide a clear and robust delineation of frog management units and highlight the importance of genetic data for effective species recovery planning.

2.3 MATERIALS AND METHODS

Sampling and DNA purification

We used 598 archived swab DNA samples (2005-2014) from 48 lake basins across four major watersheds in SEKI that were previously collected for Bd surveillance (Fig 2.1B). We sampled relatively evenly across both species (*R. sierrae*; n=304, *R. muscosa*; n=294). We define lake basins as “populations” within major watersheds (at HUC8 scale, with Kings watershed divided by two major forks), but it is important to note that lake basins are subdivided into numerous lakes and streams (as shown in Fig 2.1A). Additionally, we included two lake basins outside park boundaries (identified with an asterisk in Fig 2.1B, Mulkey Meadows & Lower Bullfrog Lakes) as they represent important populations for future frog recovery. Each individual frog was swabbed 30 times on ventral skin surfaces. DNA was extracted from swab samples using PrepMan Ultra Reagent according to manufacturer’s protocol. Typically, minimally-invasive samples contain many PCR inhibitors that can interfere with downstream data quality for DNA sequencing, so we used an isopropanol precipitation to purify swab extracts [71]. We applied 1 μ L of DNA per extract towards amplicon preparation and sequencing.

DNA sequencing

Using 50 amplicon markers previously developed for MYLFs [71], we applied a microfluidic PCR approach to generate nuclear amplicons. Briefly, the Fluidigm Access Array and Juno platforms allowed for high throughput amplification of either 48 or 192 samples, respectively, across all markers, and produced PCR products ready for amplicon library preparation. Using this type of assay provides a relatively affordable (~\$25 per sample) method to obtain robust results from lower DNA quality samples [72]. Given the small amount of DNA available from skin swabs versus traditional DNA sources, we used a pre-amplification step following the manufacturer's protocol (Fluidigm, South San Francisco, CA, USA). This initial PCR (with forward and reverse primers without tagged barcodes) increased amplification success of target regions. We then

removed other potential PCR inhibitors such as excess primers and unincorporated nucleases from PCR products using ExoSAP-IT and diluted 1:5 in nuclease-free water.

Following pre-amplification, we applied a microfluidic PCR method to amplify target regions. Each well contained a pre-amplified PCR product for each sample and multiplexed primer pools which was loaded onto an Access Array or Juno platform. Following microfluidic PCR, samples were combined into an Illumina library prep which included a barcoded tag of each amplicon and each sample. Illumina libraries were run on ¼ MiSeq plate with 2×300 bp paired-end reads, resulting in ~4.5 million reads with ~290x coverage per amplicon (unique combinations of samples and amplicons) at the University of Idaho IBEST Genomics Resources Core. Our dataset ran in two phases, 237 swabs samples on Fluidigm Access Array 48x48, followed by 361 samples on Fluidigm Juno 192x24. The two datasets were combined for sequence pre-processing and SNP genotyping.

Sequence processing and SNP genotyping

Starting with raw sequence reads, we used the `dbcAmplicons` software (<https://github.com/msettles/dbcAmplicons>) to trim adapter and primer sequences. Paired-end reads were merged to build continuous reads that extended the length of the amplicon using `flash2` [73]. Sequences were de-multiplexed using the `reduce_amplicons.R` script from the `dbcAmplicons` repository. After de-multiplexing, we used `bwa` (“mem” mode) software to align reads to our reference target regions. Using BAM files from alignments, we applied `FreeBayes`, a Bayesian genetic variant detector that identified haplotype-based SNP calls [74]. `FreeBayes` software removed singleton alleles and used phased haplotypes encoded as alleles. Following singleton removal and phasing, we used default `FreeBayes` parameters and limited SNP calls to within our 50 amplicon regions. The resulting dataset was a raw VCF file that we used for subsequent SNP filtering. We filtered SNPs using standard quality control parameters through `vcftools` (removing alignment mapping quality less than 30, supporting base quality less than 20, minimum supporting allele quality sum = 0, and proportion of genotypes called <60) [75]. Finally, we removed samples from downstream analyses that contained a high proportion of missing data (>50%), which left 385 samples in the dataset for downstream analyses.

Inferring population genetic structure

Before inferring population structure, we assessed potential pseudoreplication and associated biases in our dataset due to the physical linkage between SNPs in each of our amplicons. To do so, we first randomly subsampled one SNP per amplicon locus and conducted a principal component analysis (PCA) on that data subset. We repeated this procedure 500 times at both the basin level and the major drainage level to explore the consistency of inferred genetic relationships. We used a Procrustes transformation, implemented in R package `vegan` 2.5-6 [76], to keep a consistent orientation between PC plots for each random subset. We found some effect of subsetting on inferred genetic relationships, but patterns of relatedness were generally consistent across random subsamples, and we found no directional biases (Results, Fig 2.7). After assessing potential biases, we used multiple methods to investigate genetic structure within our SNP dataset. Using the full SNP dataset, we examined differentiation at a coarse scale by comparing F_{ST} between major watersheds and conducting a PCA, both implemented in `adegenet` [77]. We tested for departures of F_{ST} from 0 through Monte-Carlo test of 1000 simulations with pairwise F_{ST} values implemented in `hierfstat` [78]. For the PCA, we evaluated the first two principal components to visualize genetic structure at the watershed drainage scale. To more explicitly explore population structure and potential admixture among lake basins, we applied `STRUCTURE` (v. 2.3.4) to our

multi-locus genotypes. We ran an admixture model five times for each potential value of K (=1-6) with 10,000 steps burn-in and 100,000 MCMC steps. The maximum value of K was chosen as double the number of populations at the watershed scale compared to previous genetic work [33]. By using a range of K values, we evaluated all biologically reasonable groupings rather than using a single K value from a model comparison approach. Additionally, we investigated sub-structure using similar STRUCTURE model parameters within each drainage. Paired with our STRUCTURE analyses, we used conStruct v1.03 (<https://CRAN.R-project.org/package=conStruct>), which models both continuous and discrete patterns of genetic differentiation [79]. Briefly, conStruct accounts for patterns of isolation-by-distance by estimating ancestry proportions from samples while simultaneously estimating the decay of relatedness within a population due to distance across a landscape. We ran three replicate runs of conStruct for values of K between 1 and 7, each for 3000 iterations. For each analysis, we compared models across different values of K by calculating the “layer contributions” – the amounts of total covariance explained by each discrete group in the model and rejecting values of K that resulted in negligible layer contributions. Finally, we applied an AMOVA to test for hierarchical structure between lake basin and watershed scales using the *poppr* R package [80].

Measuring gene flow

We also investigated patterns of migration among major watersheds. We applied TreeMix v. 1.13 [81], which uses a maximum likelihood approach to identify patterns of population splitting and admixture across all samples. Using the four watersheds as major population groups, we simulated 2-10 migration events (-m flag), generated bootstrap replicates to ensure confidence in our inferred tree of admixture events, and chose the best fit tree based on maximum likelihood values.

Patterns of historical genetic diversity in extant and extirpated populations

Lastly, we calculated standard measures of historical genetic diversity among all 48 lake basins. In this case, we define historical as samples collected before the detection of Bd from qPCR of skin swabs. Bd epizootics in MYLF populations cause mass die-offs and many populations in SEKI were extirpated within several years of such outbreaks [17]. Bd has now been detected across nearly all of SEKI, and, as a result, robust populations are rare (Knapp & Boiano, unpublished data). Using repeated surveys of frog populations conducted over the past 20 years [17,82; Knapp, unpublished data] and associated Bd surveillance, we classified the sampled lake basins into four frog population status categories (“Status” in Table 2.1). Of the sampled lake basins, a small number remain Bd-naïve (termed “naïve” [n=6]). In addition, a few basins contain populations that are persisting or recovering following Bd-caused declines (termed “persistent” [n=6]). A larger number of basins contain populations that declined following the arrival of Bd and are trending toward extirpation due to a lack of recruitment of animals into the adult size class (termed “declining” [n=23]). The three categories of naïve, persistent, and declining are collectively referred to as “extant”. Finally, many basins contain sites from which MYLFs are entirely extirpated following Bd-caused declines (termed “extirpated” [n=13]). Especially for recently declined or extirpated lake basins, historical genetic diversity can give context for how diversity was once distributed on the landscape. We compared historical genetic diversity of frogs across the four basin categories, and calculated Watterson’s θ and observed heterozygosity using a custom R script and the *adegenet* R package, respectively [77].

2.4 RESULTS

Genetic structure

After filtering, SNP genotyping, and phasing, our dataset included 385 individuals and 1,447 SNPs. From the original 598 samples, our 385 samples for downstream analysis resulted in a 64% success rate. Percent success sequencing from swabs was similar across both species (*R. muscosa*: 67.7% [n=199], *R. sierrae*: 61.2% [n=186]); across contemporary and historical sampling periods (extant: 65.3% [n=305], extirpated: 67.7% [n=80]); and across disease status groups (naïve: 55.7% [n=44], persistent: 74.2% [n=46], declining: 66.0% [n=215], extirpated 67.8% [n=80]). The average number of SNPs per contig was 31 ± 8 SD and the average length of contig was 359 ± 60 bp SD. Inferred population genetic structure indicated that samples largely clustered by major watershed drainage (Fig 2.2). Our PCA analyses formed three groups across four watersheds with PC loadings strongly correlated with latitude or watershed (PC 1) and longitude (PC 2). STRUCTURE and conStruct results suggest three clusters forming 2-4 different groupings (Fig 2.3, 2.4). AMOVA results were consistent with major genetic groupings, with the majority of genetic variation (58.45%,) partitioned between major watersheds and remaining genetic variation partitioned among lake basins within drainages, and among all samples (38.96%, 2.58% respectively). Permutation significance testing for AMOVA showed significant differences among major watersheds ($p < 0.001$) and among samples within major watersheds ($p < 0.001$). Within watersheds, however, we found no sub-structuring from both STRUCTURE and ConStruct. Thus, the four sampled watershed basins could be described as three genetic groups, with samples from San Joaquin and Middle Fork (MF) Kings representing a northernmost cluster, samples from South Fork (SF) Kings representing a central cluster, and samples from Kern representing a southern cluster. Notably, both STRUCTURE and conStruct indicated some admixture among basins, particularly between the MF and SF Kings watersheds. The three genetic groupings we found are not entirely concordant with the previous split described between *R. sierrae* and *R. muscosa* [33]. Although we did find that *R. sierrae* and *R. muscosa* samples segregated in largely distinct clusters, we also found some admixture between the named species (notably between the MF and SF watersheds) and found additional genetic discontinuities within named species (notably between the SF and Kern watersheds).

To examine possible impacts of pseudoreplication on our results due to physical linkage between SNPs on the same amplicon, we tested for biases introduced by using the complete dataset. Using randomly subsetting SNP datasets (retaining only a single, randomly selected SNP per amplicon), we found some effect on inferred genetic relationships but no directional bias (Fig S1). Pseudoreplication due to linkage should artificially increase our certainty, but not introduce bias, in our results. Our results were broadly comparable across PCA, STRUCTURE, and ConStruct groupings (Fig 2.8). Finally, we considered a range of possible K values given the issues with identifying a single “optimal” K [83]. Overall, our results were highly consistent across approaches, so we describe biogeographic patterns based on $K=3$, which appears supported across methods and is biologically the most relevant.

Levels of differentiation based on F_{ST} among the four sampled watersheds were also consistent with clustering results (Table 2.2). The San Joaquin and MF Kings watersheds, which can be interpreted as constituting a single genetic cluster, exhibited the most limited differentiation ($F_{ST}=0.05$). Admixture between MF and SF Kings was similarly reflected by low cross-basin differentiation ($F_{ST}=0.06$). Consistent with a less porous genetic break between SF Kings and Kern, we observed greater differentiation between these basins ($F_{ST}=0.13$). As expected, F_{ST}

between non-adjacent basins was higher [MF Kings-Kern ($F_{ST}=0.17$), and San Joaquin-Kern watersheds ($F_{ST}=0.21$)]. Simulations for departures of F_{ST} showed significant differentiation between major watersheds (Monte-Carlo test, $n_{sim}=1000$, $p<0.001$).

Gene flow

Given patterns of admixture observed across watershed boundaries, we estimated relative weights of migration among watersheds. The highest likelihood tree from our TreeMix analysis inferred two migration events. Using a two-migration event tree, the strength and directionality of migration was greatest from San Joaquin to MF Kings (which together form a single genetic cluster) followed by MF Kings to SF Kings (Fig 2.5). While SF Kings and Kern cluster closely in topology, TreeMix support our structuring results that there is still a major barrier to migration between these two watersheds. It is important to note that the TreeMix model has several assumptions about the processes of gene flow. Mainly, migration is modeled as occurring in a single time point as opposed to ongoing long-term gene flow [81]. This assumption is likely violated in our case, since there is likely ongoing gene flow given our admixture, but the topology did not change by adding migration events and matches our genetic groupings.

Genetic diversity of populations differing in Bd exposure history and outcome

To examine the extent to which historical genetic diversity is distributed among frog populations with different Bd-related histories, we compared mean Watterson's θ for samples of four different types of populations (assigned at the lake basin scale): naïve, persistent, declining, and extirpated (Table 2.1). Historical genetic diversity was highest in naïve basins ($0.002\pm 0.0007SD$) followed by persistent ($0.0014\pm 0.0003SD$) and declining ($0.0014\pm 0.0008SD$) basins. Extirpated basins ($0.0012\pm 0.0007SD$) harbored the least historical genetic diversity of our status groups, but differences in genetic diversity between basin types were not significant (ANOVA, $F=1.32$, $p=0.281$). Within lake basins that still have frogs (all extant, $n=35$), mean historical genetic diversity was highest in Barrett (0.0031 , MF Kings) while Coyote basin (0.0002 , Kern) exhibited the lowest historical genetic diversity (Table 2.1, Fig 2.6).

2.5 DISCUSSION

The planning of effective translocations and reintroductions requires a baseline understanding of genetic diversity and structure for the species of interest. In cases of rapid species declines, archived samples may be the only opportunity to provide genetic context for recovery actions. Therefore, our study leveraged archived swab samples from both extant and extirpated populations of an endangered frog species complex within an actively managed protected area. Using amplicon-based Illumina sequencing, we addressed three main objectives: identifying mountain yellow-legged frog management units within SEKI, refining our understanding of gene flow across major watershed boundaries, and assessing historical genetic diversity among extant (naïve, persistent, and declining) and extirpated lake basins to identify what diversity was present in SEKI before the arrival of Bd. Overall, we found that frog populations in SEKI structured into three genetic clusters with evidence for some gene flow between the clusters. Additionally, we found that genetic diversity did not differ between populations with different disease histories. Our findings provide finer spatial and genomic resolution across the remaining frog localities in SEKI. Broadly, we demonstrate the power of combining samples from extant and extirpated populations and suggest how they can inform translocations and reintroductions for conservation.

Factors influencing frog population structure in SEKI

Our tests for genetic structure used a variety of methods (PCA, STRUCTURE, conStruct, and AMOVA) and recovered similar genetic clusters. Samples from the San Joaquin and MF Kings watersheds together composed one genetic cluster, samples from the SF Kings watershed created a second cluster, and samples from the Kern watershed comprised a third (Fig 2.2-2.4). While we identified three genetic groupings, we recovered some admixture between basins. Not only did we find evidence of significant gene flow between San Joaquin-MF Kings samples (which together comprise a single genetic group), but we also inferred more limited gene flow between the remaining adjacent watersheds (MF Kings-SF Kings and SF Kings-Kern) (Fig 2.3, Fig 2.4). Our model-based analyses suggested that a two-migration event scenario was the best fit for the data, with migration likely strongest between San Joaquin-MF Kings and MF Kings-SF Kings (Fig 2.5). In summary, there is evidence for differentiation across watershed boundaries in SEKI MYLFs, but some boundaries have been more porous to gene flow over time than others.

Several factors likely contribute to patterns of drainage-level genetic variation in MYLFs. Certain environmental characteristics, such as topography and fluvial distances, are known to separate montane amphibian populations [84–89]. Given the steep slopes and high ridges between drainages in this portion of the Sierra Nevada, the topographic isolation of lake basins, and the highly aquatic life history of MYLF, our admixture and gene flow results suggest similar characteristics could have shaped our observed genetic patterns across frog populations. These characteristics can be highlighted by the porous patterns of genetic variation between San Joaquin and MF Kings. Frog populations in these two watersheds have the least genetic differentiation between drainages (F_{ST}), and Muir Pass (elevation 3,644m), which separates them, has a relatively smooth topographic gradient. As a result, lakes and streams are in close proximity to the pass and there are fewer barriers to frog movement. Other environmental and life history factors could also impact frog movement across the landscape. Such variables could include temperature-moisture regimes, habitat permeability, presence of non-native predatory trout, and frost-free periods between sites [87]. Future work would benefit from generating explicit models to correlate patterns of genetic variation with environmental variables and landscape features.

In addition to the potential contribution of geographic barriers to observed patterns of genetic diversity, we also found a general signal of isolation-by-distance both within and across watersheds. Moreover, we identified a general pattern of asymmetrical gene flow with frogs migrating preferentially north to south across our study area (from the San Joaquin to MF Kings and from MF Kings to SF Kings, Fig 2.5). TreeMix models are likely violated if there is ongoing gene flow, but we can cautiously interpret topologies and directionality of gene flow to understand relationships between major drainages. North-south axes of differentiation have also been observed in other Sierra Nevada herpetofaunal taxa, likely influenced by one or more broad vicariant events (e.g., climatic or glacial; [33,90–95]). It is important to note that patterns of population structure and gene flow inferred here do not reflect current migration, given the small number of remaining MYLFs in SEKI. Historically, high abundances and widespread localities of MYLFs across SEKI suggest that connectivity among populations within and between lake basins would have been much higher than at present (Fig 2.1A). Thus it is also possible that observed genetic patterns could partially be a geographic artifact of recently lost MYLF populations, for example if the full complement of historical populations created more genetic continuity across the landscape [96–98].

Genetic diversity in SEKI

Our analyses - using swab samples from both extant and extirpated lake basins - also provide insight into historical genetic diversity in SEKI MYLFs given dramatic recent declines. Analyzed skin swabs were collected over the last decade (before, during, and after population declines) and provide an opportunity to describe historical genetic diversity for the species (i.e. before the arrival of Bd). In terms of rank order, Bd-naïve basins harbored the most genetic diversity, while basins from which frogs have been extirpated harbored the least. Basins where frogs have survived a Bd-outbreak were intermediate in genetic diversity. Despite this rank order, differences were not statistically significant, likely due to low total numbers of lake basins with naïve and persisting populations. Overall, mean genetic diversity varied by two orders of magnitude across all basins (Table 2.1, Fig 2.6). Inferred genetic diversity (based on sampling conducted across 20 years) may be higher than current genetic diversity given ongoing Bd-related declines. Furthermore, because samples were limited, we needed to bin samples across years, constraining our ability to estimate and identify fluctuations in genetic diversity [99,100]. However, given that many of the populations sampled represent the last remaining chance to describe historical MYLF diversity, our findings provide crucial data for translocation and reintroduction efforts by describing fine-scale patterns of diversity across the landscape.

Management implications for reintroductions and translocations

The vast majority of MYLF sites in SEKI have been extirpated in large part due to threats of non-native trout and disease, which are still present on the landscape. Only a handful of lake basins harbor frog populations that have not experienced Bd outbreaks or are persisting despite Bd presence. In our study, only twelve lake basins are considered “persistent” or “naïve” with regard to Bd. Of the twelve lake basins with persisting populations, eight had higher than average historical genetic diversity. These few basins represent the best remaining chance, if currently available genetic diversity is representative of historic levels, to bolster frog populations in SEKI. With an alarmingly small number of basins still harboring frogs, conservation managers have few options for translocations. However, even in the face of dwindling management options, our results can provide some guidance for moving frogs on the landscape.

At the broadest level, our results suggest that managing frogs by major genetic group within SEKI may be more productive than managing frogs solely based on the species-level split. Our observed patterns of genetic variation (based on multilocus nuclear data) are not entirely concordant with previous mtDNA results that indicated a species-level break at the MF-SF Kings watershed boundary [33]. Although we found that *R. sierrae* and *R. muscosa* samples segregated into largely distinct genetic clusters, we also found evidence for admixture between the named species (across the MF and SF watersheds). We also describe a genetic break within *R. muscosa* (between the SF and Kern watersheds). Such differences between mtDNA and nuclear DNA datasets are common (e.g., Toews & Brelsford, 2012), especially when one set of markers shows stronger (or different) genetic discontinuities than the other. Typically, named species are treated separately for management decisions [102]. However, when species boundaries are unclear, genetic clusters might be better functional units for conservation decision making [103]. In this case, management in SEKI might better focus on the major genetic groups as management units rather than simply relying on species designations.

A conservative management approach suggests that moving frogs between adjacent basins is more favorable than moving frogs over long distances between non-adjacent basins. Moving frogs between proximate lake basins increases the likelihood that translocated genotypes would have been historically present. Moving animals between nearby lake basins can also help maintain

locally adapted alleles. Additionally, lack of genetic substructure within watersheds suggests that moving frogs within a basin will have little impact on overall genetic structure. Therefore, managers could move frogs within watersheds to reestablish MYLFs in lake basins from which they have been extirpated. Current population census data will also be critical for assessing which basins with adequate historical genetic diversity also have viable frog numbers. Similarly, specific threats on the landscape may change which lake basins will be the best source for donor individuals. For example, translocating frogs that have persisted in the face of Bd may be a high priority given the ongoing threat of Bd on the landscape [104]. Some declining frog populations may retain high historical genetic diversity, but high Bd susceptibility and low recruitment (leading to potential loss of genetic diversity) may make them poor sources for translocations.

Our gene flow data also suggest that moving frogs from north to south would better maintain historical genetic patterns (Fig 2.5). This is less important within watersheds, where genetic substructure is not pronounced. Overall, it may be less ideal to move frogs between major watersheds, especially when they coincide with genetic breaks. However, given the low number of remaining MYLF populations in SEKI, cross-watershed translocations may be necessary. In these cases, the more conservative management action would be to maintain a north-south direction of genetic exchange.

Our recommendations prioritize maintaining historical population genetic structure and the potential for locally adapted alleles among lake basins. However, conservation managers confront complex tradeoffs, and therefore other strategies may be worth considering. For example, if reducing the threat of inbreeding depression and augmenting genetic diversity is a key concern [105,106], managers may consider moving frogs further distances than adjacent lake basins. Ultimately, translocations and reintroductions may be ineffective unless ongoing threats are mitigated. Given that Bd is still present on the landscape, introducing frogs from naïve lake basins that may be especially susceptible to chytridiomycosis increases the likelihood of recovery failure. Thus, identifying populations that are truly recovering after exposure to Bd will remain a critical objective for field research [23]. Lastly, coupling frog genetic data presented here with Bd genetic data across SEKI could illuminate whether different Bd genotypes exist among lake basins and help managers avoid moving Bd genotypes among susceptible individuals. We have recently developed a complementary Bd genotyping assay [72] and can now leverage Bd positive skin swab samples to genotype Bd across SEKI and assess whether frog and Bd genotypes co-vary spatially.

Fine-scale studies such as this genetic assessment within SEKI and similar work in Yosemite National Park [71] will be crucial for MYLF recovery in individual parks. However, remnant populations in the two national parks represent only a portion of the total MYLF range. A full rangewide analysis will be critical to resolve several outstanding issues about the species complex. Critically, additional work is required to refine our understanding of within and between species differentiation. Genetic management units identified in this study are relevant for SEKI, but a rangewide analysis would provide more clarity for conservation action on genetic variation across the range. An updated rangewide genetic assessment would increase resolution outside park boundaries (as there are many additional frog populations adjacent to the parks) and allow coordinated conservation actions across multiple jurisdictions and stakeholders. In addition, our assay could be expanded to include detection of SNPs that may be important not only for maintaining neutral processes but also candidate adaptive loci important for Bd-resistance.

Conclusions

Our study highlights the power of archived genetic samples for current conservation decision-making. Especially in cases of rapid species declines, our study provides a framework to harness critical genetic information even as populations are being extirpated. We leveraged MYLF samples from lake basins whose frog populations have been all but lost from the landscape. These samples provide crucial baseline data for understanding historical population structure and genetic diversity in SEKI. Populations will likely continue to be extirpated as disease spreads through the remaining naïve populations. Nonetheless, with a clearer understanding of historical patterns of population structure, gene flow, and genetic diversity, conservation decisions can be guided more effectively for this imperiled species complex.

Acknowledgements

We thank Thomas Poorten for assistance in bioinformatics and field crews for collecting skin swabs. Data collection and analyses performed by the IBEST Genomics Resources Core at the University of Idaho were supported in part by NIH COBRE grant P30GM103324. All sample collections were authorized by research permits provided by SEKI and the Institutional Animal Care and Use Committee at University of California, Santa Barbara and University of California, Berkeley. Funding was provided by National Park Service, National Science Foundation LTREB DEB-1557190, and US Fish and Wildlife.

2.6 FIGURES

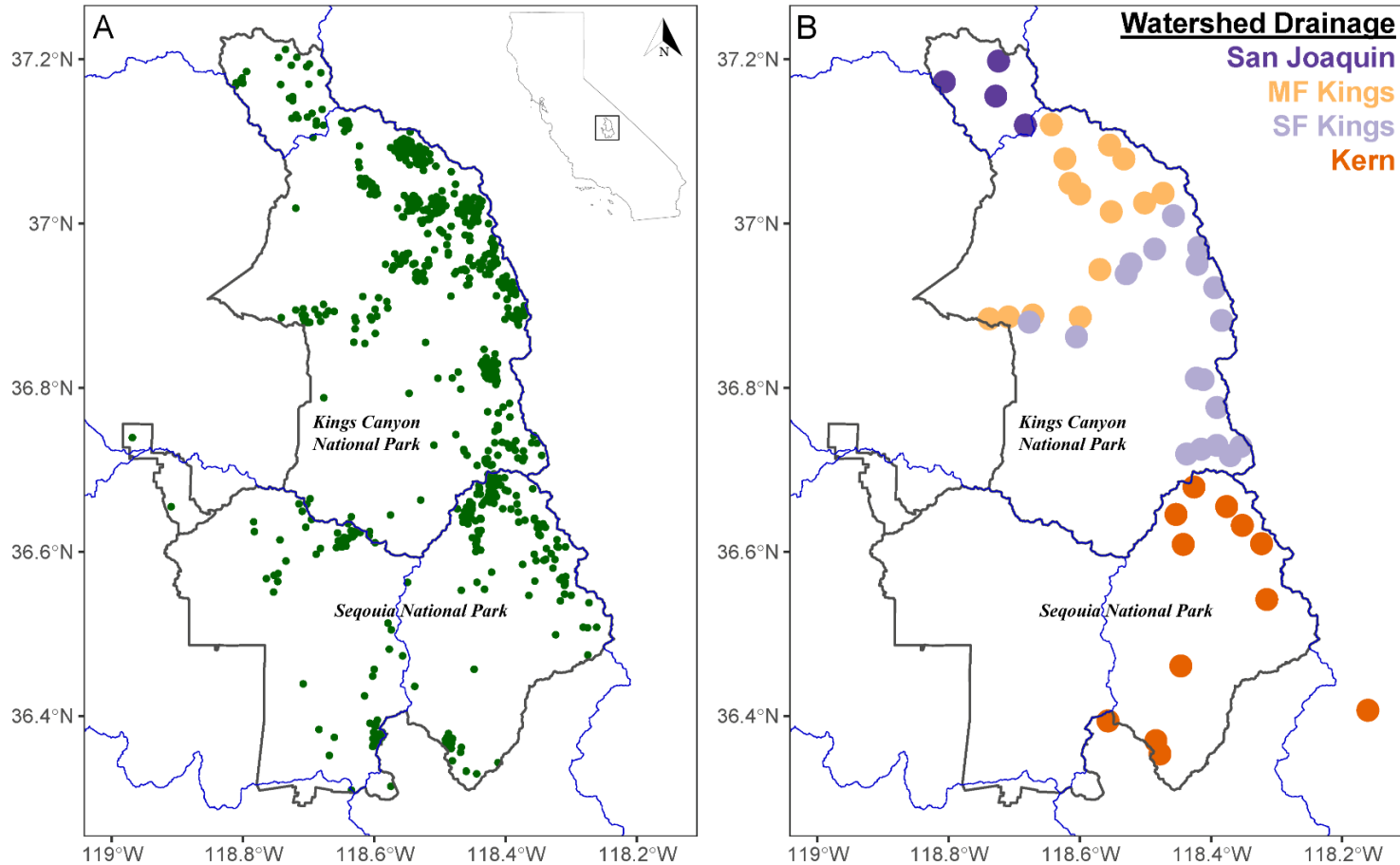


Fig 2.1. A) Map of historical MYLF localities in Sequoia-Kings Canyon National Parks (sourced from <https://nrm.dfg.ca.gov/FileHandler.ashx?DocumentID=40357>). B) Lake basins sampled in our study colored by major watershed. Lake basins shown in panel B contain multiple lakes (shown as green points in panel A, when inhabited by frogs). Solid black lines represent park boundaries, with Kings Canyon National Park to the north and Sequoia National Park to the south. Blue lines represent USGS HUC8 watershed boundaries that include San Joaquin River, Middle Fork Kings, South Fork Kings, and Kern. Species delimitation between *R. sierrae* (in the north) and *R. muscosa* (in the south) occurs across Middle Fork and South Fork Kings Rivers (based on Vredenburg et al. 2007). Two lake basins outside the park boundaries included in our study (marked with an asterisk), Mulkey Meadows (southeast of the border of Sequoia National Park located in Inyo National Forest) and Lower Bullfrog Lakes (south of the border of Sequoia National Park located in Sequoia National Forest), represent both persistent and declining sites within the Kern watershed important for frog recovery in southern Sequoia National Park.

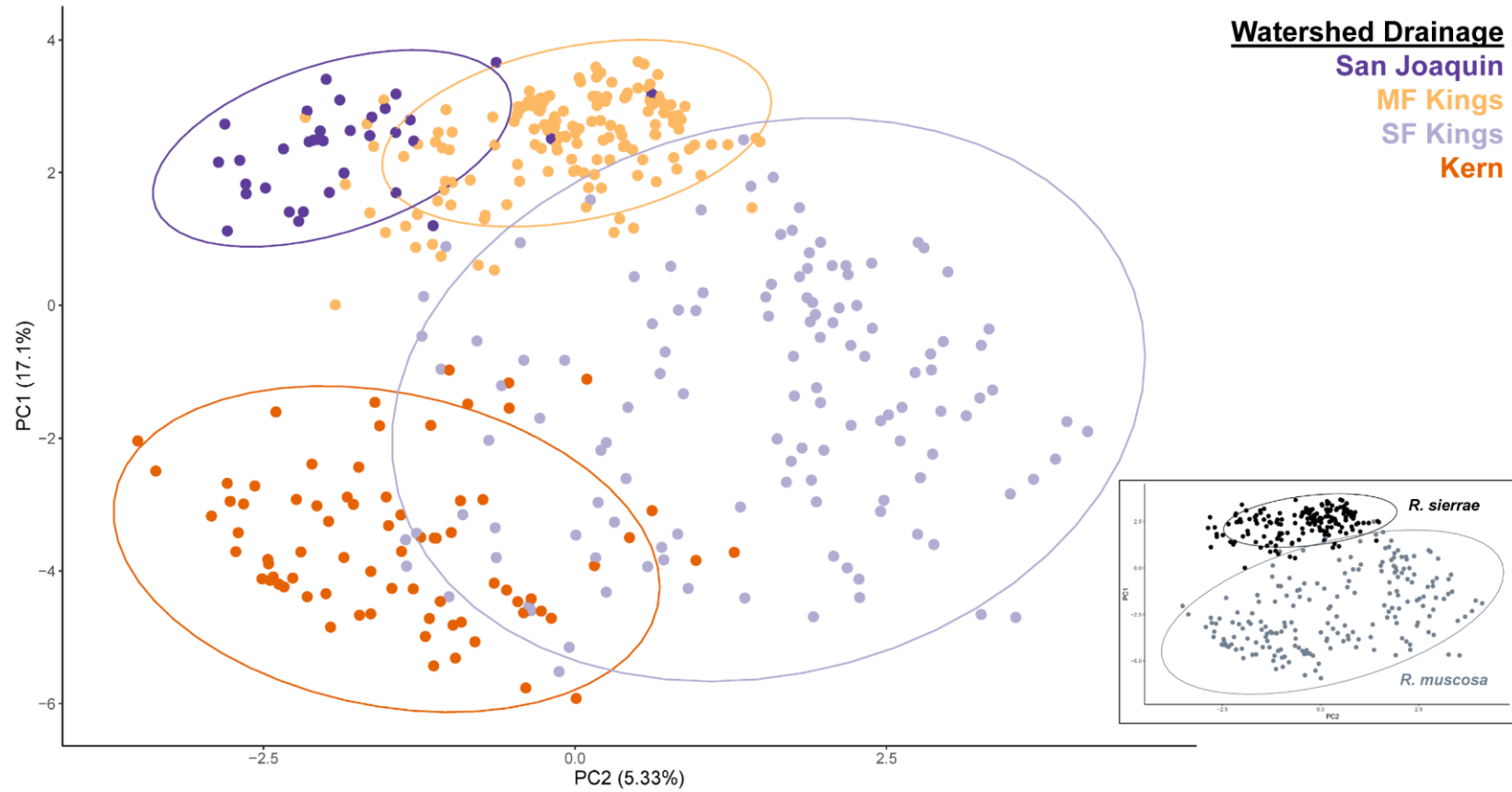
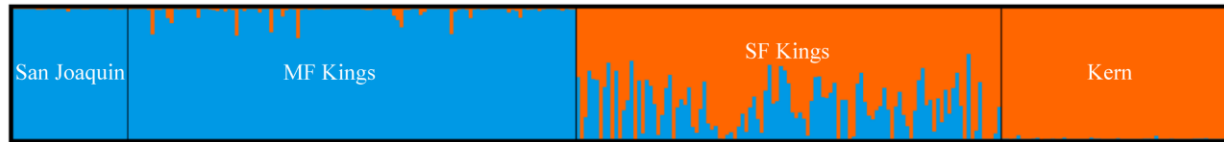
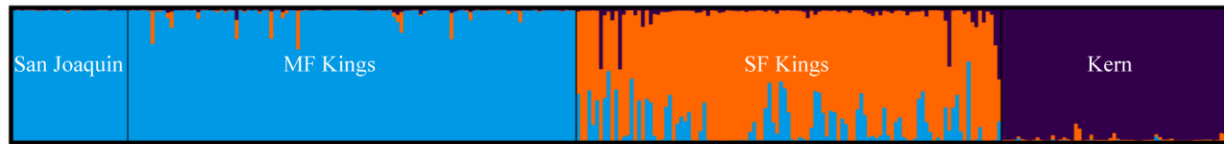


Fig 2.2. PCA plot showing genetic variation across sampling localities. Each point represents the multilocus genotype of an individual frog (colored by watershed). PC1 captured 17.1% of variation and PC 2 captured 5.33% of variation, roughly recapitulating longitude and latitude respectively. Inset PCA plot colored by species distinction. Inset PCA plot shows datapoints colored by species designations.

K=2



K=3



K=4

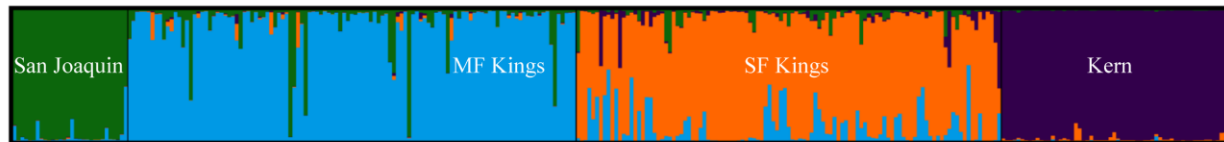


Fig 2.3. STRUCTURE results for K=2-4. K=3 represents the most biogeographically relevant cluster across the four major watersheds. Bars represent individual samples and proportion of ancestry among genetic clusters. Current species split between *R. sierrae* and *R. muscosa* occurs between the Middle Fork and South Fork of the Kings River. However, we did find admixture across all watershed boundaries.

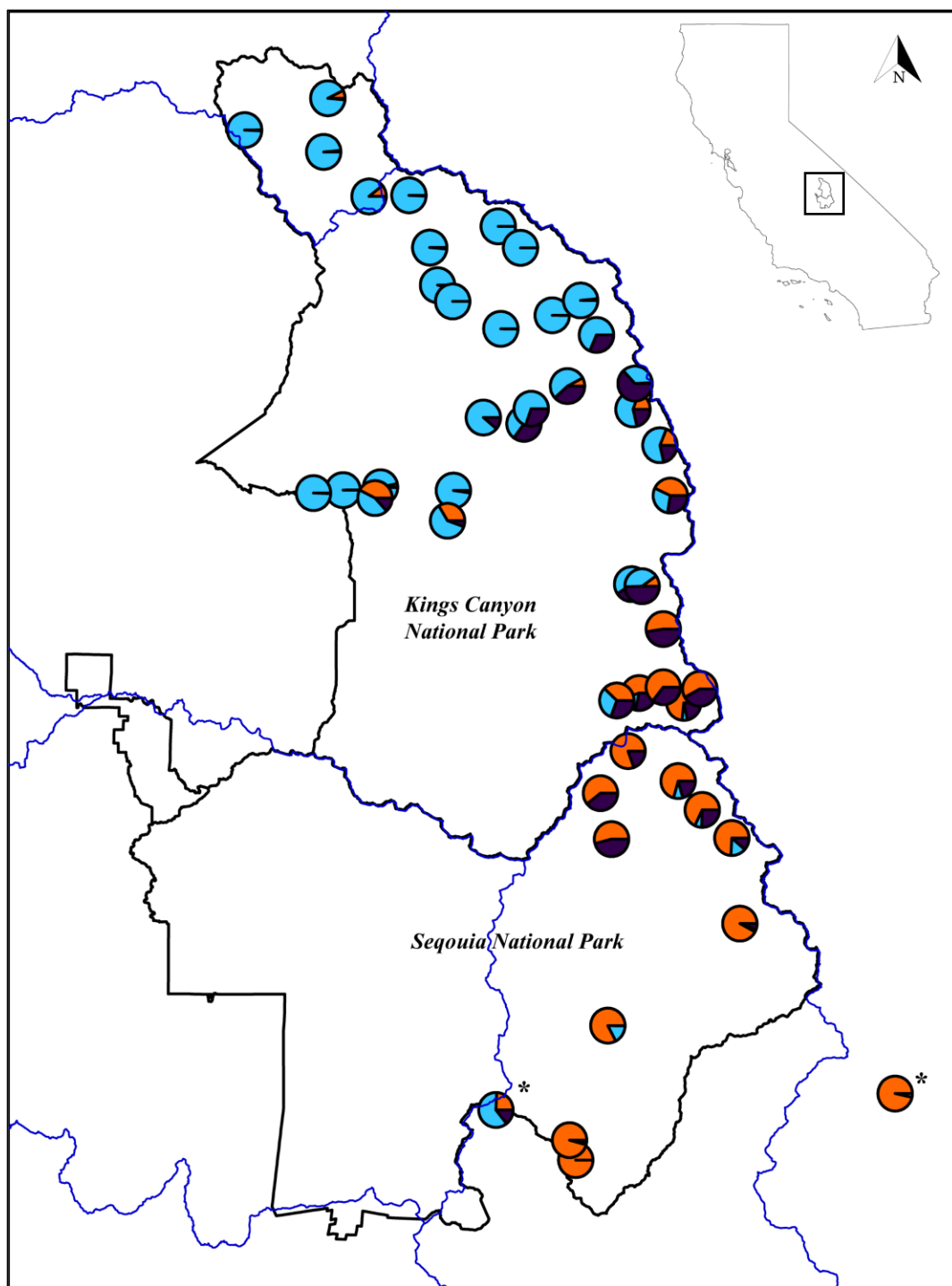


Fig 2.4. ConStruct analyses recovered three genetic groups (K=3). Pie charts show probability of ancestry from the three genetic clusters and likelihood of admixture.

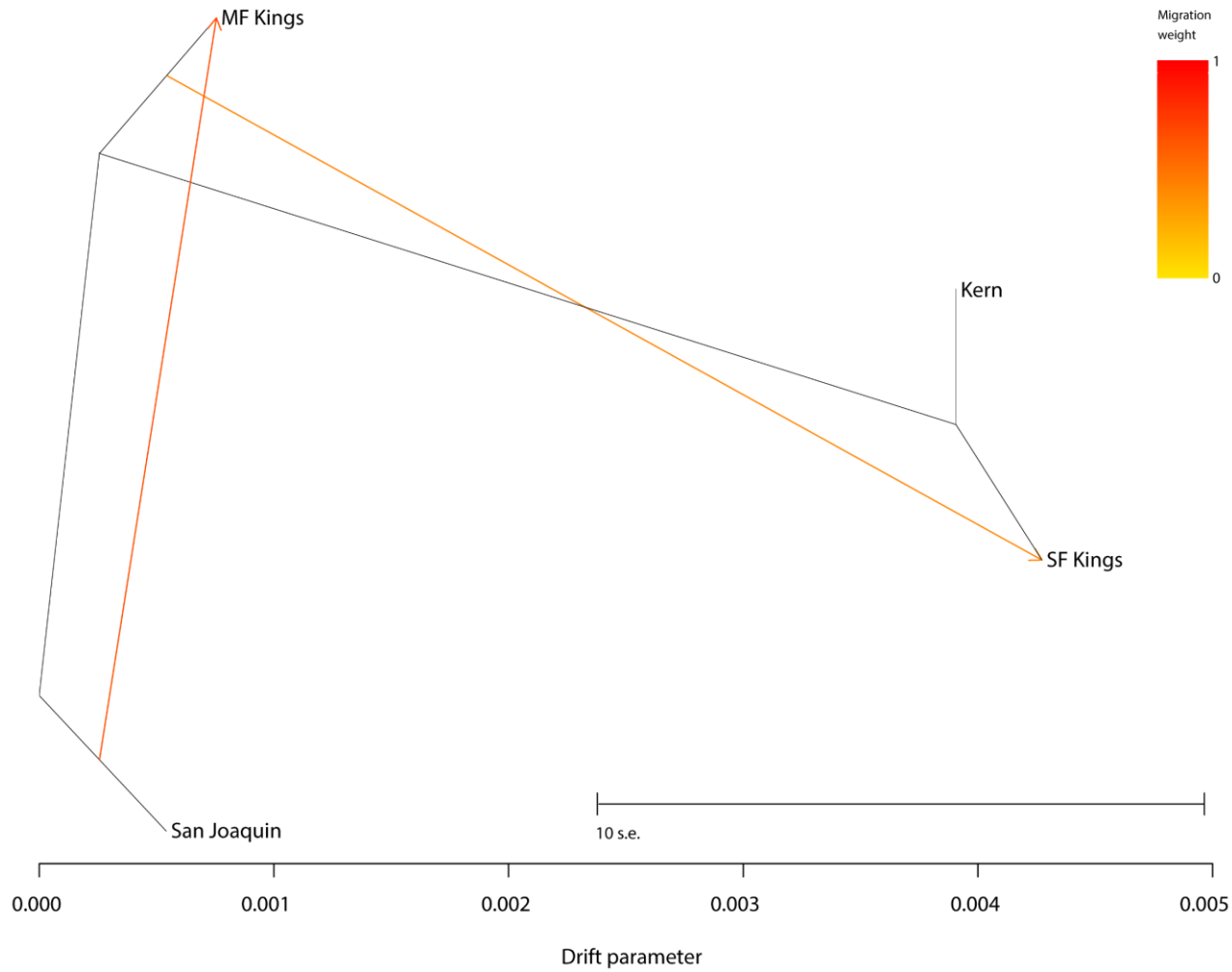


Fig 2.5. Best fit TreeMix display of two migration events. Migration is inferred to be strongest from San Joaquin to MF Kings, followed by MF Kings to SF Kings. TreeMix model was run for 2-10 migration events with two migration events resulting in best fit model. Topologies and directionality did not change by increasing migration events.

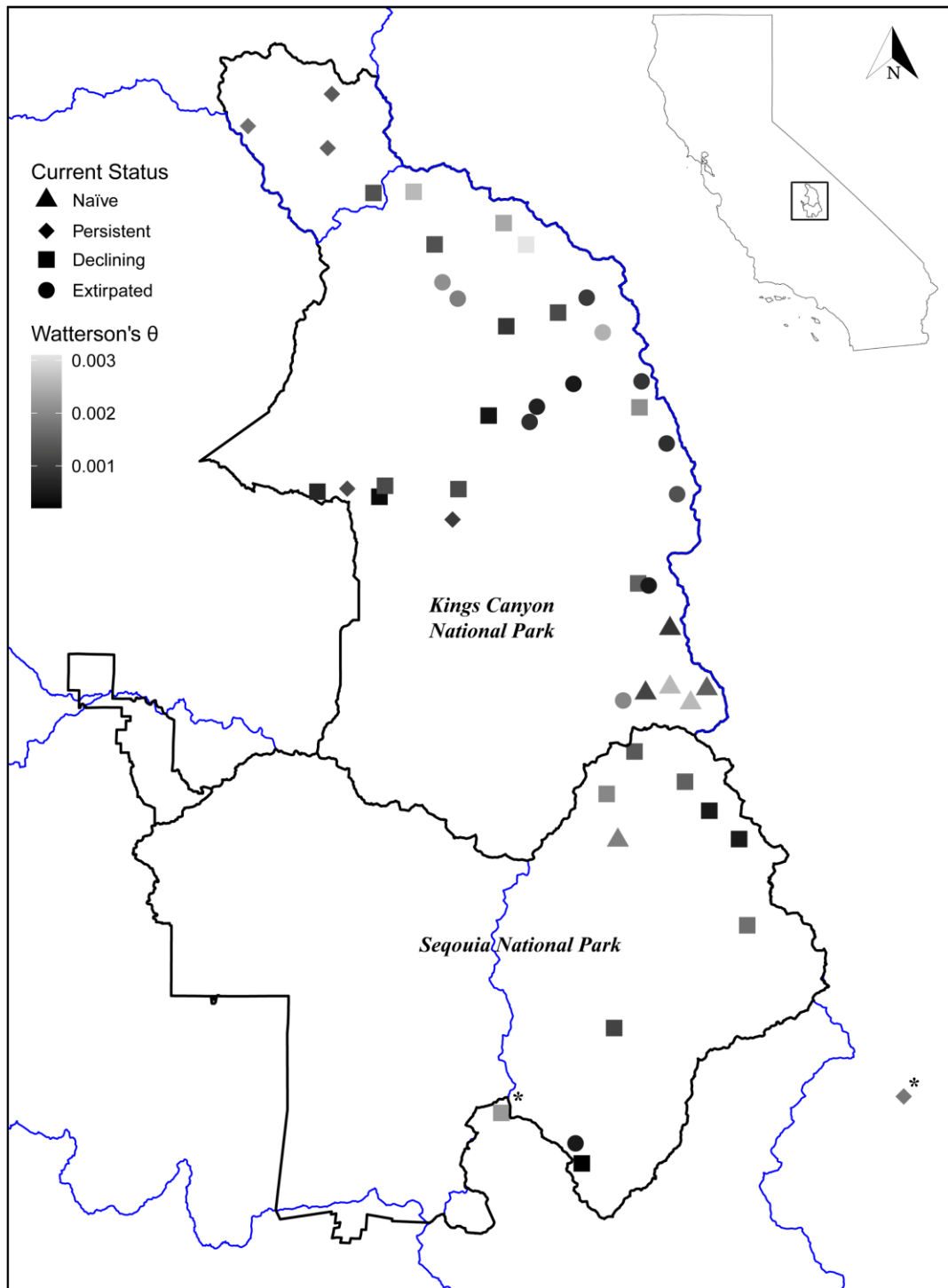


Fig 2.6. Map of genetic diversity (Watterson's θ) (grayscale) and population status (shapes). Only a small number of basins contain frog populations that are Bd-naïve or persisting after the arrival of Bd. A larger number of basins harbor frog populations that show little or no evidence of recruitment after Bd arrival (declining) or are extirpated.

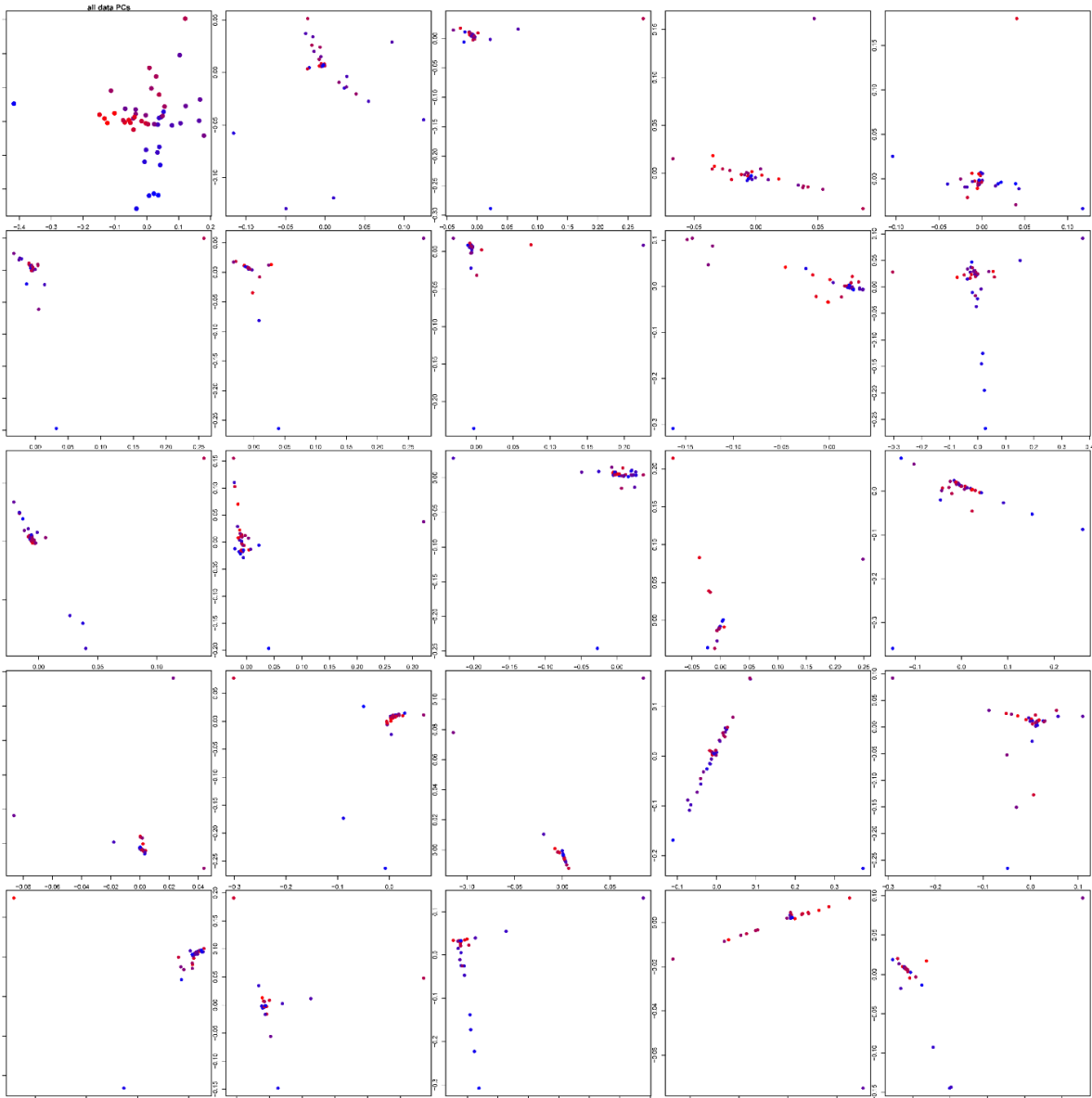


Fig 2.7. Subsetted one SNP per amplicon PCA plots. Top left represents all SNP data combined and colored by drainage group. Subsequent panels are each random subset of one SNP per amplicon. While there are subsets of SNPs that do cluster as the full data set, there are no discernible directions of bias.

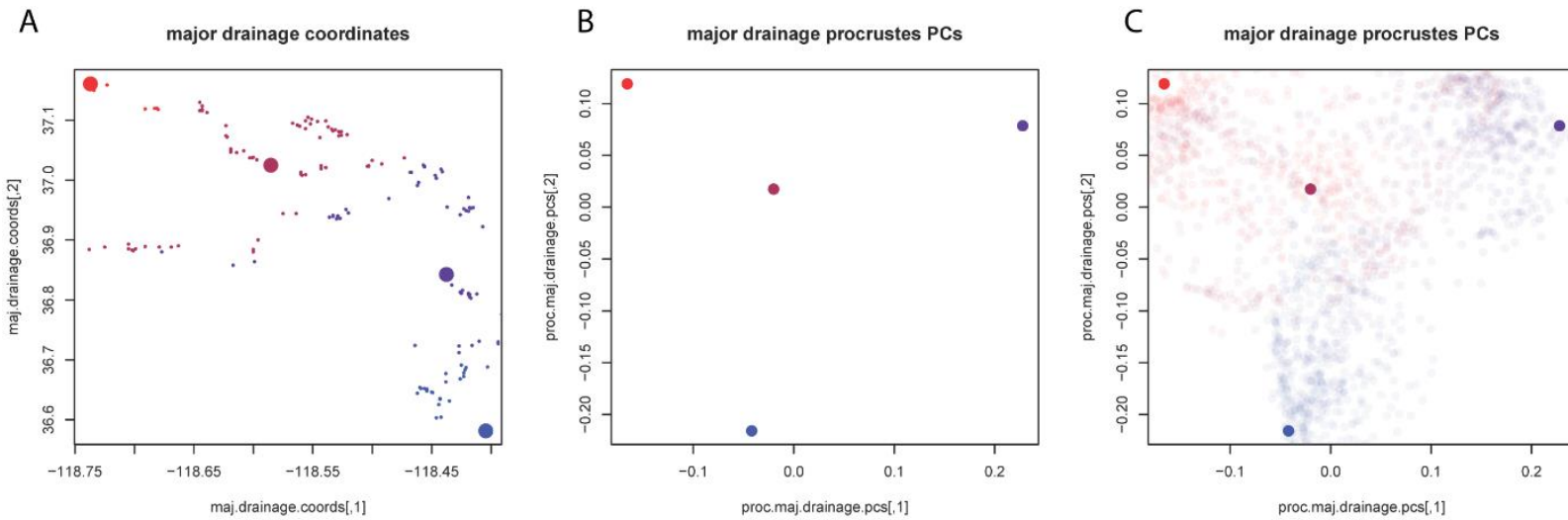


Fig 2.8. **A.** Latitude and longitude coordinates for each sample; with larger points for average among major drainages. **B.** Procrustes-transformed PC based on mean values among major drainage. **C.** Major drainage Procrustes-transformed PC representing each individual genotype (transparent points) and major drainage mean value.

2.7 TABLES

Table 2.1. Historical genetic diversity and population status by basin. Genetic diversity calculated as Watterson's θ and Nei's unbiased gene diversity. Population status divided into four categories: naïve, persistent, declining, and extirpated. (*) Mulkey Meadows and Lower Bullfrog Lake lie outside park boundaries but represent important populations for Kern Watershed lake basins.

Basin	N	Major Watershed	Species	Status	Watterson's θ	H(Nei's)
LeConte Divide	9	San Joaquin	<i>R. sierrae</i>	Persistent	0.0017	0.0015
McGee Basin	9	San Joaquin	<i>R. sierrae</i>	Persistent	0.0015	0.0022
Darwin Bench	8	San Joaquin	<i>R. sierrae</i>	Persistent	0.0014	0.0018
Evolution Basin	8	San Joaquin	<i>R. sierrae</i>	Declining	0.0013	0.0029
Barrett Basin	27	MF Kings	<i>R. sierrae</i>	Declining	0.0031	0.0061
Black Giant Basin	13	MF Kings	<i>R. sierrae</i>	Declining	0.0026	0.0023
Dusy Basin	20	MF Kings	<i>R. sierrae</i>	Declining	0.0024	0.0026
Rambaud Basin	16	MF Kings	<i>R. sierrae</i>	Extirpated	0.0021	0.0014
Devils Crag Basin	9	MF Kings	<i>R. sierrae</i>	Extirpated	0.0019	0.0011
Black Divide	3	MF Kings	<i>R. sierrae</i>	Declining	0.0013	0.001
Amphitheater Basin	13	MF Kings	<i>R. sierrae</i>	Declining	0.0012	0.0018
Volcanic Basin	10	MF Kings	<i>R. sierrae</i>	Declining	0.0012	0.0024
Slide Basin	8	MF Kings	<i>R. sierrae</i>	Declining	0.0012	0.0017
Swamp Basin	11	MF Kings	<i>R. sierrae</i>	Persistent	0.0012	0.0016
Palisade Basin	3	MF Kings	<i>R. sierrae</i>	Extirpated	0.001	0.0012
Observation Basin	13	MF Kings	<i>R. sierrae</i>	Declining	0.0009	0.0009
Gorge Basin	2	MF Kings	<i>R. sierrae</i>	Declining	0.0007	0
Horseshoe Basin	4	MF Kings	<i>R. sierrae</i>	Declining	0.0004	0.0004
Spur Basin	15	SF Kings	<i>R. muscosa</i>	Naïve	0.0026	0.005
Forester Basin	9	SF Kings	<i>R. muscosa</i>	Naïve	0.0026	0.0027
Upper Basin	15	SF Kings	<i>R. muscosa</i>	Extirpated	0.0025	0.0061
Marjorie Basin	14	SF Kings	<i>R. muscosa</i>	Declining	0.0021	0.0045
Reflection Basin	11	SF Kings	<i>R. muscosa</i>	Extirpated	0.002	0.004
Center Basin	4	SF Kings	<i>R. muscosa</i>	Naïve	0.0015	0.0014
Sixty Lake Basin	20	SF Kings	<i>R. muscosa</i>	Declining	0.0015	0.0049
Woods Basin	1	SF Kings	<i>R. muscosa</i>	Extirpated	0.0013	0
Vidette Basin	6	SF Kings	<i>R. muscosa</i>	Naïve	0.0011	0.0026
Granite Basin	3	SF Kings	<i>R. muscosa</i>	Persistent	0.001	0.0042
Bullfrog Basin	1	SF Kings	<i>R. muscosa</i>	Naïve	0.0009	0
Striped Basin	1	SF Kings	<i>R. muscosa</i>	Extirpated	0.0009	0
Muro Blanco Basin	12	SF Kings	<i>R. muscosa</i>	Extirpated	0.0008	0.0041
Pinchot Basin	3	SF Kings	<i>R. muscosa</i>	Extirpated	0.0008	0.0037

Marion Basin	2	SF Kings	<i>R. muscosa</i>	Extirpated	0.0006	0.0007
Rae Basin	3	SF Kings	<i>R. muscosa</i>	Extirpated	0.0005	0.0019
Cartridge Basin	2	SF Kings	<i>R. muscosa</i>	Extirpated	0.0005	0.0014
Lewis Basin	2	SF Kings	<i>R. muscosa</i>	Declining	0.0003	0
Lower Bullfrog Lake *	1	Kern	<i>R. muscosa</i>	Declining	0.0022	0
Milestone Basin	19	Kern	<i>R. muscosa</i>	Declining	0.002	0.0055
Kern Bench	9	Kern	<i>R. muscosa</i>	Naïve	0.0019	0.0027
Mulkey Meadows *	6	Kern	<i>R. muscosa</i>	Persistent	0.0018	0.0027
Whitney Basin	5	Kern	<i>R. muscosa</i>	Declining	0.0017	0.0053
Tyndall Basin	4	Kern	<i>R. muscosa</i>	Declining	0.0015	0.0044
Upper Kern Basin	15	Kern	<i>R. muscosa</i>	Declining	0.0014	0.0042
Sky Parlor Basin	2	Kern	<i>R. muscosa</i>	Declining	0.0011	0.0007
Wright Basin	3	Kern	<i>R. muscosa</i>	Declining	0.0005	0.0016
Wallace Basin	3	Kern	<i>R. muscosa</i>	Declining	0.0005	0
Laurel Basin	2	Kern	<i>R. muscosa</i>	Extirpated	0.0005	0.0007
Coyote Basin	6	Kern	<i>R. muscosa</i>	Declining	0.0002	0.0015

Table 2.2. Pairwise F_{ST} among watersheds. Comparisons between adjacent watersheds showed limited to moderate genetic differentiation.

<i>Major Watershed</i>	San Joaquin	MF Kings	SF Kings	Kern
San Joaquin	0	-	-	-
MF Kings	0.05	0	-	-
SF Kings	0.10	0.06	0	-
Kern	0.21	0.17	0.13	0

In **Chapter 2**, I focused on a location under intensive conservation management within *Rana muscosa/sierrae* species range. Using samples from both extant and extirpated frog populations, I laid out a comprehensive, fine-scale genetic framework to inform management actions (e.g. in the form of translocations and reintroductions). As shown in **Chapter 2**, there is a wealth of genetic information gained from using DNA from minimally invasive skin swabs. To this, in **Chapter 3**, I build on **Chapter 2** to take advantage of a similar assay to target Bd genomic regions. I compare two locations, the Sierra Nevada of California and Central Panama, and closely re-examine two of the most iconic amphibian community declines ever documented. At fine spatial resolution, we use methods in both phylogenetics and population genetics to interrogate and compare patterns of Bd evolutionary history.

CHAPTER 3 DIVERGENT EVOLUTIONARY HISTORIES OF PATHOGEN *BATRACHOCHYTRIUM DENDROBATIDIS* BETWEEN TWO REGIONS WITH EMBLEMATIC PATTERNS OF AMPHIBIAN DECLINE

Andrew P. Rothstein, Allison Q. Byrne, Roland A. Knapp, Cheryl J. Briggs, Jamie Voyles, Corinne L. Richards-Zawacki, and Erica Bree Rosenblum

3.1 ABSTRACT

Emerging infectious diseases are a pressing threat to global biological diversity. The increased incidence and severity of novel pathogens of wildlife underscores the need for methodological advances to understand pathogen emergence and spread. Here we take a genetic epidemiology approach to test – and challenge – key hypotheses about a devastating zoonotic disease impacting amphibians around the world. We used a cost-effective, amplicon-based sequencing method and non-invasive samples to retrospectively investigate the history of the fungal pathogen *Batrachochytrium dendrobatidis* (Bd) in two emblematic systems. The montane amphibian communities of the Sierra Nevada of California and Central Panama both experienced precipitous Bd-related declines. The prevailing hypothesis in both regions is that the hypervirulent Global Panzootic Lineage of Bd (BdGPL) was recently introduced and subsequently spread in a rapid and wave-like fashion. Our data challenge this hypothesis and demonstrate that disease outbreaks with similar epizootic signatures can still have radically different underlying evolutionary histories. Our genetic data from Central Panama confirm a recent and rapid spread of the pathogen in this region. However, BdGPL in the Sierra Nevada has remarkable spatial structuring, high genetic diversity, and a much older history inferred from time-dated phylogenies. The observed level of microgeographic structure within BdGPL in the Sierra Nevada has not yet been described anywhere else in the world. Thus, this deadly pathogen lineage may have a longer history in some regions than previously thought, which may provide insights into its origin and spread. Overall, our results highlight the importance of integrating field observations of wildlife die-offs with genetic data to more accurately reconstruct pathogen outbreaks.

3.2 INTRODUCTION

Globalization has contributed to a surge in the incidence, severity, and spread of emerging infectious diseases [1, e.g. 2, 107, 108]. Emerging diseases of wildlife are particularly important to global biological diversity as they can cause devastating population declines and exacerbate other threats such as habitat loss, overharvesting, invasive species, and climate change [10, 109–114]. Recent advances in the study of disease emergence and spread integrate epidemiological and genetic data to test theoretical predictions about the ecological history of the pathogen given the underlying evolutionary signal [34–36]. However, most applications of this approach have been for quickly evolving pathogens (i.e. RNA viruses) and those that directly impact human health. There have been a handful of studies applying methodological advances in genetic epidemiology to emerging wildlife diseases [see recent reviews 37–39], but such frameworks are still largely underutilized.

Amphibians are declining worldwide [12, 115]. One of the major drivers of amphibian declines is the global spread of the disease chytridiomycosis, caused by the fungal pathogen *Batrachochytrium dendrobatidis* (Bd) [13]. Bd infects the keratinized skin cells of susceptible host species, disrupts vital amphibian skin functions, and can cause mortality [18]. In some cases, Bd infections can spread quickly across individuals, populations, and species, leading to epizootic outbreaks and population and community collapses [14, 116]. Since the earliest observations of Bd related die-offs in late 1990s, Bd has emerged as a global threat to amphibian biodiversity and now impacts amphibians on every continent where they are present [12].

Bd has a complex evolutionary history with multiple lineages found in different parts of the world. Phylogenetically, Bd is characterized by several early branching lineages endemic to different regions (BdCAPE, BdASIA1, BdBrazil/ASIA2, and BdASIA3) and one more recently derived hypervirulent panzootic lineage (BdGPL) [10, 117, 118]. BdGPL has been linked to declines of amphibian communities around the world and is the only Bd lineage with a truly global distribution [10]. Whole-genome data have been important for revealing dynamics of BdGPL spread [10, 119]. BdGPL typically exhibits little phylogenetic or spatial genetic structure (with the exception of two subclades BdGPL-1 and BdGPL-2) [120, 121], suggesting that this lineage spread rapidly around the world [118, 119]. Moreover, compared to other Bd lineages, BdGPL genomes have fewer pairwise genetic differences among them and highly variable genetic diversity values [10]. Observations of minimal pairwise genetic differences are consistent with rapid BdGPL spatial radiation, and variability in genetic diversity suggests episodes of population size fluctuation. However, we still lack a connection between our understanding of Bd evolutionary history at a global scale and regional Bd emergence and spread.

Two of the most emblematic BdGPL-related declines occurred in the montane amphibian communities of the Sierra Nevada of California and Central Panama. In the Sierra Nevada of California, mountain-yellow legged frogs (*Rana sierrae/muscosa*), were historically one of the most abundant vertebrates [122]. Over the last century, these frogs vanished from more than 90% of their historic range, and Bd (along with invasive fish) was a significant factor in their decline [123]. Available information suggests that Bd has been spreading across the Sierra Nevada since at least the 1960s [124, 125] and has caused epizootics and subsequent extirpations in hundreds of populations [31, 32, 116]. Some populations that experienced Bd-related declines are beginning to rebound, but remaining naïve populations are still at risk for Bd epizootics [126]. Similarly, in Central America, amphibian population declines were first observed in the late 1980s [127–129]. As Bd spread southeast into Central Panama starting in the early 2000s [14], many susceptible

amphibian host species declined –or even disappeared completely – across the region [14,130–134]. Although some species seem to be recovering [133], Bd-related declines have fundamentally reshaped these tropical communities [131,135,136].

From an epizootiological perspective, amphibian declines in the Sierra Nevada and Central Panama appear quite similar. In both regions, initial detection of Bd was followed by devastating outbreaks and host mortality. Patterns of decline in both the Sierra Nevada and Central Panama also appear to provide evidence of a “wave”-like spread of Bd across the landscape [116,137]. Pathogen prevalence and population decline data in both systems suggest that new infections appear in a predictable spatial direction and that Bd outbreaks move a predictable distance each year [14,116,137]. Coupled with a global phylogenetic view of Bd, the prevailing hypothesis suggests that BdGPL is recent invasive pathogen in these two regions [138]. However, epizootiological data based on observed outbreaks and host outcomes may or may not reflect the true history of Bd arrival and spread. The Sierra Nevada and Central Panama differ dramatically in climate, habitat, and amphibian community composition. Therefore, although it is often assumed that Bd arrived recently and spread in a wave-like fashion in both regions, it is possible that different evolutionary histories of Bd underlie these observed patterns.

Molecular data can reveal nuances of a pathogen’s history that cannot be obtained by field observations alone. Genetic and genomic approaches have previously been used to investigate the evolutionary history of Bd at regional and global scales [10,118,119,139]. However, most studies of the evolutionary history of Bd in emblematic systems like the Sierra Nevada and Central Panama have relied on a small number of Bd isolates for any one region. Live and pure Bd cultures have been the source of high-quality DNA for genomic sequencing (e.g., [10,119,140]) but are inherently challenging to obtain, isolate, and maintain. Low sample sizes and poor spatial coverage has made it difficult to test fine-scale hypotheses about Bd emergence and spread. However, advances in sequencing technology now allow for leveraging fine-scale sampling of frog skin swabs, previously used to determine Bd presence/absence and load, to robustly characterize Bd genotypes across relevant spatial scales [141]. Thus, we can now test whether patterns of Bd emergence that appear similar across systems result from shared underlying processes.

We used fine-scale genetic sampling to investigate assumptions about the history of BdGPL in the Sierra Nevada and Central Panama. Using non-invasive skin swabs collected across similar spatial and temporal scales, we targeted hundreds of loci across the Bd genome to examine the hypothesis of recent Bd emergence and unidirectional epizootic spread in these two emblematic systems. Our work provides an in-depth understanding of pathogen evolutionary dynamics in natural systems and highlights the importance of integrating genetic and epizootiological approaches for emerging wildlife diseases.

3.3 MATERIALS AND METHODS

Sampling and Sequencing

We used skin swab DNA samples collected from the Sierra Nevada and Central Panama across similar timescales (2011-2017) and across equivalent spatial scales (~130km across Euclidean distance between furthest two sites) (Fig 3.1A). Sites are defined as collections of lakes and streams that cluster together geographically within a region. We sampled 10 sites from both the Sierra Nevada (n=130 swabs) and Central Panama (n=80 swabs). Sierra Nevada samples comprised skin swabs from two sister species of frogs (*R. sierrae/muscosa*) [123] and Central Panama samples comprised skin swabs from 16 different frog species. Additionally, we included

120 previously sequenced samples from a global BdGPL dataset for downstream analyses to compare Sierra Nevada and Central Panama regions [117]. The global BdGPL dataset included samples across 59 frog species from continental regions of Africa (n=3), Americas (n=69), Asia (n=24), Australia (n=1), and Europe (n=23).

We genotyped Sierra Nevada and Central Panama Bd from skin swab samples across 240 regions (each 150-200bp long) of the Bd genome using a custom assay [141]. We extracted DNA using either PrepMan Ultra Reagent or Qiagen DNEasy kits. DNA from skin swabs typically contains many PCR inhibitors that can interfere with downstream data quality, so we used an isopropanol precipitation to purify swab extractions. Given the small amount of DNA available from skin swabs versus traditional DNA sources, we used a pre-amplification step in two pools of 120 primer pairs (416.6nM concentration). Each pre-amplification PCR reaction used the FastStart High Fidelity Reaction PCR System (Roche) with the following concentrations: 1x FastStart High Fidelity Reaction Buffer with MgCl₂, 4.5mM MgCl₂, 5% DMSO, 200μM PCR Grade Nucleotide Mix, 0.1 U/μl FastStart High Fidelity Enzyme Blend. We removed other potential PCR inhibitors, such as excess primers and unincorporated nucleases, using 4 μl ExoSAP-it (Affymetrix Inc.) and diluted 1:5 in nuclease-free water.

Following pre-amplification, we applied a microfluidic PCR approach using the Fluidigm Access Array platform. Pre-amplified products were loaded into a Fluidigm Access Array IFC, individually barcoded, then pooled for sequencing on ¼ of an Illumina MiSeq lane with 2 x 300bp paired-end reads at the University of Idaho IBEST Genomics Resources Core. From raw sequence reads, we used the dbcAmplicons software (<https://github.com/msettles/dbcAmplicons>) to trim adapter and primer sequences. Paired-end reads were merged to build continuous reads to extend the length of amplicon using flash2. We de-multiplexed and filtered sequences using the *reduce_amplicons.R* script within the dbcAmplicons repository into two sequence types: ambiguities and raw fastq for each sample. Ambiguities sequence files used IUPAC ambiguity codes to identify multiple alleles. Raw fastq files are all sequences for each sample. Ambiguity sequences were used for phylogenetic analyses and the fastq by sample was used for alignment, variant calling, and PCA.

Variant Calling

After de-multiplexing, we used bwa software (“mem” mode) to align reads to our reference target regions [142]. From the resulting BAM files, we filtered by read depth for each amplicon for each individual. We required that each individual had an average read depth >5 for per amplicon to pass the filter. All reads from amplicons that passed the depth filter were moved into a new .bam file for that individual. Using a filtered BAM file from alignments, we applied FreeBayes, a Bayesian genetic variant detector that identified haplotype-based SNP calls [143]. FreeBayes software was used to remove singleton alleles and created phased haplotypes encoded as alleles. Following singleton removal and phasing, we used default FreeBayes parameters and called SNPs only within reference sequences for all 240 amplicons. The resulting dataset was a raw VCF file that we used for subsequent SNP filtering. We filtered SNPs using standard quality control parameters through *vcftools* (removed alignment mapping quality less than 30, supported base quality less than 20, minimum supported allele quality sum = 0, and proportion of genotypes called <50%). Lastly, we removed samples from analyses that contained a high proportion of missing data (>50%) [144]. Post filtering, we recovered 2,268 variable sites across 235 amplicons. Our resulting VCF included 130 Sierra Nevada samples, 80 Central Panama samples, and 120 global BdGPL samples for downstream analyses.

Genetic Diversity

Using our filtered VCF, we applied PCA to examine genetic clustering and structuring among the Sierra Nevada, Central Panama, and global samples. We estimated PCs using *adegenet* [145] and visualized in R (v.3.6.1). We calculated summary diversity statistics using ANGSD [146]. Given that sample sizes can greatly impact diversity metrics, we randomly subsampled our Sierra Nevada and global BdGPL samples to equal the number of Central Panama samples (n=80). Additionally, 49 amplicons were previously developed as Central Panama-specific markers and were removed, leaving 186 amplicons for diversity statistics. Using our filtered BAMs from our variant calls, we generated a folded site frequency spectrum given an unknown ancestral state. After estimating site frequency spectrum for each region, we calculated per-site Watterson's θ and π for the Sierra Nevada, Central Panama, and global BdGPL samples. We tested for significant differences in mean Watterson's θ and π and using analysis of variance followed by Tukey's HSD in R (v. 3.6.1), given that we had multiple pairwise comparisons of our global BdGPL reference, Sierra Nevada, and Central Panama samples.

Phylogenetics

We created a phylogeny including Sierra Nevada, Central Panama and our global BdGPL reference panel. We removed amplicons that had no data and included samples that had least 20 amplicons. We trimmed loci that had >5bp difference between minimum and maximum sequence length to control for improper alignments near large indels. A final list of 206 loci were individually aligned using the MUSCLE package in R [v.3.6.1, 147] and concatenated (28,688 bp in length). We also included an outgroup of BdBrazil using previously published sequences from UM142 [117].

With our concatenated alignment and recorded sampling years, we inferred time-measured phylogenies using both BEAST2 [148] and Nextstrain [149]. For BEAST2 we used a GTR substitution model with estimated mutation rates 7.29×10^{-7} (lower; 3.41×10^{-7} , upper; 1.14×10^{-6}) and extended Bayesian skyline plot as demographic parameter [10]. Using this model, we ran a chain which drew samples every 3,000 MCMC steps from a total of 575,000,000 steps, after a discarded burn-in of 57,500,000 steps. Convergence of distribution and effective sample size >150 were checked through *Tracer* (v.1.7.1) [150]. Our best supported tree was estimated using maximum clade credibility through *TreeAnnotator* (v. 2.6) and was visualized using *FigTree* (v.1.4.4).

We used Nextstrain for visualization comparison. Briefly, Nextstrain applies a maximum likelihood ancestral state reconstruction of discrete traits (e.g. sites) and also uses locations and timing to infer potential transmission events across nodes of a tree [149]. Using the *augur* pipeline within Nextstrain, we applied a GTR substitution model with the same substitution rate as our BEAST2 model at 7.29×10^{-7} substitutions per year ($SD \pm 4.0 \times 10^{-7}$). We estimated standard deviation using the average distance between O'Hanlon et. al. (2018) substitution rate compared to both the lower and upper bound values. The model assumed an uncorrelated lognormal relaxed clock and, to minimize demographic history assumptions, we applied an extended Bayesian skyline plot. Using *auspice* within Nextstrain, we built a single tree and map that color coded by region and global BdGPL reference panel as well as by site for Sierra Nevada and Central Panama to infer within-region transmission events.

It is important to note that we used BEAST2 and Nextstrain as analytical frameworks to compare patterns between the Sierra Nevada and Central Panama but not to infer exact introduction

dates. Applying the same evolutionary models across two geographic regions provides a powerful comparative tool and allows us to infer *relative* evolutionary rates and introduction timings. However, we interpret specific dates with great caution given that patterns of Bd genome evolution may violate a number of model assumptions (e.g., variation across the genome in recombination and mutation rates, variation in chromosomal copy numbers, potential for both meiotic and mitotic recombination) [119,140] and because our sampling dates do not necessarily correspond to first introduction dates. Given that any violation of basic model assumptions would be shared across study regions, comparisons between the Sierra Nevada and Central Panama can be used to draw conclusions about the relative invasion history in these regions.

3.4 RESULTS

Bd from the Sierra Nevada shows greater population structure than Bd from Central Panama

When comparing within regions, we found significant genetic clustering across the Sierra Nevada (Fig 3.1B) but no genetic clustering across Central Panama (Fig 3.1C). Samples collected from the same site in the Sierra Nevada clustered together, regardless of collection year. Starting with Unicorn Ponds at the north, samples generally follow a pattern of isolation by distance. LeConte Divide and Conness Pond are somewhat anomalous however because they overlap in PC space but are geographically separated by ~80 km (Fig 3.1B). In contrast, Central Panama genotypes exhibited panmictic patterns, regardless of locality or collection year, indicating no genetic structuring across a similar spatiotemporal scale (Fig 3.1C).

Bd from the Sierra Nevada shows greater variation and diversity than Bd from Central Panama

We confirmed that Bd from Sierra Nevada and Central Panama belong to the global BdGPL lineage. However, Sierra Nevada and Central Panama samples clustered separately from each other in PC space when compared to global BdGPL samples (Fig 3.2A). Additionally, we found that overall genetic diversity was significantly higher in the Sierra Nevada as compared to Central Panama [Tukey HSD, $p < 0.0001$] (Fig 3.2B-C). Remarkably, we also found that Sierra Nevada Bd samples have comparable and, in the case of Watterson's θ , higher diversity than the set of global BdGPL samples [Tukey HSD, $p < 0.0001$]. When comparing Central Panama and the Sierra Nevada using individual sites with similar sample sizes, we found that the majority of Sierra Nevada sites had higher mean diversity compared to Central Panama sites (both Watterson's θ and π) [Tukey HSD, $p < 0.001$], except in the lowest sample size pairing (N=5) where El Valle S. had significantly higher mean diversity than LeConte Divide (Fig 3.4).

Bd in the Sierra Nevada is inferred to be older than Bd in Central Panama

Using a time-dated phylogenetic approach that included previously published global BdGPL samples for reference [117], we found branches from Sierra Nevada samples were comparatively older than those in Central Panama (Fig 3.3, Fig 3.5). As discussed in the Materials and Methods, we do not assume the specific inferred dates are accurate given the likelihood that dynamics of Bd genome evolution violate several model assumptions. However, comparing the results across regions provides important data on relative invasion histories. For BEAST2, the time to most recent common ancestor (tMRCA) for Sierra Nevada samples was estimated to be 474 years from present day (95%HPD 510-393 years from present day) and estimated tMRCA in Central Panama was 277 years from present day (95%HPD 389-60 years from present day) (Fig 3.3). For Nextstrain, tMRCA for Sierra Nevada samples was estimated as 1407 years from present

day (95% CI 4,498 - 1,151) and tMRCA for Central Panama was estimated as 666 years from present day (95% CI 1,914 - 534) (Fig 3.5); dynamic Nextstrain visualizations are available at: <https://nextstrain.org/community/andrew-rothstein/bd-gpl/auspice/viz>. Therefore, even without ascribing weight to specific inferred dates, Bd in the Sierra Nevada appears to be much older than Bd in Panama. Confidence intervals for the inferred tMRCA do not overlap between regions with either analysis. The BEAST2 and Nexstrain time-dated phylogenetic approaches also corroborated PCA results (Fig 3.1). Sierra Nevada samples largely clustered by site while Central Panama samples had little to no structure based on site location. (Fig 3.5 B, C) Finally, phylogenetic trees show an expected split within BdGPL. The groupings correspond to a previously reported split separating BdGPL into two subclades: BdGPL-1 and BdGPL-2[120,121]. Only GPL-2 is represented in Panama samples while GPL-1 and GPL-2 are both found in the Sierra Nevada samples.

3.5 DISCUSSION

Bd has caused mass amphibian declines in many regions of the world [12,14,15,116,137,151,152]. However, assessments of Bd emergence and spread have yet to incorporate genetically-informed epizootology to examine Bd dynamics at fine spatial scales. Our study used comparative population genetics to examine the genetic signatures of BdGPL across two emblematic regions with disease-related amphibian declines. The alpine lakes of the Sierra Nevada and the tropical forests of Central Panama have dramatically different climate, habitat, and host communities. However, they have been described as having similar histories of recent Bd emergence and spread. We tested the assumption that BdGPL was recently introduced to these two regions and swept through each in a unidirectional epizootic wave. We found dramatic differences in Bd evolutionary history across regions, with an unexpectedly deep history of Bd in the Sierra Nevada. Here we explore differences across regions, providing a new perspective on these important historic declines.

How do patterns of pathogen genetic variation differ across regions?

BdGPL in Central Panama is genetically similar and spatially unstructured

Our results from Central Panama support the hypothesis of a recent introduction, with Bd in this region lacking any spatial structure. All Bd genotypes from Central Panama group tightly together, are generally distinct from Bd collected in the Sierra Nevada, and are all part of the GPL-2 subclade. This pattern supports previous studies reporting a single fast-moving outbreak of Bd through Central Panama [137]. Our samples from Central Panama were collected approximately 8 years after observed outbreaks (between 2012-2016), and the observed lack of genetic structure indicates that Bd did not diverge on a site-specific basis over this time period. Our findings supports other recent studies showing a lack of genetic, phenotypic, and functional shifts in Central Panama Bd across similar temporal scales [133]. BdGPL appears to have arrived in Panama relatively recently (within the last 250+ years), maintained low levels of genetic diversity, and, over the last two decades, currently has no detectable genetic sub-structure.

BdGPL in Sierra Nevada is genetically diverse and spatially structured

We observed a dramatically different pattern in the Sierra Nevada, where we found high levels of genetic variation between sampling sites and spatial structuring of Bd genotypes.

Although Bd samples were collected across a similar spatial and temporal scale as those from Panama, our genetic data indicates that BdGPL has likely had a much longer historical presence in the Sierra Nevada than it has in Panama. This conclusion is supported by multiple lines of evidence. First, Sierra Nevada Bd contains more genetic variation and diversity than Central Panama (Fig 3.2A). Measures of nucleotide diversity (π), are higher in Sierra Nevada Bd samples compared to Central Panama and Sierra Nevada Bd genetic diversity (Watterson's θ) is significantly higher than the entire global panel of BdGPL samples (Fig 3.2B). This result is consistent with previous evidence that BdGPL in the Sierra Nevada has higher levels of genetic diversity than BdGPL from Arizona, Mexico, or Central Panama [153]. Second, we also observed a surprising pattern of spatially-structured genetic diversity for BdGPL in the Sierra Nevada. Sierra Nevada BdGPL genotypes typically cluster by site and segregate by geographic distance in PC space and in the phylogeny (Fig 3.1B, Fig 3.3B). Much of the observed genetic structure in the Sierra Nevada is consistent with a pattern of isolation by distance, suggesting a much longer history of Bd on the landscape. Third, even the exceptions to the pattern of isolation by distance suggests a deeper and more complex history of Bd in the Sierra Nevada. Samples from LeConte Divide and Conness Pond are genetically distinct from all other samples in the Sierra Nevada and cluster in PC space (Fig 3.1B). These samples belong to a separate, early-branching clade referred to as GPL-1 (Fig 3.3). The presence of both BdGPL-1 and BdGPL-2 subclades could represent multiple independent introductions or much deeper in-situ divergence, possibilities we revisit below.

What do regional differences suggest about BdGPL origin and invasion history?

BdGPL in Sierra Nevada likely predates the most recently observed wave of declines

One key factor that could contribute to radically different patterns of Bd genetic variation between Central Panama and the Sierra Nevada is invasion history (the timing and number of introductions). Our Nextstrain and BEAST2 analyses infer that Bd from the Sierra Nevada is older than Bd from Central Panama (Fig 3.3, Fig 3.5). While our inference indicates that BdGPL has been in the Sierra Nevada longer than Central Panama, it is difficult to assert specific invasion dates. As discussed in the Materials and Methods section, patterns of Bd genome evolution may violate a number of model assumptions. Although our analyses used a species-specific mutation rate inferred from Bd whole genome analyses [10] our assay targets regions of the Bd genome that are most informative for discriminating among Bd lineages [141] and therefore may not evolve with a shared background mutation rate. Even without specific introduction dates, studies using histology and qPCR to test for Bd presence in museum specimens have often shown Bd presence prior to field-observed die-offs [124,154,155], which could indicate older introduction timings than previously assumed. As such, Bd presence has been detected in samples as far back as 1932 in Sierra Nevada [124] and 1964 in Costa Rica (adjacent to Panama) [154].

Moreover, field observations suggest that Bd may be present in the environment well before an outbreak is observed. In some lakes, Bd is present at almost undetectably low prevalence and load for years before Bd loads spike and die-offs occur [82,116,126]. In some systems, Bd can even be detected from eDNA surveys before die-offs occur [156]. Such dynamics challenge our *a priori* expectations that Bd die-offs occur immediately after the pathogen first arrives in an area. In some systems, such as the Sierra Nevada and parts of Costa Rica [124,154,155], it is possible that Bd had a more wide-spread presence earlier than perceived. Whether there actually were earlier Bd-caused die-offs remains an open question. Increased surveillance of Bd before and

during early outbreaks is needed to decouple initial pathogen invasion from observed pathogen-induced declines.

The Sierra Nevada is a potential source for BdGPL

High levels of genetic variation, deep spatial genetic structure, and the presence of both sub-clades of BdGPL in the Sierra Nevada suggest a longer evolutionary history of Bd in the region than previously appreciated. Presence of both BdGPL-1 and BdGPL-2 could represent multiple asynchronous invasions of BdGPL, a hypothesis raised by another recent spatial-temporal study of Bd presence in the Sierra Nevada [124]. An alternative explanation is that California is a potential *source* of Bd that has spread to other regions. As sampling resolution improves, it is possible that we will find other regions of the world with highly diverse and spatially structured BdGPL populations. However, it is also worth continuing to challenge our assumptions about the origin and spread of this lineage. While the most basal lineage of Bd is from Asia [10], the origin of BdGPL remains highly uncertain. Although we often assume that BdGPL presence results from recent invasions, the region from which BdGPL originated would be expected to have general characteristics similar to what we observe in the Sierra Nevada (i.e., relatively high genetic diversity and deep spatial structure). No such region other than the Sierra Nevada has yet been identified. Global sampling with greater spatial and temporal resolution will be needed to ultimately determine the origins of this highly virulent Bd lineage.

How do biotic and abiotic factors influence observed Bd genetic variation?

Differences in topography, host life-history, community structure, and climate also likely contribute to divergent patterns of pathogen genetic structure across regions

Biotic and abiotic factors also likely influence patterns of Bd genetic variation in a consistent direction, with increased opportunity for pathogen mixing in Central Panama relative to the Sierra Nevada. Central Panama is home to a diverse amphibian assemblage, with dozens of sympatric species that use a variety of microhabitats and have different reproductive modes [14,131]. A diverse host community in Panama with year-round activity and some direct developing species (i.e., those without an aquatic larval phase) could provide more opportunities for Bd spread [131,157]. Central Panama contains landscape features that may be barriers to dispersal for some amphibian species [158], but interconnected stream networks still allow for fairly high connectivity among sites. In contrast, in the Sierra Nevada, our samples are from the only common - and highly susceptible - amphibian species in the alpine lake habitats (*Rana sierrae/muscosa*) [159,160]. *Rana sierrae/muscosa* have high site fidelity, limited overland movements, spend the majority of each year under ice, and inhabit disjunct alpine lakes separated by high mountain passes [161–163]. These features all impede connectivity among host populations and provide fewer opportunities for Bd dispersal [164]. Therefore, landscape and host factors consistently provide decreased opportunities for Bd gene flow in the Sierra Nevada, which is reflected in greater pathogen spatial structure in this region.

In addition, Central Panama is significantly warmer and wetter than the Sierra Nevada. Temperature differences are particularly important because warmer temperatures (to a point) can lead to faster pathogen growth, increased number of generations per year, and greater opportunity for rapid evolutionary change [165–167]. Slower Bd growth, generation time, and evolutionary rates in the Sierra Nevada compared to Central Panama, make the patterns of higher genetic diversity and strong spatial genetic structure in the Sierra Nevada all the more interesting.

How can pathogen genetic data help inform wildlife disease mitigation efforts?

Ultimately, integrating genetic, spatial, and epizootic data within an evolutionary framework is a powerful way to understand dynamics of emerging diseases of wildlife. Typically, studies of wildlife disease dynamics rely on *a priori* assumptions about pathogen introductions (i.e., based on earliest infection known from wild populations or museum records). However, our results clearly demonstrate that outbreaks with similar epizootological signatures can still have radically different underlying pathogen histories. In our study, two regions with similar observed epizootological patterns in the field exhibit dramatically different pathogen evolutionary histories. In fact, one of the regions – the Sierra Nevada – has considerable pathogen diversity and genetic structure. Supporting evidence suggests that Bd in this region may persist in populations of highly susceptible host species at very low levels over many years without causing epizootics, opening the possibility that the pathogen has a much longer evolutionary history than previously appreciated. When we treat all population declines as the same, we overlook important nuances that could assist on-the-ground recovery and mitigation efforts. For example, if we incorporate Bd genotype data into choices of donor frog populations when planning translocations and reintroductions, we can mitigate human-induced mixing of Bd genotypes. Such actions could be an important component for species recovery efforts. By combining genetic and epizootological data, we can better understand differences in pathogen invasion history across regions and support more effective policies for biodiversity conservation and management.

Acknowledgements

We thank the Sierra Nevada Aquatic Research Laboratory field crew, Danny Boiano from the National Park Service, Matt Robak, Angie Estrada, Renwei Chen, and Mary Toothman for assisting in field collection and pathogen qPCR. This work was supported by DOD SERDP (to E.B.R, C.L.R.Z., J.V., C.J.B), NSF DEB-1557190 (to E.B.R., C.J.B, R.A.K), NSF DEB-1551488 (to E.B.R., C.L.R.Z., J.V.), NSF DEB-1457695 (to J.V.), NSF DEB-166311 (to C.L.R.Z), and the National Park Service. Sequencing done at IBEST Genomics Resources Core at the University of Idaho was supported in part by NIH COBRE grant P30GM103324. All sample collections were authorized by research permits provided by NPS, USFWS, and the Institutional Animal Care and Use Committees of UC Berkeley, UC Santa Barbara, University of Nevada – Reno, and University of Pittsburgh.

3.6 FIGURES

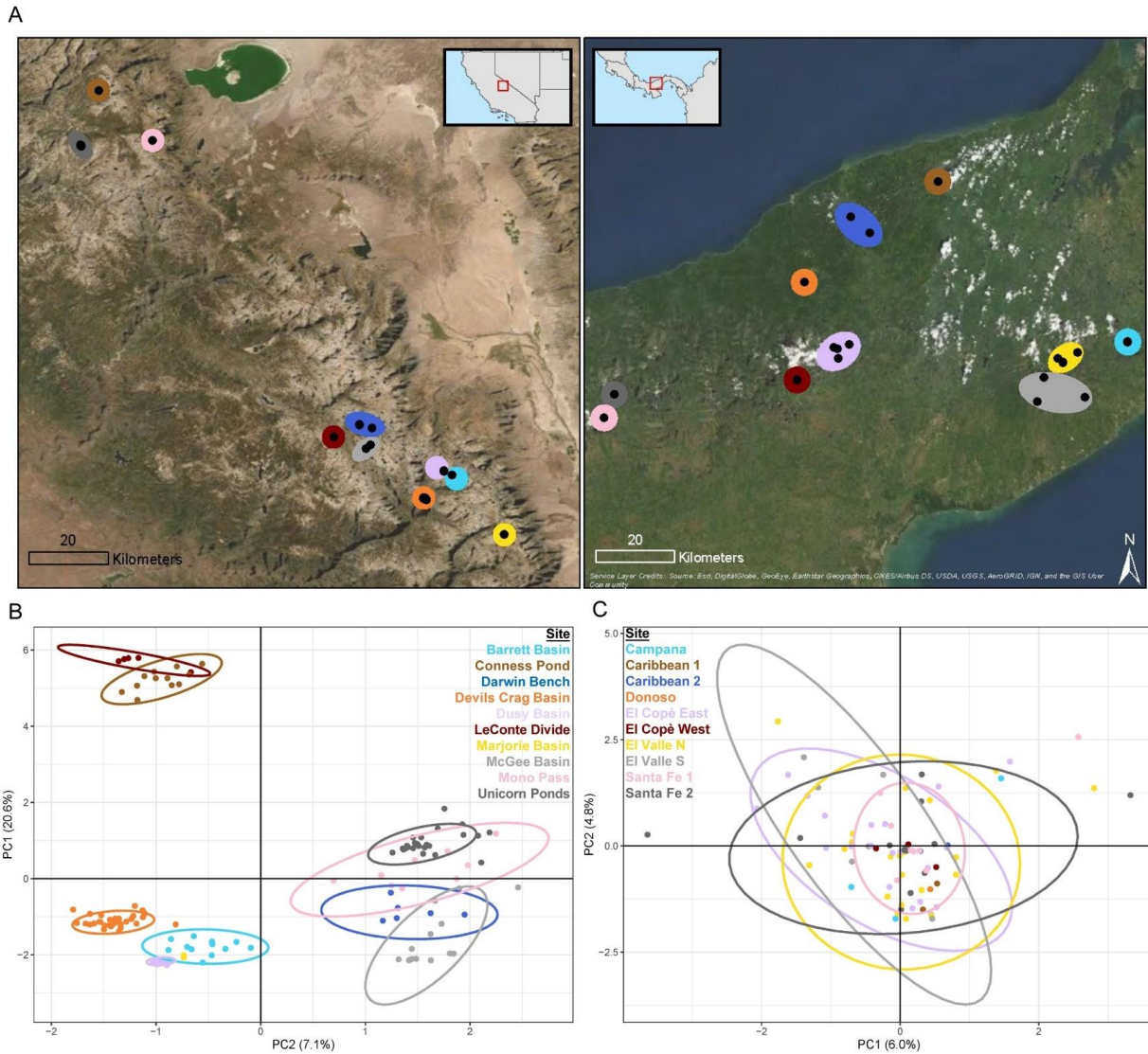


Fig 3.1. Study system map and principal component analysis of within region genotypes. (A) Map of sites sampled in the study in the Sierra Nevada and Central Panama. (B) PCA within Sierra Nevada samples, colored by major site. Samples cluster by site, suggesting strong genetic structuring across the Sierra Nevada. (C) PCA within Central Panama samples, colored by site. Compared to samples from the Sierra Nevada, Central Panama samples exhibit a dramatically different pattern, i.e., panmixis, despite a similar spatial and temporal scale of sampling.

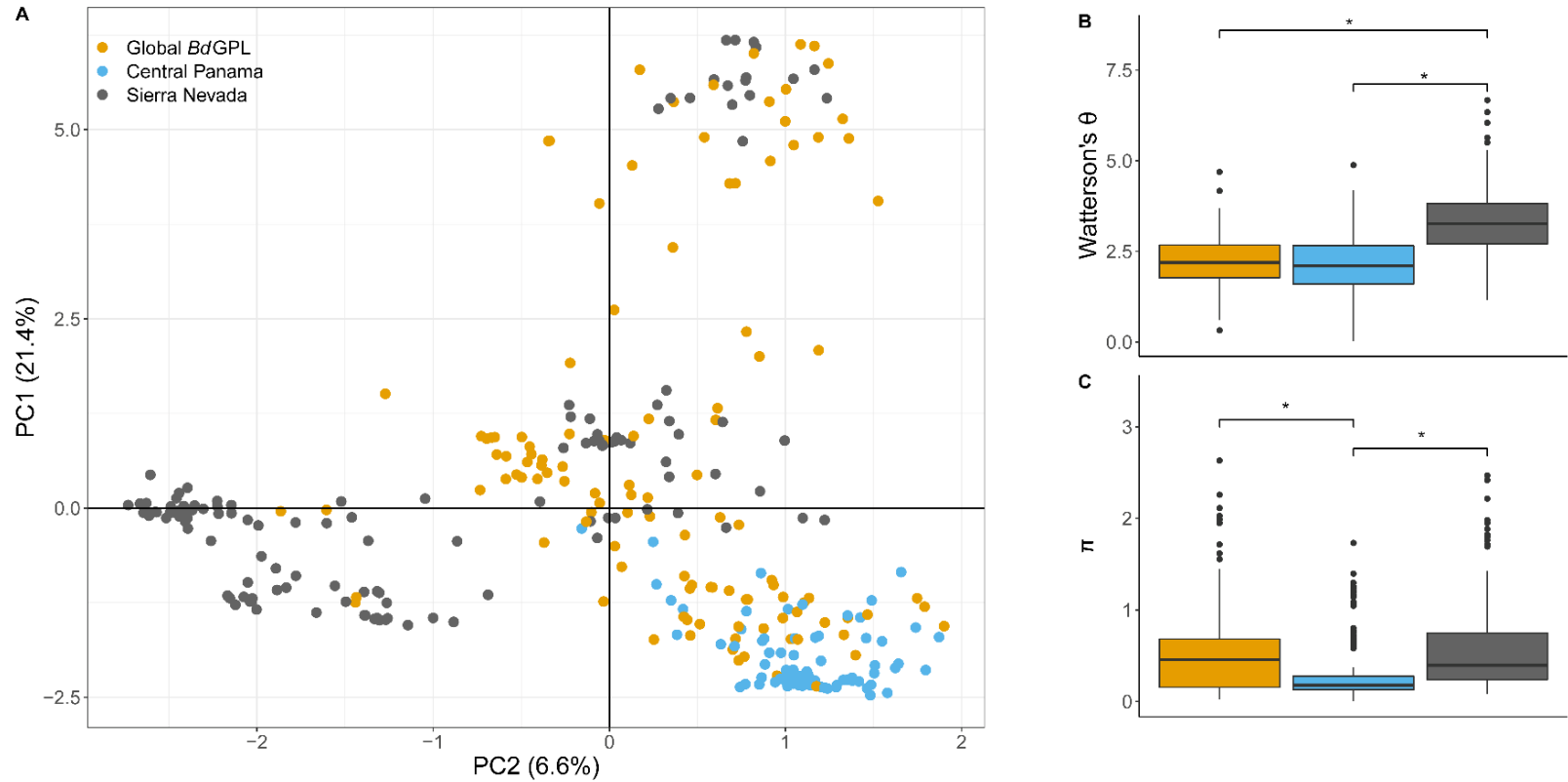


Fig 3.2. Genetic differentiation and diversity among Sierra Nevada, Central Panama, and Global *Bd*GPL samples. (A) PCA based on *Bd*GPL genotypes from the Sierra Nevada ($n=130$), Central Panama ($n=80$), and global reference panel ($n=120$). Colors indicate samples from each region. The global reference panel included samples from dozens of frog species across all continents with *Bd*GPL. Samples from Sierra Nevada and Central Panama are almost entirely separated in PC space with the Sierra Nevada samples showing greater genetic variation than Central Panama samples. (B) Distribution of mean genetic diversity (Watterson's Θ) for all variable sites based on region. Samples from Sierra Nevada and global panels were randomly subsampled to match Central Panama sample size (all regions $n=80$). Mean genetic diversity was significantly higher for Sierra Nevada samples compared to Central Panama samples and to the global *Bd*GPL panel [Tukey HSD, $p < 0.0001$]. (C) Distribution of mean nucleotide diversity (π) for all variable sites based on region using the same samples as panel B. Mean nucleotide diversity was significantly lower for Central Panama samples compared to Sierra Nevada samples and the global *Bd*GPL panel [Tukey HSD, both $p < 0.0001$]. Each box plot shows the median (horizontal line), first and third quartiles (bottom and top of box, "hinges"), lowest and highest values within inter-quartile range of the lower and upper hinges (vertical lines), and outliers (points).

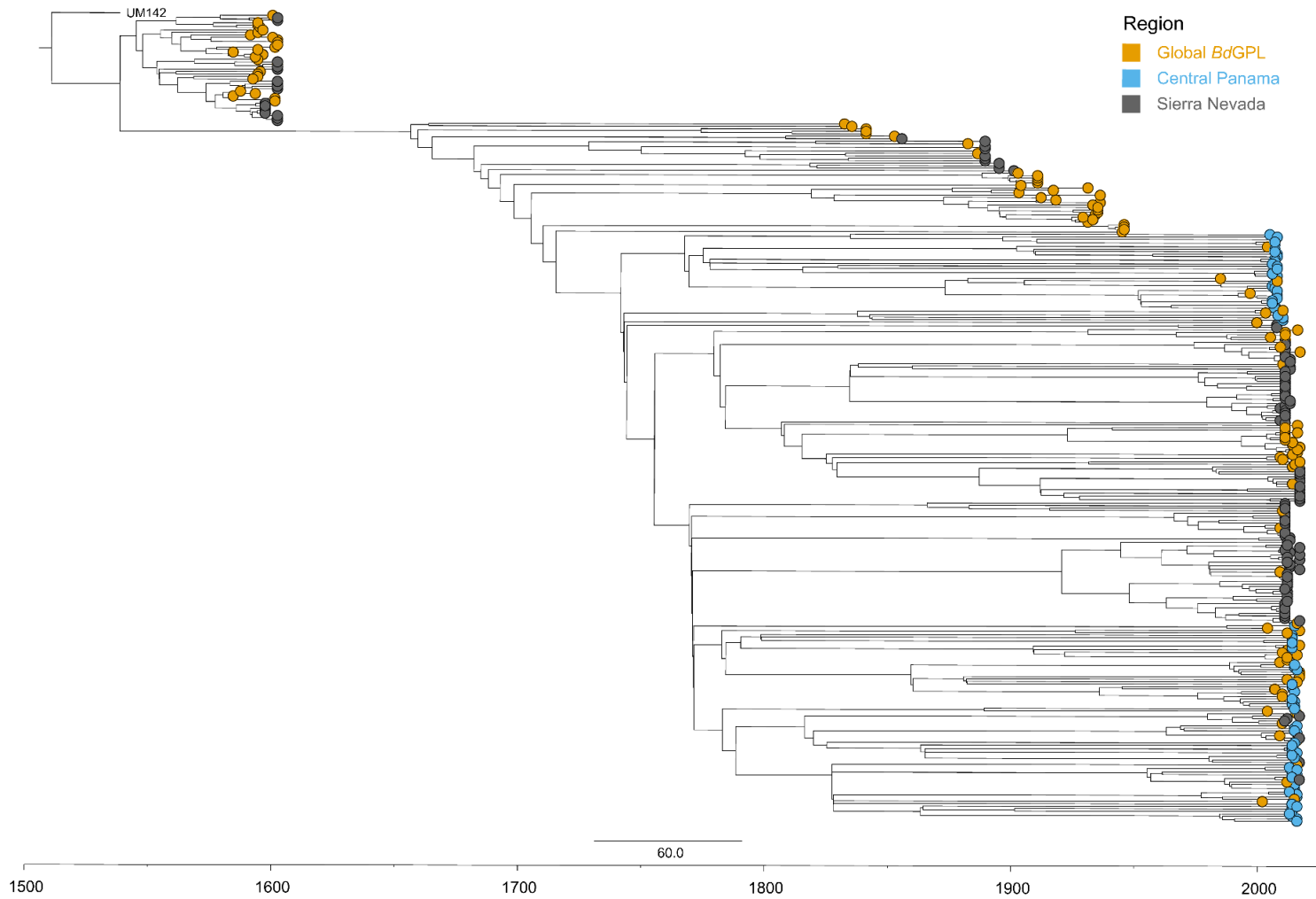


Fig 3.3. BEAST2 timed dated phylogeny among Sierra Nevada, Central Panama, and Global BdGPL samples. Branch tips are color coded by region. The tree is rooted by an outgroup from a more basal Bd lineage (BdBrazil isolate UM142). Sierra Nevada samples are found across the tree, in multiple clusters, and with longer branch lengths than Central Panama samples suggesting a longer history of Bd in this region.

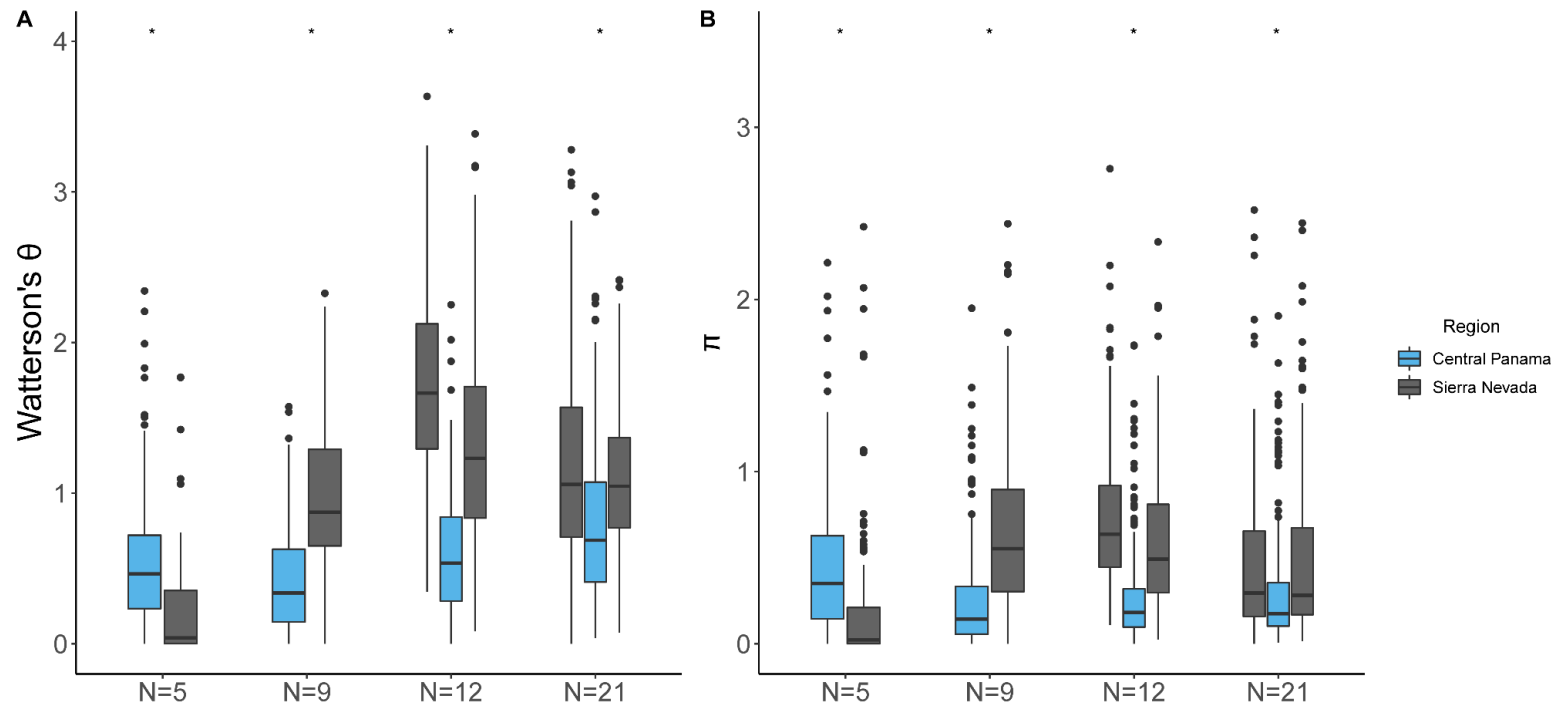


Fig 3.4. Regional site comparisons of genetic diversity between Sierra Nevada and Central Panama. (A) Distribution of mean genetic diversity (Watterson's Θ) of variable sites paired by Sierra Nevada and Central Panama locations with equal samples sizes. (B) Distributions of mean nucleotide diversity (π) for all variable for same locations as panel A. In both measures of diversity, samples from Sierra Nevada were significantly higher in all cases except N=5 where Central Panama was higher [Tukey HSD, $p < 0.0001$]. Each box plot shows the median (horizontal line), first and third quartiles (bottom and top of box, "hinges"), lowest and highest values within inter-quartile range of the lower and upper hinges (vertical lines), and outliers (points).

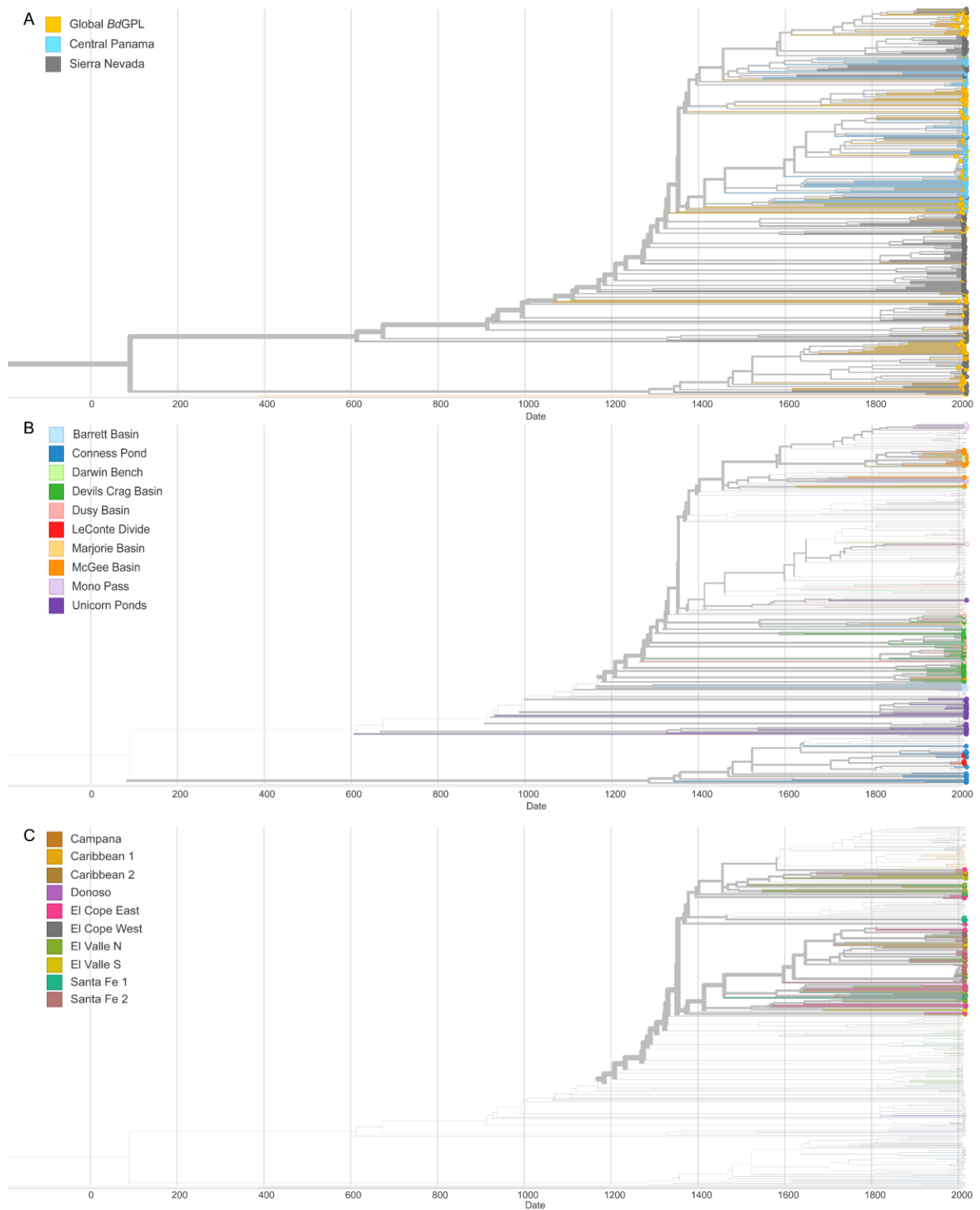


Fig 3.5. Static Nextstrain visualizations for time-dated phylogenies. (A) all samples colored by region, (B) Sierra Nevada samples colored by site, (C) and Central Panama samples colored by site. Sierra Nevada samples are highly structured by site across the phylogeny while Central Panama samples lack structuring by site. Although the specific inferred dates are not biologically meaningful, the comparison across regions is important and suggests that Bd/GPL has a much longer history in the Sierra Nevada than in Central Panama.

In **Chapter 3**, I focused on two regions that are exemplars of dramatic amphibian declines from Bd: the temperate alpine lakes of the Sierra Nevada of California and the tropical montane forests of Central Panama. Decades of work in these two areas have characterized Bd as a novel, recently introduced pathogen that subsequently spread in a “wave-like” progression across the landscape. Despite similar stories of disease emergence, we find remarkably different patterns of evolutionary history. Specifically, the Sierra Nevada of California, we found evidence of a highly structured Bd population, indicating a long historical presence in the area. The high genetic structuring of Bd in the Sierra largely aligns with genetic structuring of frog populations by location in **Chapter 2**. The results of **Chapter 2** and **Chapter 3** provides a framework to expand sampling in **Chapter 4** across the entire range of *Rana muscosa/sierrae* to build a comprehensive genomic assessment to inform conservation efforts. Collective results from **Chapter 3** and **Chapter 4**, conservation of *Rana muscosa/sierrae* will have the most complete genomic picture of both endangered host populations and the pathogen implicated in its decline.

CHAPTER 4 RANGEWIDE CONSERVATION GENOMICS USING AMPLICON-BASED SEQUENCING FOR THE MOUNTAIN YELLOW-LEGGED FROG SPECIES COMPLEX (*RANA MUSCOSA/SIERRAE*)

Andrew P. Rothstein, Lydia L. Smith, Hannah Kania, Roland K. Knapp, Daniel M. Boiano, Cheryl J. Briggs, Adam R. Backlin, Robert N. Fisher, and Erica Bree Rosenblum

4.1 ABSTRACT

Insights from conservation genomics have dramatically improved the recovery plans for numerous endangered species. However, certain imperiled groups, such as amphibians, have yet to benefit from the full application of genomic technologies. Despite a critical need for genomics-informed recovery actions, amphibians' large and complex genomes create a barrier for rapid and affordable genomic applications. One species complex, *Rana muscosa* and *sierrae*, that inhabit the Sierra Nevada Mountains of California are an exemplar of this tension. *Rana muscosa/sierra* have declined precipitously throughout their range, but conservation management plans are still based off a single mitochondrial gene. Our study took advantage of archived skin swabs, previously used in the detection of the amphibian chytrid fungus (*Batrachochytrium dendrobatidis*) to genotype frog populations across the range. With a robust data set from 373 samples across 276 frog populations and 50 nuclear markers, we found eight major genetic clusters. Though we observed strong genetic clustering, we also found some admixture across these boundaries, suggesting a stepping stone model of population structure. We also found that genetic diversity is relatively uniform across genetic clusters with a few exceptions. We explore how these insights could immediately and drastically inform on-the-ground conservation efforts. Overall, our results provide clarity on management units across the range of a highly endangered species and highlight how genomics can be used to interrogate complexities of disease-related amphibian declines.

4.2 INTRODUCTION

The era of genomics has ushered in countless methodological approaches for the conservation of natural and managed populations [29,40,168]. Historically, conservation genetics used only a handful of genetic markers (e.g. microsatellites or mtDNA) to examine fundamental patterns of population structure, diversity, and gene flow [169]. Now, with decreasing cost and increasing ease of implementation, researchers can routinely interrogate hundreds and thousands of genetic markers and even obtain whole genome-wide resolution for non-model species [24–27]. Indeed, methodological advances now allow researchers to answer previously intractable questions in conservation biology and pursue more advanced applications of genetic management (e.g. inclusion of markers related to adaptive variation and evolutionary rescue) [28,170].

Amphibians are declining worldwide due to numerous factors such as habitat loss, climate change, invasive species, and disease [12,115]. Amphibian conservation often relies on a genetic foundation to guide recovery efforts [171]. Usually, species recovery plans include identifying management units with the objective of bolstering populations while maintaining historical genetic structure and diversity [26,172–175]. To effectively maintain conservation management units across populations (e.g. through translocations and reintroduction programs) amphibian recovery efforts require comprehensive genetic frameworks [44,176,177].

Especially in amphibians, securing genomic resources can be costly and sometimes methodologically prohibitive due to large and complex genomes sizes [41–43]. Given these restrictions, conservation genomic applications need to identify the appropriate genomic scale to match species recovery priorities. More genomic data will always increase resolution and confidence in conservation management recommendations. However, at what point does this increase become no longer necessary? Answering this question requires balancing an increase in genomic resolution while maintaining practical outcomes for conservation [178].

The mountain yellow-legged frog species complex (*R. muscosa/sierrae*) in the Sierra Nevada of California is a prime example of active recovery efforts that would benefit from increased genomic resolution. *R. muscosa/sierrae* were once abundant in the high alpine communities of California [122,179] but have, since the mid-20th century, precipitously declined due to invasive fish [180–184] and the fungal pathogen *Batrachochytrium dendrobatidis* (Bd) [32,116]. Given dramatic declines of these species (over 90% of their historical range) there has been an intensive focus on recovering frog populations in the form of translocations and reintroductions [164]. Many of these conservation actions have used genetics as a blueprint for informing which donor populations to use in recovery actions.

The existing genetic framework for *R. muscosa/sierrae* is based on a single mitochondrial marker that described the major genetic management units across the species complex [123]. Recent frog population genetic work in both Yosemite National Park and Sequoia and Kings-Canyon National Parks have shown that - when many nuclear genetic markers are used in tandem with higher spatial resolution - these species contain high levels of spatial genetic structure [164,185]. Moreover, genetic breaks inferred with multi-locus nuclear data are not always the same as those observed in the existing mitochondrial tree [164,185]. Therefore, an updated genetic framework for this species complex is critical for managing population and species recovery across the landscape.

For protected amphibian species, like *R. muscosa/sierrae*, there are some challenges to obtaining genome-wide data. The protected status of these species limits collecting high-quality DNA sources (e.g. tissue samples). Moreover, even with high quality DNA, the large and complex

genomes in these species make building genome-wide resources difficult [186]. To address these limitations, our study used a microfluidic amplicon sequencing approach that was developed to successfully genotype low DNA quality and quantity skin swab samples. These minimally invasive skin swabs were previously collected for Bd surveillance from 276 localities across the species range. We assessed patterns of genetic structure and admixture among frog populations and explored patterns of genetic diversity among major conservation units. Our goal was to provide a definitive analysis of genetic variation for the *R. muscosa/sierrae* species complex and create a framework to inform conservation management decisions.

4.3 MATERIALS AND METHODS

Sampling and DNA extraction

Given that *R. muscosa/sierrae* are state and federally protected species, we used a readily available and minimally invasive source of DNA - archived skin swabs previously collected for Bd surveillance. Samples were originally collected with a standardized approach with each individual frog swabbed 30 times on the ventral skin surface. We compiled 373 archived skin swab samples from 276 lake basins across the range of *R. muscosa/sierrae*. Lake basins, which represent “populations” in the system, are typically comprised of a series of nearby lakes and streams. We sampled both named species *Rana muscosa* (n=46) and *Rana sierrae* (n=327). Additionally, we incorporated a subset of samples from previously published studies from Yosemite National Park (n= 21) (Poorten *et al.*, 2017) and Sequoia and Kings-Canyon National Parks (n=32) [164]. We also included phylogenetic outgroups of related *Rana* species including *Rana aurora*, *Rana boylei*, *Rana cascadae*, *Rana draytonii*, *Rana castbeinna*, and *Rana sylvatica*. DNA was extracted from swab samples using PrepMan Ultra Reagent and Qiagen DNeasy kits according to manufacturer’s protocol. Due to PCR inhibitors present in skin swab extracts, we used an isopropanol precipitation to purify DNA extracts. From this purified extract we applied 1 uL of DNA per extract to be used in amplicon preparation and sequencing.

Fluidigm amplicon sample preparation and sequencing

We used 50 amplicon markers (400-600bp in length) previously developed for *Rana muscosa/sierrae* and implemented a microfluidic PCR approach to recover nuclear amplicons [185]. We used Fluidigm Access Array and Juno microfluidic PCR platforms because they allow high throughput amplification to produce PCR products used in library preparation and sequencing. Because since skin swabs typically have low quantities of DNA, we implemented a pre-amplification step based on manufacturer’s protocols (Fluidigm, South San Francisco, CA, USA). We used forward and reverse primers without tagged barcodes in an initial PCR step which increased success for downstream amplification of target amplicons. Following initial PCR, we applied an ExoSAP-IT treatment that removed PCR inhibitors (e.g. excess primers and unincorporated nucleases) and used a 1:5 dilution in nuclease-free water. Pre-amplified products were used in Illumina library preparation to include a barcoded tag of each amplicon and each sample. Illumina libraries were ran on MiSeq with 2 × 300 bp paired-end reads at the University of Idaho IBEST Genomics Resources Core similar to Poorten *et al.* [185] and Rothstein *et al.* [164].

Variant Calling

From raw sequence reads with primers sequences removed, we implemented the dbcAmplicons software (<https://github.com/msettles/dbcAmplicons>) to trim adapters sequences.

Paired-end reads were merged and extended across the length of target amplicons using flash2 [187]. We de-multiplexed sequences using *reduce_amplicons.R* script from the dbcAmplicons repository into raw .fastq for each sample. Fastq files included all sequences for each sample and were used for alignment, variant calling, and population genetic analyses.

We used bwa software (“mem” mode) to align reads to target amplicon regions and created BAM files for each individual [142]. From resulting BAM files, we filtered by read depth for each amplicon by sample and required an average read depth of ≥ 5 reads per amplicon to pass filtering. All reads from amplicons that passed this depth filter were subsequently put into a new .bam file for each individual. Using filtered BAM files, we applied bcftools to call and output only variant sites for our unfiltered VCF [188]. We limited calls to only within reference sequences for all 50 amplicons. From our raw VCF, we filtered variant sites using standard filtering parameters using vcftools (removed alignment mapping quality less than 30, supported base quality less than 20, include sites with $MAF \geq 0.02$, exclude sites with 55% or more missing, and removed indels). We removed individual samples that had a high proportion of missing data ($>55\%$) [144].

Genetic structure

Using our filtered VCF, we inferred population genetic structure using multiple methods including measures of genetic differentiation (F_{ST} and isolation by distance), discriminant principal components analysis (DPCA), and ADMIXTURE. Both F_{ST} calculations and DPCA were implemented in *adegenet*. To assess number of groupings we implemented the *find.clusters* function to approximate the ideal number of clusters among our groupings. Briefly, *find.clusters* uses a *k*-means approach to find a given number of groups and maximizing the variation between groups while simultaneously transforming data to retain principal components. To identify groups, the *find.clusters* function used increasing values of *k* (=1-15). We identified the ideal number of clusters (lowest Bayesian Information Criterion values) by a flattening of criterion scores. Once an ideal number of clusters was found, we plotted for visual interpretation of cluster differentiation. Using these groupings, we also compared the amount of genetic differentiation across populations. We assessed patterns of isolation by distance by comparing genetic distance (Nei’s) to geographic distance (km) and used Monte-Carlo test of 1000 simulations test to assess significant patterns of isolation by distance in *adegenet*.

We also used ADMIXTURE to explicitly infer population structure among our samples [189]. We ran ADMIXTURE on across a range of potential *K* (=1-15) values. The maximum value of *K* was chosen as more than double the number of clades identified within the mtDNA phylogeny [123]. From these individual *K* runs, we plotted the cross-validation error, similar to DPCA Bayesian Information Criterion, and identified the ideal number of clusters. Even with an optimal value for *K*, we evaluated genetic structure amongst a subset of *K* values within a biologically reasonable grouping. Finally, we used an AMOVA for hierarchical structure between identified major clusters and sub-lake basins of our samples using *ade4*.

Genetic Diversity

We calculated summary diversity statistics using ANGSD [146]. Using filtered BAMs from our variant calls, we generated a folded site frequency spectrum with an unknown ancestral state. We calculated per-site diversity (Watterson’s θ) and per-site nucleotide diversity (π) across amplicons for each major cluster from our DPCA and ADMIXTURE results. Because estimates of Watterson’s θ can be impacted by sample size, we randomly subsampled clusters to have equal sample sizes limited by the cluster with the lowest sample size ($n=7$). We compared significant

differences in Watterson's θ and π by cluster compared to all other clusters (base mean) using pairwise Wilcoxon tests. We also calculated significant pairwise comparisons in Watterson's θ and π by group using ANOVA and TukeyHSD correction due to comparisons of multiple means. Both tests were implemented in R (v. 3.6.3).

4.4 RESULTS

Pattern of isolation by distance across species range

From our amplicon sequence dataset, we recovered 161 samples across 134 populations (Fig 4.1A). Site filtering yielded 212 variant sites across 44 nuclear amplicon markers. Percent success of our samples was equivalent across all samples (43%) and within species (*R. muscosa*; 43% [n=20], *R. sierrae*; 43% [n=147]). Both Bayesian Information Criterion for DPCA and cross-validation error in ADMIXTURE identified eight major clusters across our samples (Fig 4.1B-C, S1). DPC loadings largely recapitulated geographic locations with LD1 representing latitude and LD2 representing longitude. Additionally, our DPCA included 30 PCs which represented 83% of variance from our principal components. AMOVA results identified the majority of genetic variation was found among our eight clusters (39.8%) with the remainder being represented at the population scale (12.1%) and across all samples (34.2%). Monte-Carlo permutation tests (permutations=1000) were significant for variation between major clusters ($p < 0.001$) and within samples ($p < 0.001$).

There was largely a pattern of isolation by distance with samples grouping by major cluster in both DPC and geographic space (Fig 4.1). Major clusters identified in our study exhibit a continuous pattern of grouping by geographic location but there is significant admixture across cluster boundaries (Fig 4.1C). Clusters are named based on the primary jurisdictions in which they reside: *Plumas* (Plumas National Forest), *Tahoe* (Tahoe National Forest), *Emigrant* (El Dorado National Forest and Emigrant Wilderness), *Yosemite North* (Yosemite National Park), *Yosemite South* (Yosemite National Park), *Kings Canyon* (Kings Canyon National Park), *Sequoia* (Sequoia National Park), and *Sequoia-Southern* (Sequoia National Park and Angeles-San Bernardino National Forests). We found a significant pattern of isolation by distance across all samples ($p < 0.004$). Additionally, given DPCA and ADMIXTURE distinction of Yosemite North and South, we found significant difference in levels of genetic differentiation of these clusters against all other clusters ($p < 0.001$) (Fig 4.2).

Patterns of genetic diversity

Overall, measures of Watterson's θ and π were relatively even across clusters. In pairwise comparisons of mean diversity, there were no significant differences across cluster comparisons. However, we found certain clusters that exhibited significant levels of genetic diversity compared when grouping all other clusters (Fig 4.3). Tahoe exhibited higher levels of genetic diversity in both measures compared to all other clusters (θ ; $p < 0.0001$, π ; $p < 0.01$). Additionally, Yosemite North had significantly lower genetic diversity for both measures compared to all clusters (θ ; $p < 0.01$; π ; $p < 0.05$). Yosemite South (θ ; $p < 0.05$) and Kings Canyon (θ ; $p < 0.01$) were significantly different in levels of Watterson's θ (lower and higher respectively) but this was not observed in measures of π .

4.5 DISCUSSION

The power of massively parallel sequencing has dramatically transformed the field of conservation genetics. However, there are still constraints for many taxa, such as amphibians, that have limited genomic resources and complex genomes [26,171,190]. Our study leveraged archived skin swab samples across the range of an imperiled species and a custom amplicon-based sequencing approach to obtain robust data to inform *R. muscosa/sierrae* conservation and recovery efforts. Previous work identified phylogenetic groupings in *R. muscosa/sierrae* and named a species level split based on mitochondrial, morphometric, and acoustic data [123]. Our work – with increased numbers of genetic markers and finer-scale spatial sampling – provides new insight on - and challenges current assumptions about - the *R. muscosa/sierrae* species complex.

Distinct genetic clusters but with some admixture across groups

In our multi-locus data set, tests for genetic differentiation consistently identified eight major clusters (Fig 4.1, Fig 4.2). These genetic clusters are distinct across space and, through multiple methods, suggest there is stepping stone model of population genetic structure across the species range of *R. muscosa/sierrae*. A stepping stone model implies that gene flow occurs most readily between neighboring genetic groups [191]. Similar to conclusions discussed in Poorten et. al. [185] and Rothstein et. al. [164], our results indicate that the boundaries between clusters appeared permeable to gene flow (Fig 4.1C). Pairwise F_{ST} values were lowest between spatially adjacent clusters indicating higher levels of gene flow between closer geographic populations (Fig 4.5). Importantly, while we observed moderate admixture between adjacent genetic groups, this did not erode the distinctness of the eight primary genetic clusters.

Increased gene flow between proximate populations can also lead to a pattern of isolation by distance. Our observation of isolation by distance in this range-wide dataset is consistent with previous work within the species complex [123,164,185] and also with other species distributed across the Sierra Nevada [192–194]. The observed pattern of isolation by distance and the signature of gene flow between neighboring genetic clusters, may result more from historical – rather than contemporary - gene flow. In the past, frog populations were more continuously distributed across the landscape, but exceptional population declines have left remaining populations more spatially disjunct [164]. It is possible that large-scale extirpations have contributed to observed genetic patterns. If historical frog populations were still present on the landscape, it is possible that genetic variation would appear more continuous than what is contemporarily observed.

In addition, measures of diversity were relatively uniform among clusters. Only three out of the eight clusters had significant differences in genetic diversity compared to mean of all other clusters (Fig 4.3). In terms of diversity rank, the Tahoe cluster had the most genetic diversity. Yosemite North and Yosemite South showed the least amount of genetic diversity (discussed below). Remaining clusters had relatively similar measures of genetic diversity indicated by no significant differences in pairwise comparisons. It is interesting to observe relatively uniform levels of genetic diversity in a species that has experiences intense population declines and extirpations. However, genetic diversity can take a long time to erode (e.g. more than 10 generations), even when populations experience precipitous declines and extirpations [195].

High genetic distinctness and reduced genetic diversity in Yosemite populations

An important exception to the general patterns observed were Yosemite North and South clusters. One reason these populations may have distinct genetic signatures coupled with lower genetic diversity is due to historical isolation from the rest of the species range. Frog populations in Yosemite inhabit high alpine elevation lakes that are characterized by sharp elevational gradients coupled with high mountain ridgelines. Such landscape features likely impeded historical gene flow across the region. Additionally, periods of Pleistocene glacial retreat, which isolated taxa across the Sierra Nevada [196–198], have been found to be earliest in areas near Yosemite (McGee Till) [199] and could have isolated Yosemite frog populations. While Yosemite populations may be isolated by elevation and topography, we do not see similar patterns with populations in Sequoia and Kings Canyon National Parks (genetic clusters Kings Canyon, Sequoia, and Sequoia-Southern), which also inhabit high alpine lakes. A similar genetic pattern between populations in Yosemite versus Sequoia and Kings Canyon National Parks has been observed in the Yosemite Toad (*Bufo canorus*) suggesting this may be a common pattern among high alpine Sierra Nevada amphibians [192].

In addition to historical biogeographic factors, recent population declines may also have impacted genetic patterns in Yosemite. *R. muscosa/sierrae* populations in this region have experienced particularly intense population reductions due to invasive fish and disease. Bd has been detected in museum specimens from Yosemite as far back as 1972 [124], and Bd related amphibian declines in Yosemite (in *Anaxyrus canorus* populations) have been documented as early as 1978 [200,201]. Bd is hypothesized to have emerged in the northern part of the Sierras followed by emergence in southern Sierras in the early 2000s [124]. Samples in our study from Yosemite National Park were collected between 2005-2014 during which time population abundances were increasing following removal of non-native rainbow trout and Bd [126]. If *R. muscosa/sierrae* Yosemite declines began decades before the rest of the Sierra Nevada, longer term bottleneck may have contributed to outcomes such as reduced genetic diversity. The remaining populations that survived epizootic outbreaks may be more genetically distinct because of the heightened strength of genetic drift in small populations and spatial genetic signatures reflecting selection [202–204]. However, *R. muscosa/sierrae* have experience precipitous declines across the range, and therefore it is not clear whether recent dynamics alone can explain the distinctive genetic signature in Yosemite populations. Better understanding the timing of populations declines across the range could help determine whether Yosemite populations genetic signatures are indeed a result of recent declines.

New conservation units for an endangered amphibian

Previous range-wide genetic studies for *R. muscosa/sierrae* made two key conclusions that impacted conservation. Based on mitochondrial data, six major mitochondrial clades across the species range were identified, and *R. muscosa/sierrae* were divided into sister species with a split located within Sequoia and Kings Canyon National Parks [123]. Our results are discordant with prior mitochondrial results in several key ways and can provide guidance for future local and range-wide conservation actions. First, we observed eight distinct genetic clusters with varying levels of admixture across cluster boundaries suggesting a stepping stone model of population structure. Second, we did not observe a more dramatic genetic discontinuity across the Sequoia-Kings Canyon divide. Therefore, managing *R. muscosa/sierrae* as eight genetic units rather than two species may be more appropriate for conservation. A detailed study of the populations in Sequoia-Kings Canyon also came to a similar conclusion that genetic breaks across several clusters

were of equal strength rather than finding a single species-level break [164]. Therefore, genetic clusters could be used operationally as functional conservation units.

Given observed patterns of isolation by distance, there are some clear management actions suggested from our results. In cases of translocation and reintroductions, moving frogs between adjacent clusters is an appropriate management strategy to preserve historical genetic structure. Such adjacent movements would also likely better maintain any locally adapted alleles. In a separate study, we also found strong spatial structure of Bd in the Sierra Nevada (Chapter 2). Therefore, restricting movement of frogs to only adjacent populations would also reduce mixing of Bd genotypes, which could lead to unknown consequences.

A conservative approach to maintaining historical genetic structure may be appropriate in many cases. However, in certain parts of the range, a more aggressive management strategy might be warranted. For instance, high genetic distinctiveness and low genetic diversity in Yosemite National Park could be a warning sign for the genetic health of these populations [205]. While population abundance data can be one measure of success for conservation, continued genetic monitoring of Yosemite North and South will be necessary to assess if additional interventions are needed to boost overall genetic diversity. Additionally, Sequoia-Southern cluster contains populations in Sequoia and Kings Canyon National Parks and disjunct southern populations. Currently, southern populations have been grouped as a separate, distinct cluster [123,206]. Southern populations of *R. muscosa* have experienced some of the worst declines of the species complex (up to 98% of historical populations lost) and have limited options for local donors to bolster frog populations [207]. Management options for southern populations have always seemed limited because previous results suggested no historical admixture between southern frogs and the rest of the range. Our study had only small sample sizes for southern populations (n=3), and we acknowledge that ADMIXTURE results can occasionally lead to an over-simplification of complex genomic histories [208]. However, our data suggest that there may be an opportunity to use donor individuals from large, persistent populations in Sequoia and Kings Canyon National Parks to bolster dwindling southern populations while maintaining historical population structure. Future investigations could aim to assess viability of translocations between these two regions.

Conclusions

Creating a comprehensive genetic framework for conservation is crucial for declining species. Delineating historical population genetic structure and diversity, especially when current populations are vanishing, can guide and strengthen species recovery efforts. Here, we took advantage of archived skin swabs from across the range of *R. muscosa/sierrae*, an endangered amphibian species complex, to investigate historical genetic population structure and diversity. By identifying key genetic units across the *R. muscosa/sierrae* range, our work provides a comprehensive framework to guide ongoing conservation management. We found that genetic clusters primarily exhibit a pattern of isolation by distance and that clusters are somewhat permeable to gene flow. Importantly, we found that some genetic clusters are more genetically isolated and less genetically diverse than others, a signature that may result from a volatile history of population declines and nascent recoveries. We also found less evidence for a primary species-level split and that some clusters could be used as donors to support recovery efforts in neighboring clusters. This may alleviate current management restrictions based on previous genetic frameworks. Overall, our results create a more explicit blueprint for framing management actions for an imperiled species.

4.6 FIGURES

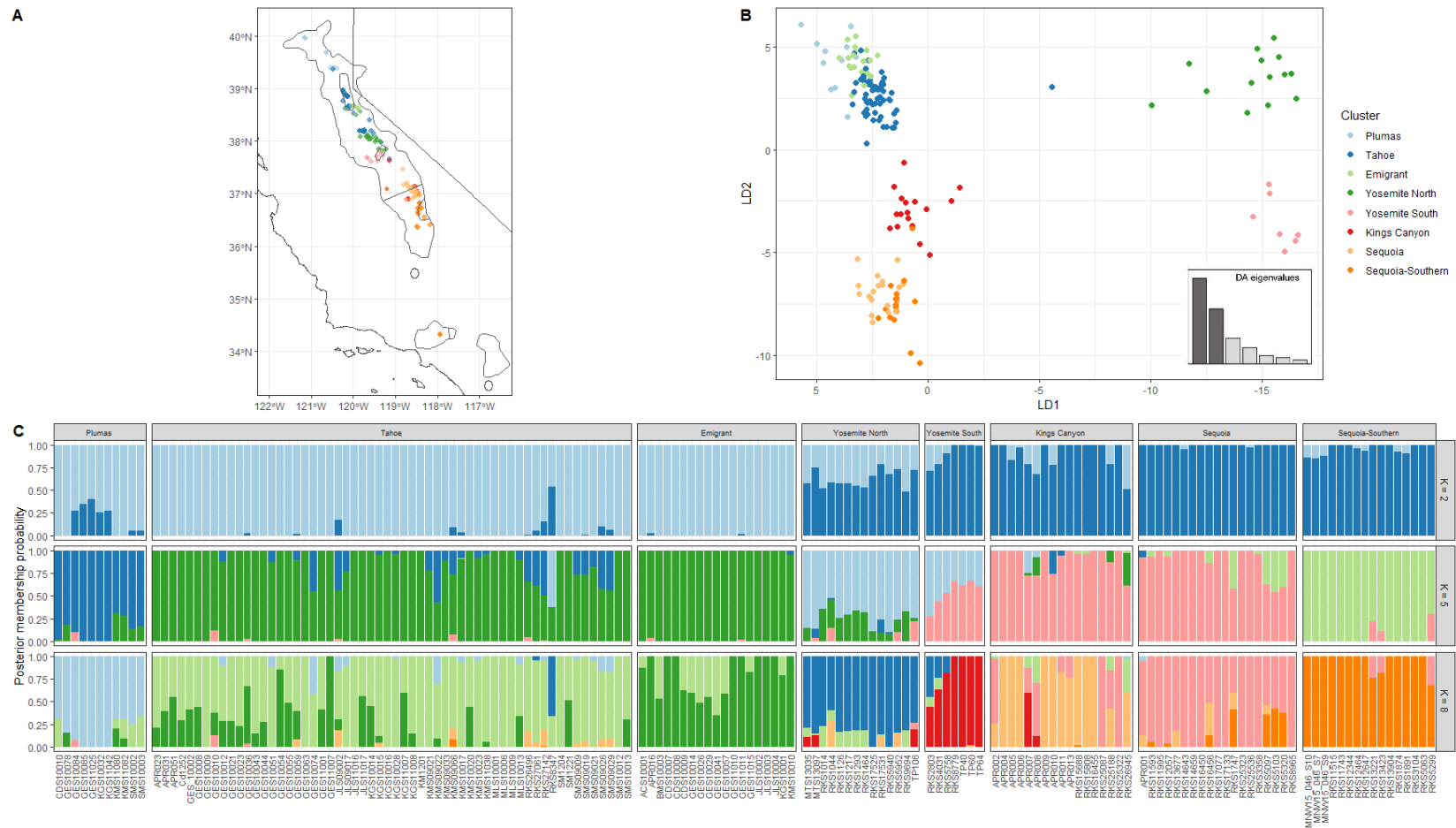


Fig 4.1. (A) Map of sampling locations with points colored by major genetic cluster. (B) DPCA plot of genetic variation among samples. Each point represents an individual sample genotype colored by major cluster based on discriminant analysis. Bottom right corner is plot of discriminant analysis eigenvalues indicating the majority of variation is represent in LD1 and LD2. (C) ADMIXTURE results for K=2, K=5, and K=8. K=8 was consistently identified in both DPCA and ADMIXTURE as “best- k ”. Bars represent individual samples and posterior probability of membership. K=8 ADMIXTURE plots find the same eight groupings identified in DPCA (and colors in the two plots correspond). Individual swabs as x-axis labels.

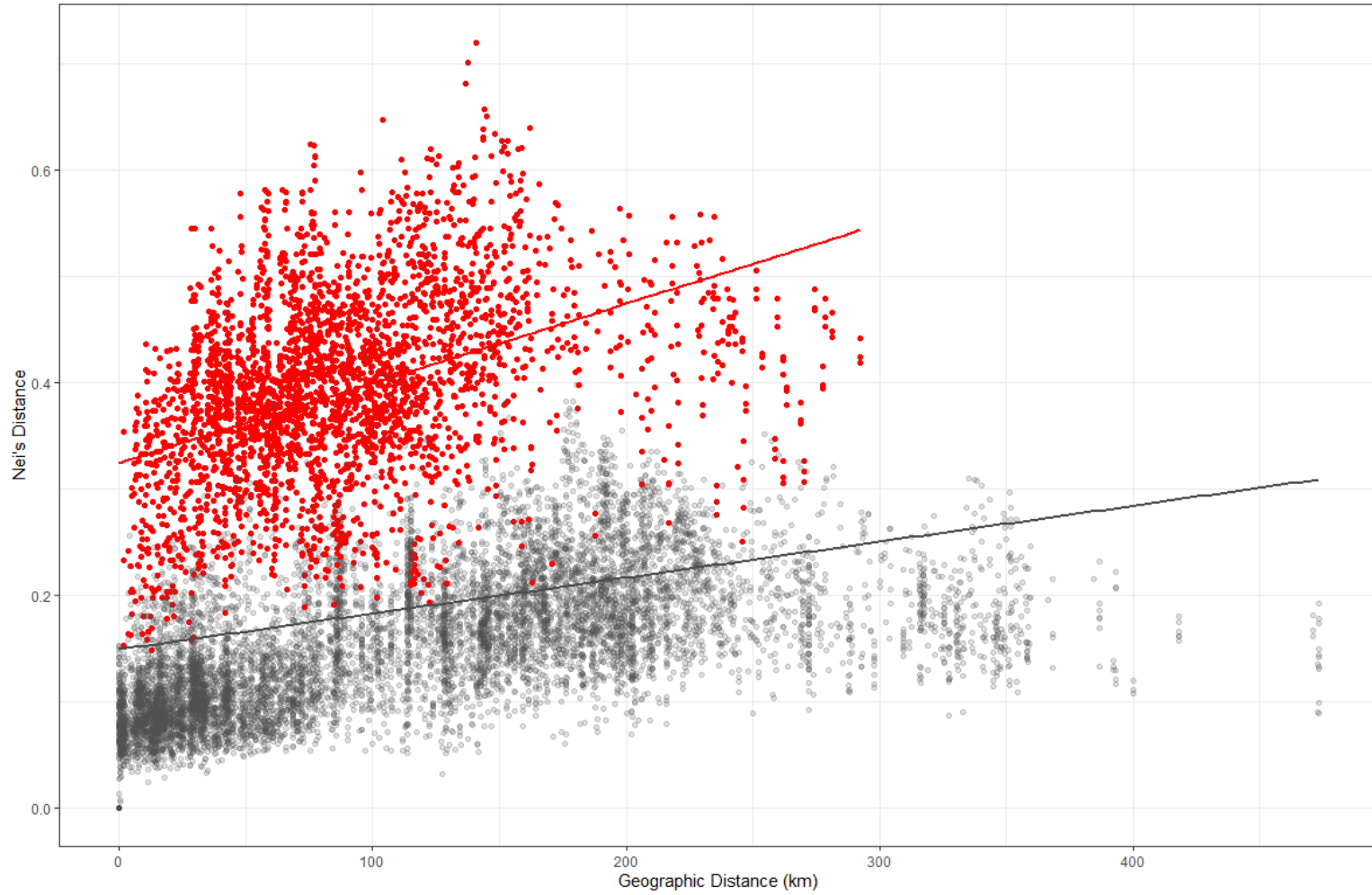


Fig 4.2. Regression of pairwise geographic distance. All comparisons to Yosemite National Park samples (Yosemite North & South) are shown as red points and all other comparisons are shown as black points. Black line represents regression for all samples, red line represent regression for only among Yosemite pairwise comparisons. Comparisons with samples from Yosemite National Park show an increased slope to the pattern of isolation by distance, due to the fact Yosemite samples are quite distinct from all other genetic clusters.

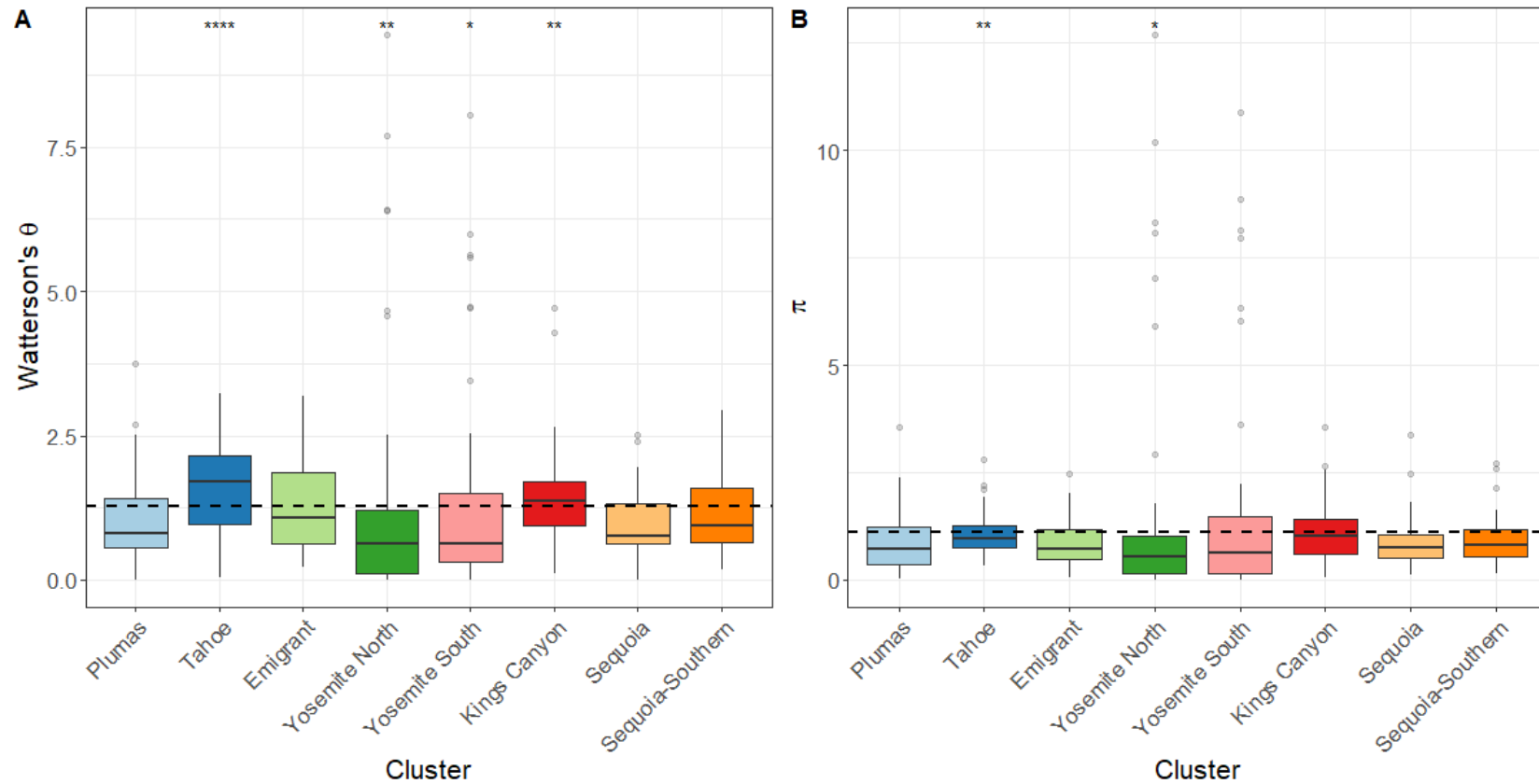


Fig 4.3. (A) Distribution of genetic diversity (Watterson's θ) per variable site by major cluster group. Each cluster represents a randomly selected subset ($n=7$). Tahoe ($p<0.0001$), Yosemite North ($p<0.01$), Yosemite South ($p<0.05$), and Kings Canyon ($p<0.01$) all show significant differences in genetic diversity when compared base mean. However, there were no significant differences in pairwise comparisons of genetic diversity by cluster. (B) Distribution of nucleotide diversity (π) per variable site by major cluster group. Tahoe ($p<0.01$) and Yosemite North ($p<0.05$) showed significant differences in nucleotide diversity compared to base mean. Similar to Watterson's θ , we observed no significant differences in pairwise comparisons. Each box plot shows the median (horizontal line), first and third quartiles (bottom and top of box), lowest and highest values within inter-quartile range of the lower and upper hinges (vertical lines), and outliers (points). Dotted horizontal line represent mean across all groups.

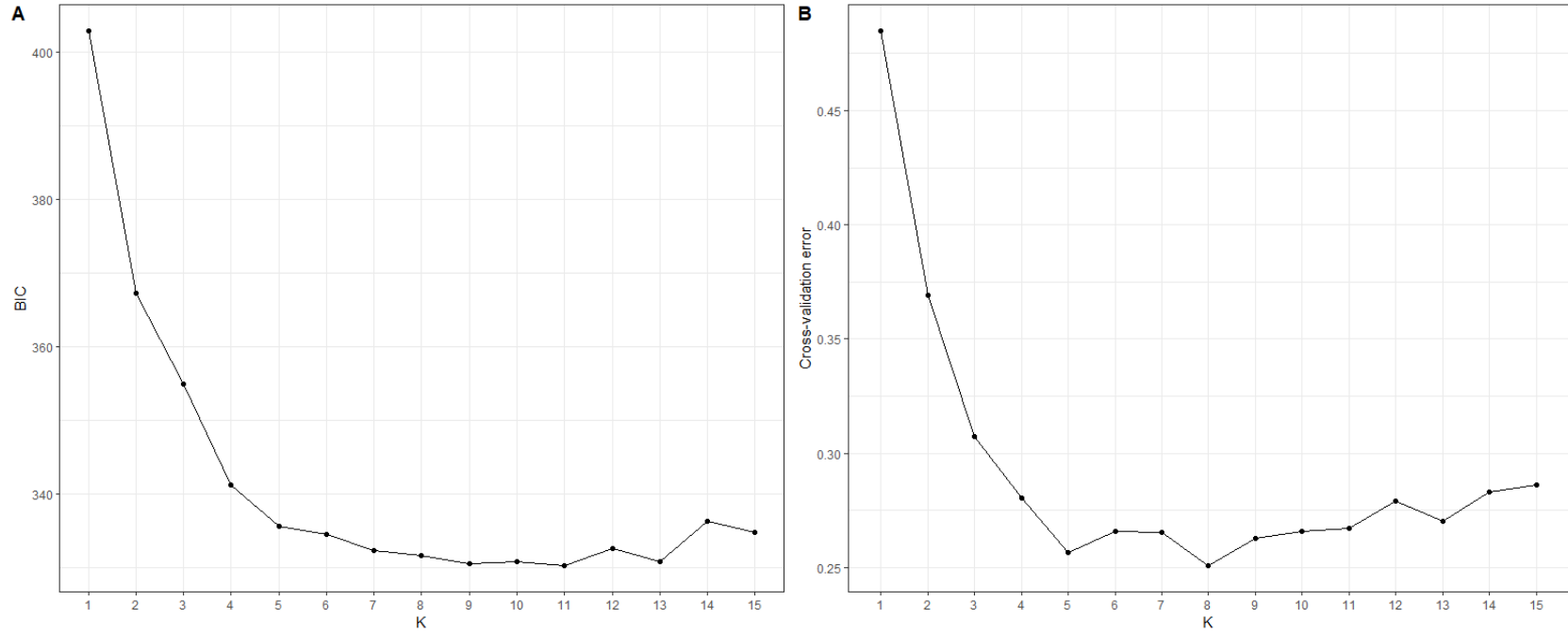


Fig 4.4. (A) Bayesian Information Criterion for DPCA analyses. Best-K indicated by flattening of Bayesian Information Criterion values. (B) Cross-validation error values for K=1-15 in ADMIXTURE. Best-K identified as K=8 based on lowest cross-validation error value.

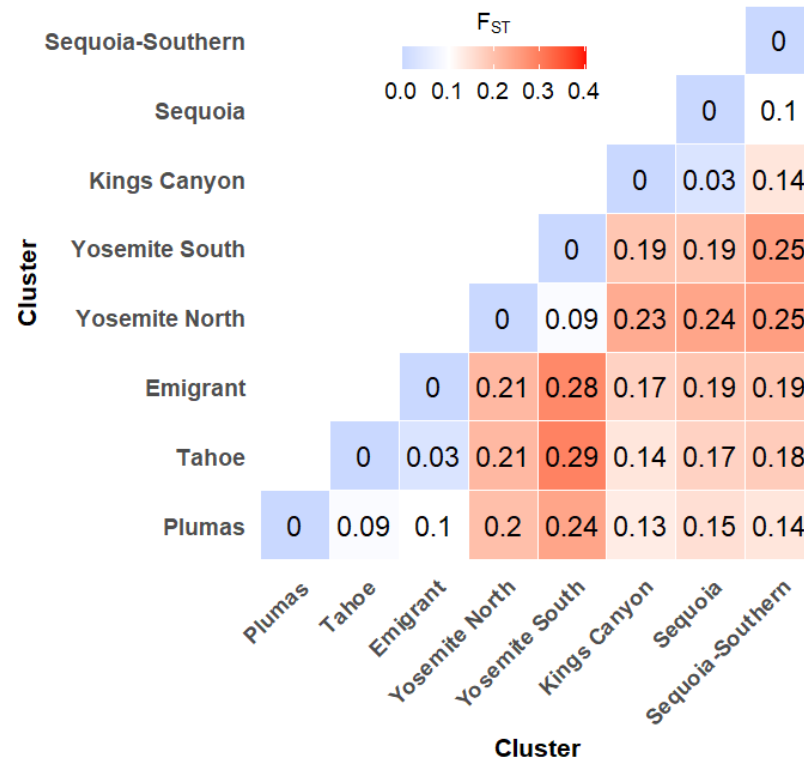


Fig 4.5. Pairwise heatmap of F_{ST} by major genetic cluster. Blue values represent relatively lower values of F_{ST} while red values represent higher ranges of F_{ST} . With exception of Yosemite North and Yosemite South comparisons, clusters generally follow a pattern of isolation by distance (e.g. geographically adjacent clusters have lower F_{ST} values).

CHAPTER 5 CONCLUSIONS

Curtailing declines of wildlife species due to disease involves a multifaceted and interdisciplinary approach. My dissertation explores disease mitigation through the lens of genomics. Using its application to the conservation of an imperiled amphibian species and a globally distributed pathogen, I applied population genetics and evolutionary biology tools toward critical applied questions for conserving contemporary declining populations.

Currently, multiple management agencies, including state and federal governments, are actively involved in several types of species recovery efforts for *Rana muscosa/sierrae* including frog translocations, reintroductions, and disease treatments to reduce susceptibility to Bd. Having a genomic context for the on-the-ground conservation decisions will undoubtedly ensure a better way forward for the successful recovery of this species. The collection of my chapters will be integral in conservation management of *Rana muscosa/sierrae* but also for how we interrogate disease mitigation broadly. Results from Chapter 2 involving fine-scale genetic work across one of the most heavily invested conservation actions for *Rana muscosa/sierrae*. By including both extant and extirpated frog populations, our work provide a critical framework for the few remaining frog populations in Sequoia and Kings Canyon National Parks. For Chapter 3, my results comparing the of Bd genetics in two classic systems identified how *a priori* assumptions of disease emergence are clouded without interrogating underlying pathogen evolutionary histories. Finally, in Chapter 4, my results resolved data gaps to maintain the historical genetic structure of both species to the maximum extent possible, assisting in recovery programs across California.

By framing my chapters based on theory related to infectious diseases, spatial epizootology, population genetics, and conservation biology, results of my work will impact both basic and applied research communities. As global threats continue to impact vulnerable populations, conservation practitioners will need to utilize genomics for continued protection, restoring, and reviving species on the brink of extinction. My dissertation highlights the effective use of genomics in applied conservation efforts.

REFERENCES

1. Jones KE, Patel NG, Levy MA, Storeygard A, Balk D, Gittleman JL, et al. Global trends in emerging infectious diseases. *Nature*. 2008;451: 990–993. doi:10.1038/nature06536
2. Daszak P, Cunningham AA, Hyatt AD. Emerging Infectious Diseases of Wildlife--Threats to Biodiversity and Human Health. *Science*. 2000;287: 443–449. doi:10.1126/science.287.5452.443
3. Fisher MC, Henk DA, Briggs CJ, Brownstein JS, Madoff LC, McCraw SL, et al. Emerging fungal threats to animal, plant and ecosystem health. *Nature*. 2012;484: 186–194.
4. Joseph MB, Mihaljevic JR, Arellano AL, Kueneman JG, Preston DL, Cross PC, et al. Taming wildlife disease: bridging the gap between science and management. *Journal of Applied Ecology*. 2013;50: 702–712. doi:https://doi.org/10.1111/1365-2664.12084
5. Wobeser G. Disease management strategies for wildlife. *Revue Scientifique et Technique-Office international des epizooties*. 2002;21: 159–178.
6. Bozzuto C, Schmidt BR, Canessa S. Active responses to outbreaks of infectious wildlife diseases: objectives, strategies and constraints determine feasibility and success. *Proceedings of the Royal Society B: Biological Sciences*. 2020;287: 20202475. doi:10.1098/rspb.2020.2475
7. Cunningham AA, Daszak P, Wood JLN. One Health, emerging infectious diseases and wildlife: two decades of progress? *Philosophical Transactions of the Royal Society B: Biological Sciences*. 2017 [cited 4 Dec 2020]. doi:10.1098/rstb.2016.0167
8. Daszak P, Berger L, Cunningham AA, Hyatt AD, Green DE, Speare R. Emerging Infectious Diseases and Amphibian Population Declines. *Emerg Infect Dis*. 1999;5: 735–748. doi:10.3201/eid0506.990601
9. Skerratt LF, Berger L, Speare R, Cashins S, McDonald KR, Phillott AD, et al. Spread of Chytridiomycosis Has Caused the Rapid Global Decline and Extinction of Frogs. *EcoHealth*. 2007;4: 125–134. doi:10.1007/s10393-007-0093-5
10. O’Hanlon SJ, Rieux A, Farrer RA, Rosa GM, Waldman B, Bataille A, et al. Recent Asian origin of chytrid fungi causing global amphibian declines. *Science*. 2018;360: 621–627. doi:10.1126/science.aar1965
11. Fisher MC, Garner TWJ. Chytrid fungi and global amphibian declines. *Nat Rev Microbiol*. 2020; 1–12. doi:10.1038/s41579-020-0335-x
12. Wake DB, Vredenburg VT. Are we in the midst of the sixth mass extinction? A view from the world of amphibians. *Proceedings of the National Academy of Sciences*. 2008;105: 11466–11473.
13. Longcore JE, Pessier AP, Nichols DK. *Batrachochytrium Dendrobatidis* gen. et sp. nov., a Chytrid Pathogenic to Amphibians. *Mycologia*. 1999;91: 219–227. doi:10.2307/3761366
14. Lips KR, Brem F, Brenes R, Reeve JD, Alford RA, Voyles J, et al. Emerging infectious disease and the loss of biodiversity in a Neotropical amphibian community. *PNAS*. 2006;103: 3165–3170. doi:10.1073/pnas.0506889103
15. Berger L, Speare R, Daszak P, Green DE, Cunningham AA, Goggin CL, et al. Chytridiomycosis causes amphibian mortality associated with population declines in the rain forests of Australia and Central America. *Proceedings of the National Academy of Sciences*. 1998;95: 9031–9036.

16. James TY, Litvintseva AP, Vilgalys R, Morgan JAT, Taylor JW, Fisher MC, et al. Rapid global expansion of the fungal disease chytridiomycosis into declining and healthy amphibian populations. *PLoS Pathogens*. 2009;5: e1000458–e1000458.
17. Vredenburg VT, Knapp RA, Tunstall TS, Briggs CJ. Dynamics of an emerging disease drive large-scale amphibian population extinctions. *PNAS*. 2010;107: 9689–9694.
18. Voyles J, Young S, Berger L, Campbell C, Voyles WF, Dinudom A, et al. Pathogenesis of chytridiomycosis, a cause of catastrophic amphibian declines. *Science*. 2009;326: 582–585.
19. Voyles J, Vredenburg VT, Tunstall TS, Parker JM, Briggs CJ, Rosenblum EB. Pathophysiology in Mountain Yellow-Legged Frogs (*Rana muscosa*) during a Chytridiomycosis Outbreak. *PLOS ONE*. 2012;7: e35374. doi:10.1371/journal.pone.0035374
20. Cheng TL, Rovito SM, Wake DB, Vredenburg VT. Coincident mass extirpation of neotropical amphibians with the emergence of the infectious fungal pathogen *Batrachochytrium dendrobatidis*. *Proceedings of the National Academy of Sciences*. 2011;108: 9502–9507. doi:10.1073/pnas.1105538108
21. Ryan MJ, Lips KR, Eichholz MW. Decline and extirpation of an endangered Panamanian stream frog population (*Craugastor punctariolus*) due to an outbreak of chytridiomycosis. *Biological Conservation*. 2008;141: 1636–1647.
22. Knapp RA, Boiano DM, Vredenburg VT. Removal of nonnative fish results in population expansion of a declining amphibian (mountain yellow-legged frog, *Rana muscosa*). *Biological Conservation*. 2007;135: 11–20.
23. Knapp RA, Fellers GM, Kleeman PM, Miller DAW, Vredenburg VT, Rosenblum EB, et al. Large-scale recovery of an endangered amphibian despite ongoing exposure to multiple stressors. *PNAS*. 2016; 201600983–201600983.
24. Primmer CR. From conservation genetics to conservation genomics. *Annals of the New York Academy of Sciences*. 2009;1162: 357–368.
25. Ouborg N, Pertoldi C, Loeschcke V, Bijlsma RK, Hedrick PW. Conservation genetics in transition to conservation genomics. *Trends in Genetics*. 2010;26: 177–187.
26. Shaffer HB, Gidiş M, McCartney-Melstad E, Neal KM, Oyamaguchi HM, Tellez M, et al. Conservation Genetics and Genomics of Amphibians and Reptiles. *Annual Review of Animal Biosciences*. 2015;3: 113–138. doi:10.1146/annurev-animal-022114-110920
27. Allendorf FW. Genetics and the conservation of natural populations: allozymes to genomes. *Molecular Ecology*. 2017;26: 420–430.
28. Funk WC, McKay JK, Hohenlohe PA, Allendorf FW. Harnessing genomics for delineating conservation units. *Trends Ecol Evol*. 2012;27: 489–496. doi:10.1016/j.tree.2012.05.012
29. Supple MA, Shapiro B. Conservation of biodiversity in the genomics era. *Genome Biology*. 2018;19: 131. doi:10.1186/s13059-018-1520-3
30. Bradford DF, Graber DM, Tabatabai F. Population Declines of the Native Frog, *Rana muscosa*, in Sequoia and Kings Canyon National Parks, California. *The Southwestern Naturalist*. 1994;39: 323–327.
31. Bradford DF. Mass Mortality and Extinction in a High-Elevation Population of *Rana muscosa*. *Journal of Herpetology*. 1991;25: 174–177. doi:10.2307/1564645

32. Rachowicz LJ, Knapp RA, Morgan JAT, Stice MJ, Vredenburg VT, Parker JM, et al. Emerging Infectious Disease as a Proximate Cause of Amphibian Mass Mortality. *Ecology*. 2006;87: 1671–1683. doi:10.1890/0012-9658(2006)87[1671:EIDAAP]2.0.CO;2
33. Vredenburg VT, Bingham R, Knapp R, Morgan JA, Moritz C, Wake D. Concordant molecular and phenotypic data delineate new taxonomy and conservation priorities for the endangered mountain yellow-legged frog. *Journal of Zoology*. 2007;271: 361–374.
34. Grenfell BT, Pybus OG, Gog JR, Wood JLN, Daly JM, Mumford JA, et al. Unifying the Epidemiological and Evolutionary Dynamics of Pathogens. *Science*. 2004;303: 327–332. doi:10.1126/science.1090727
35. Rife BD, Mavian C, Chen X, Ciccozzi M, Salemi M, Min J, et al. Phylodynamic applications in 21st century global infectious disease research. *Global Health Research and Policy*. 2017;2: 13. doi:10.1186/s41256-017-0034-y
36. Volz EM, Pond SLK, Ward MJ, Brown AJL, Frost SDW. Phylodynamics of Infectious Disease Epidemics. *Genetics*. 2009;183: 1421–1430. doi:10.1534/genetics.109.106021
37. Benton CH, Delahay RJ, Trewby H, Hodgson DJ. What has molecular epidemiology ever done for wildlife disease research? Past contributions and future directions. *Eur J Wildl Res*. 2015;61: 1–16. doi:10.1007/s10344-014-0882-4
38. Blanchong JA, Robinson SJ, Samuel MD, Foster JT. Application of genetics and genomics to wildlife epidemiology. *The Journal of Wildlife Management*. 2016;80: 593–608. doi:10.1002/jwmg.1064
39. White LA, Forester JD, Craft ME. Dynamic, spatial models of parasite transmission in wildlife: Their structure, applications and remaining challenges. *Journal of Animal Ecology*. 2018;87: 559–580. doi:10.1111/1365-2656.12761
40. Meek MH, Larson WA. The future is now: Amplicon sequencing and sequence capture usher in the conservation genomics era. *Molecular Ecology Resources*. 2019;19: 795–803. doi:10.1111/1755-0998.12998
41. Gregory TR. Genome size and developmental complexity. *Genetica*. 2002;115: 131–146.
42. McCartney-Melstad E, Mount GG, Shaffer HB. Exon capture optimization in amphibians with large genomes. *Molecular Ecology Resources*. 2016;16: 1084–1094. doi:10.1111/1755-0998.12538
43. Sun Y-B, Zhang Y, Wang K. Perspectives on studying molecular adaptations of amphibians in the genomic era. *Zool Res*. 2020;41: 351–364. doi:10.24272/j.issn.2095-8137.2020.046
44. Griffiths RA, Pavajeau L. Captive Breeding, Reintroduction, and the Conservation of Amphibians. *Conservation Biology*. 2008;22: 852–861. doi:10.1111/j.1523-1739.2008.00967.x
45. Griffith B, Scott JM, Carpenter JW, Reed C. Translocation as a Species Conservation Tool: Status and Strategy. *Science*. 1989;245: 477–480.
46. Seddon PJ, Armstrong DP, Maloney RF. Developing the science of reintroduction biology. *Conservation biology*. 2007;21: 303–312.
47. Armstrong DP, Seddon PJ. Directions in reintroduction biology. *Trends in Ecology & Evolution*. 2008;23: 20–25. doi:10.1016/J.TREE.2007.10.003
48. Germano JM, Bishop PJ. Suitability of amphibians and reptiles for translocation. *Conservation Biology*. 2009;23: 7–15.
49. Dodd CK, Seigel RA. Relocation, repatriation, and translocation of amphibians and reptiles: are they conservation strategies that work? *Herpetologica*. 1991; 336–350.

50. Fischer J, Lindenmayer DB. An assessment of the published results of animal relocations. *Biological Conservation*. 2000;96: 1–11. doi:10.1016/S0006-3207(00)00048-3
51. Seigel RA, Dodd CK. Translocations of amphibians: proven management method or experimental technique? *Conservation biology*. 2002;16: 552–554.
52. Stuart SN, Chanson JS, Cox NA, Young BE, Rodrigues ASL, Fischman DL, et al. Status and trends of amphibian declines and extinctions worldwide. *Science*. 2004;306: 1783–1786.
53. Griffiths RA, Pavajeau L. Captive Breeding, Reintroduction, and the Conservation of Amphibians. *Conservation Biology*. 2008;22: 852–861. doi:10.1111/j.1523-1739.2008.00967.x
54. Harding G, Griffiths RA, Pavajeau L. Developments in amphibian captive breeding and reintroduction programs. *Conservation Biology*. 2016;30: 340–349.
55. Kriger KM, Hero J-M. Chytridiomycosis, amphibian extinctions, and lessons for the prevention of future panzootics. *EcoHealth*. 2009;6: 6.
56. Woodhams DC, Bosch J, Briggs CJ, Cashins S, Davis LR, Lauer A, et al. Mitigating amphibian disease: strategies to maintain wild populations and control chytridiomycosis. *Frontiers in Zoology*. 2011;8: 8.
57. Garner TWJ, Schmidt BR, Martel A, Pasmans F, Muths E, Cunningham AA, et al. Mitigating amphibian chytridiomycoses in nature. *Phil Trans R Soc B*. 2016;371: 20160207.
58. Reinert HK. Translocation as a Conservation Strategy for Amphibians and Reptiles: Some Comments, Concerns, and Observations. *Herpetologica*. 1991;47: 357–363.
59. Stebbins RC. A field guide to western reptiles and amphibians. Houghton Mifflin Harcourt; 2003.
60. Grinnell J, Storer TI. Animal life in the Yosemite. University Press; 1924.
61. California Fish and Game Commission. A status review of the mountain yellow-legged frog (*Rana sierrae* and *Rana muscosa*). 2011 Nov.
62. US Fish and Wildlife Service. Endangered and threatened wildlife and plants; endangered species status for Sierra Nevada yellow-legged frog and northern distinct population segment of the mountain yellowlegged frog, and threatened species status for Yosemite toad; final rule. *Federal Register*. 2014;79: 24256–24310.
63. Bradford DF, Tabatabai F, Graber DM. Isolation of remaining populations of the native frog, *Rana muscosa*, by introduced fishes in Sequoia and Kings Canyon National Parks, California. *Conservation biology*. 1993;7: 882–888.
64. Knapp RA. Effects of nonnative fish and habitat characteristics on lentic herpetofauna in Yosemite National Park, USA. *Biological Conservation*. 2005;121: 265–279. doi:10.1016/j.biocon.2004.05.003
65. Knapp RA, Matthews KR. Non-native fish introductions and the decline of the mountain yellow-legged frog from within protected areas. *Conservation Biology*. 2000;14: 428–438.
66. Vredenburg VT. Reversing introduced species effects: Experimental removal of introduced fish leads to rapid recovery of a declining frog. *PNAS*. 2004;101: 7646–7650. doi:10.1073/pnas.0402321101
67. Lips KR. Overview of chytrid emergence and impacts on amphibians. *Philosophical Transactions of the Royal Society B: Biological Sciences*. 2016;371: 20150465. doi:10.1098/rstb.2015.0465

68. Bradford DF. Mass Mortality and Extinction in a High-Elevation Population of *Rana muscosa*. *Journal of Herpetology*. 1991;25: 174–177. doi:10.2307/1564645
69. Rachowicz LJ, Knapp RA, Morgan JAT, Stice MJ, Vredenburg VT, Parker JM, et al. Emerging Infectious Disease as a Proximate Cause of Amphibian Mass Mortality. *Ecology*. 2006;87: 1671–1683. doi:10.1890/0012-9658(2006)87[1671:EIDAAP]2.0.CO;2
70. Brown C, Hayes M, Green G, Macfarlane D. Mountain Yellow-Legged Frog Conservation Assessment For The Sierra Nevada Mountains Of California, USA - A Collaborative Inter-Agency Project. 2014. doi:10.13140/2.1.4787.5204
71. Poorten TJ, Knapp RA, Rosenblum EB. Population genetic structure of the endangered Sierra Nevada yellow-legged frog (*Rana sierrae*) in Yosemite National Park based on multi-locus nuclear data from swab samples. *Conservation Genetics*. 2017;18: 731–744. doi:10.1007/s10592-016-0923-5
72. Byrne AQ, Rothstein AP, Poorten TJ, Erens J, Settles ML, Rosenblum EB. Unlocking the story in the swab: A new genotyping assay for the amphibian chytrid fungus *Batrachochytrium dendrobatidis*. *Molecular ecology resources*. 2017;17: 1283–1292.
73. Magoč T, Salzberg SL. FLASH: fast length adjustment of short reads to improve genome assemblies. *Bioinformatics*. 2011;27: 2957–2963. doi:10.1093/bioinformatics/btr507
74. Garrison E, Marth G. Haplotype-based variant detection from short-read sequencing. 2012 [cited 6 Dec 2018]. Available: <https://arxiv.org/abs/1207.3907>
75. Danecek P, Auton A, Abecasis G, Albers CA, Banks E, DePristo MA, et al. The variant call format and VCFtools. *Bioinformatics*. 2011;27: 2156–2158. doi:10.1093/bioinformatics/btr330
76. Oksanen J, Blanchet F, Friendly M, Kindt R, Legendre P, McGlinn D, et al. *vegan: Community Ecology Package*. R package version 2.5–6. 2019. 2019.
77. Jombart T. *ade4*: a R package for the multivariate analysis of genetic markers. *Bioinformatics*. 2008;24: 1403–1405.
78. Goudet J. Hierfstat, a package for R to compute and test hierarchical F-statistics. *Molecular Ecology Notes*. 2005;5: 184–186.
79. Bradburd GS, Coop GM, Ralph PL. Inferring Continuous and Discrete Population Genetic Structure Across Space. *Genetics*. 2018;210: 33–52. doi:10.1534/genetics.118.301333
80. Kamvar ZN, Tabima JF, Grünwald NJ. Poppr: an R package for genetic analysis of populations with clonal, partially clonal, and/or sexual reproduction. *PeerJ*. 2014;2: e281.
81. Pickrell JK, Pritchard JK. Inference of population splits and mixtures from genome-wide allele frequency data. *PLoS genetics*. 2012;8: e1002967.
82. Jani AJ, Knapp RA, Briggs CJ. Epidemic and endemic pathogen dynamics correspond to distinct host population microbiomes at a landscape scale. *Proceedings of the Royal Society B: Biological Sciences*. 2017;284: 20170944. doi:10.1098/rspb.2017.0944
83. Meirmans PG. Seven common mistakes in population genetics and how to avoid them. *Molecular Ecology*. 2015;24: 3223–3231. doi:10.1111/mec.13243
84. Funk WC, Blouin MS, Corn PS, Maxell BA, Pilliod DS, Amish S, et al. Population structure of Columbia spotted frogs (*Rana luteiventris*) is strongly affected by the landscape. *Molecular Ecology*. 2005;14: 483–496. doi:10.1111/j.1365-294X.2005.02426.x

85. Giordano AR, Ridenhour BJ, Storfer A. The influence of altitude and topography on genetic structure in the long-toed salamander (*Ambystoma macrodactylum*). *Molecular Ecology*. 2007;16: 1625–1637. doi:10.1111/j.1365-294X.2006.03223.x
86. Lowe WH, Likens GE, McPeck MA, Buso DC. Linking Direct and Indirect Data on Dispersal: Isolation by Slope in a Headwater Stream Salamander. *Ecology*. 2006;87: 334–339. doi:10.1890/05-0232
87. Murphy MA, Dezzani R, Pilliod DS, Storfer A. Landscape genetics of high mountain frog metapopulations. *Molecular Ecology*. 2010;19: 3634–3649. doi:10.1111/j.1365-294X.2010.04723.x
88. Richards-Zawacki CL. Effects of slope and riparian habitat connectivity on gene flow in an endangered Panamanian frog, *Atelopus varius*. *Diversity and Distributions*. 2009;15: 796–806. doi:10.1111/j.1472-4642.2009.00582.x
89. Spear SF, Peterson CR, Matocq MD, Storfer A. Landscape genetics of the blotched tiger salamander (*Ambystoma tigrinum melanostictum*). *Molecular Ecology*. 2005;14: 2553–2564. doi:10.1111/j.1365-294X.2005.02573.x
90. Feldman CR, Spicer GS. Comparative phylogeography of woodland reptiles in California: repeated patterns of cladogenesis and population expansion. *Molecular Ecology*. 2006;15: 2201–2222. doi:10.1111/j.1365-294X.2006.02930.x
91. Moritz C, Schneider CJ, Wake DB. Evolutionary Relationships Within the *Ensatina* *Eschscholtzii* Complex Confirm the Ring Species Interpretation. *Syst Biol*. 1992;41: 273–291. doi:10.1093/sysbio/41.3.273
92. Recuero E, Martínez-Solano Í, Parra-Olea G, García-París M. Phylogeography of *Pseudacris regilla* (Anura: Hylidae) in western North America, with a proposal for a new taxonomic rearrangement. *Molecular Phylogenetics and Evolution*. 2006;39: 293–304. doi:10.1016/j.ympev.2005.10.011
93. Rissler LJ, Hijmans RJ, Graham CH, Moritz C, Wake DB. Phylogeographic Lineages and Species Comparisons in Conservation Analyses: A Case Study of California Herpetofauna. *The American Naturalist*. 2006;167: 655–666. doi:10.1086/503332
94. Shaffer HB, Fellers GM, Magee A, Voss SR. The genetics of amphibian declines: population substructure and molecular differentiation in the Yosemite Toad, *Bufo canorus* (Anura, Bufonidae) based on single-strand conformation polymorphism analysis (SSCP) and mitochondrial DNA sequence data. *Molecular Ecology*. 2000;9: 245–257. doi:10.1046/j.1365-294x.2000.00835.x
95. Shaffer HB, Pauly GB, Oliver JC, Trenham PC. The molecular phylogenetics of endangerment: cryptic variation and historical phylogeography of the California tiger salamander, *Ambystoma californiense*. *Molecular Ecology*. 2004;13: 3033–3049. doi:10.1111/j.1365-294X.2004.02317.x
96. Froufe E, Alekseyev S, Knizhin I, Alexandrino P, Weiss S. Comparative phylogeography of salmonid fishes (Salmonidae) reveals late to post-Pleistocene exchange between three now-disjunct river basins in Siberia. *Diversity and Distributions*. 2003;9: 269–282. doi:10.1046/j.1472-4642.2003.00024.x
97. Waters JM, Rowe DL, Apte S, King TM, Wallis GP, Anderson L, et al. Geological Dates and Molecular Rates: Rapid Divergence of Rivers and Their Biotas. *Syst Biol*. 2007;56: 271–282. doi:10.1080/10635150701313855
98. Lind AJ, Spinks PQ, Fellers GM, Shaffer HB. Rangelwide phylogeography and landscape genetics of the Western U.S. endemic frog *Rana boylei* (Ranidae): implications for the

- conservation of frogs and rivers. *Conserv Genet.* 2011;12: 269–284. doi:10.1007/s10592-010-0138-0
99. Palm S, Laikre L, Jorde PE, Ryman N. Effective population size and temporal genetic change in stream resident brown trout (*Salmo trutta*, L.). *Conservation Genetics.* 2003;4: 249–264. doi:10.1023/A:1024064913094
 100. Tessier N, Bernatchez L. Stability of population structure and genetic diversity across generations assessed by microsatellites among sympatric populations of landlocked Atlantic salmon (*Salmo salar* L.). *Molecular Ecology.* 1999;8: 169–179. doi:10.1046/j.1365-294X.1999.00547.x
 101. Toews DPL, Brelsford A. The biogeography of mitochondrial and nuclear discordance in animals. *Molecular Ecology.* 2012;21: 3907–3930. doi:10.1111/j.1365-294X.2012.05664.x
 102. Mace GM. The role of taxonomy in species conservation. *Philosophical Transactions of the Royal Society of London Series B: Biological Sciences.* 2004;359: 711–719.
 103. Coates DJ, Byrne M, Moritz C. Genetic Diversity and Conservation Units: Dealing With the Species-Population Continuum in the Age of Genomics. *Front Ecol Evol.* 2018;6. doi:10.3389/fevo.2018.00165
 104. Joseph MB, Knapp RA. Disease and climate effects on individuals drive post-reintroduction population dynamics of an endangered amphibian. *Ecosphere.* 2018; e02499. doi:10.1002/ecs2.2499@10.1002/(ISSN)2150-8925.disease-ecology
 105. Moritz C. Conservation Units and Translocations: Strategies for Conserving Evolutionary Processes. *Hereditas.* 1999;130: 217–228. doi:10.1111/j.1601-5223.1999.00217.x
 106. Weeks AR, Sgro CM, Young AG, Frankham R, Mitchell NJ, Miller KA, et al. Assessing the benefits and risks of translocations in changing environments: a genetic perspective. *Evolutionary Applications.* 2011;4: 709–725.
 107. El Amri H, Boukharta M, Zakham F, Ennaji MM. Chapter 27 - Emergence and Reemergence of Viral Zoonotic Diseases: Concepts and Factors of Emerging and Reemerging Globalization of Health Threats. In: Ennaji MM, editor. *Emerging and Reemerging Viral Pathogens.* Academic Press; 2020. pp. 619–634. doi:10.1016/B978-0-12-819400-3.00027-2
 108. Tompkins DM, Carver S, Jones ME, Krkošek M, Skerratt LF. Emerging infectious diseases of wildlife: a critical perspective. *Trends in Parasitology.* 2015;31: 149–159. doi:10.1016/j.pt.2015.01.007
 109. Altizer S, Ostfeld RS, Johnson PT, Kutz S, Harvell CD. Climate change and infectious diseases: from evidence to a predictive framework. *science.* 2013;341: 514–519.
 110. Crowl TA, Crist TO, Parmenter RR, Belovsky G, Lugo AE. The spread of invasive species and infectious disease as drivers of ecosystem change. *Frontiers in Ecology and the Environment.* 2008;6: 238–246. doi:10.1890/070151
 111. Fisher MC, Garner TWJ. The relationship between the emergence of *Batrachochytrium dendrobatidis*, the international trade in amphibians and introduced amphibian species. *Fungal Biology Reviews.* 2007;21: 2–9. doi:10.1016/j.fbr.2007.02.002
 112. Gallana M, Ryser-Degiorgis M-P, Wahli T, Segner H. Climate change and infectious diseases of wildlife: Altered interactions between pathogens, vectors and hosts. *Curr Zool.* 2013;59: 427–437. doi:10.1093/czoolo/59.3.427
 113. Lafferty KD. The ecology of climate change and infectious diseases. *Ecology.* 2009;90: 888–900.

114. McCallum H, Dobson A. Disease, habitat fragmentation and conservation. *Proc R Soc Lond B*. 2002;269: 2041–2049. doi:10.1098/rspb.2002.2079
115. Stuart SN, Chanson JS, Cox NA, Young BE, Rodrigues ASL, Fischman DL, et al. Status and trends of amphibian declines and extinctions worldwide. *Science*. 2004;306: 1783–1786.
116. Vredenburg VT, Knapp RA, Tunstall TS, Briggs CJ. Dynamics of an emerging disease drive large-scale amphibian population extinctions. *PNAS*. 2010;107: 9689–9694.
117. Byrne AQ, Vredenburg VT, Martel A, Pasmans F, Bell RC, Blackburn DC, et al. Cryptic diversity of a widespread global pathogen reveals expanded threats to amphibian conservation. *PNAS*. 2019;116: 20382–20387. doi:10.1073/pnas.1908289116
118. Farrer RA, Weinert LA, Bielby J, Garner TWJ, Balloux F, Clare F, et al. Multiple emergences of genetically diverse amphibian-infecting chytrids include a globalized hypervirulent recombinant lineage. *Proceedings of the National Academy of Sciences*. 2011;108: 18732–18736. doi:10.1073/pnas.1111915108
119. Rosenblum EB, James TY, Zamudio KR, Poorten TJ, Ilut D, Rodriguez D, et al. Complex history of the amphibian-killing chytrid fungus revealed with genome resequencing data. *Proceedings of the National Academy of Sciences*. 2013;110: 9385–9390. doi:10.1073/pnas.1300130110
120. James TY, Toledo LF, Rödder D, da Silva Leite D, Belasen AM, Betancourt-Román CM, et al. Disentangling host, pathogen, and environmental determinants of a recently emerged wildlife disease: lessons from the first 15 years of amphibian chytridiomycosis research. *Ecology and Evolution*. 2015;5: 4079–4097. doi:10.1002/ece3.1672
121. Schloegel LM, Toledo LF, Longcore JE, Greenspan SE, Vieira CA, Lee M, et al. Novel, panzootic and hybrid genotypes of amphibian chytridiomycosis associated with the bullfrog trade. *Molecular Ecology*. 2012;21: 5162–5177.
122. Grinnell J, Storer TI. *Animal life in the Yosemite*. University Press; 1924.
123. Vredenburg VT, Bingham R, Knapp R, Morgan JA, Moritz C, Wake D. Concordant molecular and phenotypic data delineate new taxonomy and conservation priorities for the endangered mountain yellow-legged frog. *Journal of Zoology*. 2007;271: 361–374.
124. Vredenburg VT, McNally SVG, Sulaeman H, Butler HM, Yap T, Koo MS, et al. Pathogen invasion history elucidates contemporary host pathogen dynamics. *PLOS ONE*. 2019;14: e0219981. doi:10.1371/journal.pone.0219981
125. Zhou H, Hanson T, Knapp R. Marginal Bayesian nonparametric model for time to disease arrival of threatened amphibian populations. *Biometrics*. 2015;71: 1101–1110. doi:10.1111/biom.12345
126. Knapp RA, Fellers GM, Kleeman PM, Miller DAW, Vredenburg VT, Rosenblum EB, et al. Large-scale recovery of an endangered amphibian despite ongoing exposure to multiple stressors. *PNAS*. 2016; 201600983–201600983.
127. Lips KR. Decline of a tropical montane amphibian fauna. *Conservation Biology*. 1998;12: 106–117.
128. Pounds JA, Fogden MP, Savage JM, Gorman GC. Tests of null models for amphibian declines on a tropical mountain. *Conservation biology*. 1997;11: 1307–1322.
129. Pounds JA, Crump ML. Amphibian declines and climate disturbance: the case of the golden toad and the harlequin frog. *Conservation Biology*. 1994;8: 72–85.

130. Brem FM, Lips KR. Batrachochytrium dendrobatidis infection patterns among Panamanian amphibian species, habitats and elevations during epizootic and enzootic stages. *Diseases of aquatic organisms*. 2008;81: 189–202.
131. Crawford AJ, Lips KR, Bermingham E. Epidemic disease decimates amphibian abundance, species diversity, and evolutionary history in the highlands of central Panama. *PNAS*. 2010;107: 13777–13782. doi:10.1073/pnas.0914115107
132. Kilburn VL, Ibáñez R, Sanjur O, Bermingham E, Suraci JP, Green DM. Ubiquity of the pathogenic chytrid fungus, *Batrachochytrium dendrobatidis*, in anuran communities in Panamá. *EcoHealth*. 2010;7: 537–548.
133. Voyles J, Woodhams DC, Saenz V, Byrne AQ, Perez R, Rios-Sotelo G, et al. Shifts in disease dynamics in a tropical amphibian assemblage are not due to pathogen attenuation. *Science*. 2018;359: 1517–1519. doi:10.1126/science.aao4806
134. Woodhams DC, Kilburn VL, Reinert LK, Voyles J, Medina D, Ibáñez R, et al. Chytridiomycosis and amphibian population declines continue to spread eastward in Panama. *EcoHealth*. 2008;5: 268–274.
135. Whiles MR, Hall RO, Dodds WK, Verburg P, Huryn AD, Pringle CM, et al. Disease-Driven Amphibian Declines Alter Ecosystem Processes in a Tropical Stream. *Ecosystems*. 2013;16: 146–157. doi:10.1007/s10021-012-9602-7
136. Zipkin EF, DiRenzo GV, Ray JM, Rossman S, Lips KR. Tropical snake diversity collapses after widespread amphibian loss. *Science*. 2020;367: 814–816. doi:10.1126/science.aay5733
137. Lips KR, Diffendorfer J, Mendelson III JR, Sears MW. Riding the wave: reconciling the roles of disease and climate change in amphibian declines. *PLoS biology*. 2008;6.
138. Collins JP, Storfer A. Global amphibian declines: sorting the hypotheses. *Diversity and distributions*. 2003;9: 89–98.
139. Morgan JAT, Vredenburg VT, Rachowicz LJ, Knapp RA, Stice MJ, Tunstall T, et al. Population genetics of the frog-killing fungus *Batrachochytrium dendrobatidis*. *PNAS*. 2007;104: 13845–50. doi:10.1073/pnas.0701838104
140. Farrer RA, Henk DA, Garner TWJ, Balloux F, Woodhams DC, Fisher MC. Chromosomal Copy Number Variation, Selection and Uneven Rates of Recombination Reveal Cryptic Genome Diversity Linked to Pathogenicity. *PLOS Genetics*. 2013;9: e1003703. doi:10.1371/journal.pgen.1003703
141. Byrne AQ, Rothstein AP, Poorten TJ, Erens J, Settles ML, Rosenblum EB. Unlocking the story in the swab: A new genotyping assay for the amphibian chytrid fungus *Batrachochytrium dendrobatidis*. *Molecular ecology resources*. 2017;17: 1283–1292.
142. Li H. Aligning sequence reads, clone sequences and assembly contigs with BWA-MEM. *arXiv preprint arXiv:13033997*. 2013.
143. Garrison E, Marth G. Haplotype-based variant detection from short-read sequencing. 2012 [cited 6 Dec 2018]. Available: <https://arxiv.org/abs/1207.3907>
144. Danecek P, Auton A, Abecasis G, Albers CA, Banks E, DePristo MA, et al. The variant call format and VCFtools. *Bioinformatics*. 2011;27: 2156–2158. doi:10.1093/bioinformatics/btr330
145. Jombart T. adegenet: a R package for the multivariate analysis of genetic markers. *Bioinformatics*. 2008;24: 1403–1405.
146. Korneliussen TS, Albrechtsen A, Nielsen R. ANGSD: analysis of next generation sequencing data. *BMC bioinformatics*. 2014;15: 356.

147. Bodenhofer U, Bonatesta E, Horejš-Kainrath C, Hochreiter S. msa: an R package for multiple sequence alignment. *Bioinformatics*. 2015;31: 3997–3999.
148. Bouckaert R, Heled J, Kühnert D, Vaughan T, Wu C-H, Xie D, et al. BEAST 2: a software platform for Bayesian evolutionary analysis. *PLoS computational biology*. 2014;10: e1003537.
149. Hadfield J, Megill C, Bell SM, Huddleston J, Potter B, Callender C, et al. Nextstrain: real-time tracking of pathogen evolution. *Bioinformatics*. 2018;34: 4121–4123.
150. Rambaut A, Drummond AJ, Xie D, Baele G, Suchard MA. Posterior Summarization in Bayesian Phylogenetics Using Tracer 1.7. *Syst Biol*. 2018;67: 901–904. doi:10.1093/sysbio/syy032
151. Walker SF, Bosch J, Gomez V, Garner TWJ, Cunningham AA, Schmeller DS, et al. Factors driving pathogenicity vs. prevalence of amphibian panzootic chytridiomycosis in Iberia. *Ecology Letters*. 2010;13: 372–382. doi:10.1111/j.1461-0248.2009.01434.x
152. Gillespie G, Hunter D, Berger L, Marantelli G. Rapid decline and extinction of a montane frog population in southern Australia follows detection of the amphibian pathogen *Batrachochytrium dendrobatidis*. *Animal Conservation*. 2015;18: 295–302.
153. Velo-Antón G, Rodríguez D, Savage AE, Parra-Olea G, Lips KR, Zamudio KR. Amphibian-killing fungus loses genetic diversity as it spreads across the New World. *Biological Conservation*. 2012;146: 213–218. doi:10.1016/j.biocon.2011.12.003
154. León MED, Zumbado-Ulate H, García-Rodríguez A, Alvarado G, Sulaeman H, Bolaños F, et al. *Batrachochytrium dendrobatidis* infection in amphibians predates first known epizootic in Costa Rica. *PLOS ONE*. 2019;14: e0208969. doi:10.1371/journal.pone.0208969
155. Puschendorf R, Bolaños F, Chaves G. The amphibian chytrid fungus along an altitudinal transect before the first reported declines in Costa Rica. *Biological Conservation*. 2006;132: 136–142. doi:10.1016/j.biocon.2006.03.010
156. Kamoroff C, Goldberg C. Using environmental DNA for early detection of amphibian chytrid fungus *Batrachochytrium dendrobatidis* prior to a rapid die-off. *Dis Aquat Org*. 2017;127: 75–79. doi:10.3354/dao03183
157. Paz A, Ibáñez R, Lips KR, Crawford AJ. Testing the role of ecology and life history in structuring genetic variation across a landscape: A trait-based phylogeographic approach. *Molecular Ecology*. 2015;24: 3723–3737.
158. Richards-Zawacki CL. Effects of slope and riparian habitat connectivity on gene flow in an endangered Panamanian frog, *Atelopus varius*. *Diversity and Distributions*. 2009;15: 796–806. doi:10.1111/j.1472-4642.2009.00582.x
159. Bradford DF. Allotopic distribution of native frogs and introduced fishes in high Sierra Nevada lakes of California: implication of the negative effect of fish introductions. *Copeia*. 1989;1989: 775–778.
160. Zweifel RG. *Ecology, Distribution and Systematics of Frogs of the "Rana Boylei" Group*, by Richard G. Zweifel. University of California Press; 1955.
161. Matthews KR, Pope KL. A telemetric study of the movement patterns and habitat use of *Rana muscosa*, the mountain yellow-legged frog, in a high-elevation basin in Kings Canyon National Park, California. *Journal of Herpetology*. 1999; 615–624.
162. Pope KL, Matthews KR. Movement ecology and seasonal distribution of mountain yellow-legged frogs, *Rana muscosa*, in a high-elevation Sierra Nevada basin. *Copeia*. 2001;2001: 787–793.

163. Bradford DF. Winterkill, Oxygen Relations, and Energy Metabolism of a Submerged Dormant Amphibian, *Rana Muscosa*. *Ecology*. 1983;64: 1171–1183. doi:10.2307/1937827
164. Rothstein AP, Knapp R, Bradburd G, Boiano D, Briggs CJ, Rosenblum EB. Stepping into the past to conserve the future: archived skin swabs from extant and extirpated populations inform genetic management of an endangered amphibian. *Molecular Ecology*. 2020.
165. Stevenson LA, Alford RA, Bell SC, Roznik EA, Berger L, Pike DA. Variation in thermal performance of a widespread pathogen, the amphibian chytrid fungus *Batrachochytrium dendrobatidis*. *PloS one*. 2013;8.
166. Voyles J, Johnson LR, Briggs CJ, Cashins SD, Alford RA, Berger L, et al. Temperature alters reproductive life history patterns in *Batrachochytrium dendrobatidis*, a lethal pathogen associated with the global loss of amphibians. *Ecology and Evolution*. 2012;2: 2241–2249. doi:10.1002/ece3.334
167. Voyles J, Johnson LR, Rohr J, Kelly R, Barron C, Miller D, et al. Diversity in growth patterns among strains of the lethal fungal pathogen *Batrachochytrium dendrobatidis* across extended thermal optima. *Oecologia*. 2017;184: 363–373.
168. Allendorf FW, Hohenlohe PA, Luikart G. Genomics and the future of conservation genetics. *Nature Reviews Genetics*. 2010;11: 697–709. doi:10.1038/nrg2844
169. Allendorf FW, Luikart GH. Conservation and the genetics of populations. Blackwell Publishing; 2007.
170. Whiteley AR, Fitzpatrick SW, Funk WC, Tallmon DA. Genetic rescue to the rescue. *Trends in Ecology & Evolution*. 2015;30: 42–49. doi:10.1016/j.tree.2014.10.009
171. McCartney-Melstad E, Shaffer HB. Amphibian molecular ecology and how it has informed conservation. *Molecular Ecology*. 2015;24: 5084–5109. doi:10.1111/mec.13391
172. Waples RS. Pacific salmon, *Oncorhynchus* spp., and the definition of "species" under the Endangered Species Act. *Marine Fisheries Review*. 1991;53: 11–22.
173. Moritz C. Defining 'evolutionarily significant units' for conservation. *Trends in ecology & evolution*. 1994;9: 373–375.
174. Bowen BW. Preserving genes, species, or ecosystems? Healing the fractured foundations of conservation policy. *Molecular Ecology*. 1999;8: S5–S10. doi:10.1046/j.1365-294X.1999.00798.x
175. Jehle R, Burke T, Arntzen J. Delineating fine-scale genetic units in amphibians: probing the primacy of ponds. *Conservation Genetics*. 2005;6: 227–234.
176. Moritz C. Conservation Units and Translocations: Strategies for Conserving Evolutionary Processes. *Hereditas*. 1999;130: 217–228. doi:10.1111/j.1601-5223.1999.00217.x
177. Harding G, Griffiths RA, Pavajeau L. Developments in amphibian captive breeding and reintroduction programs. *Conservation Biology*. 2016;30: 340–349.
178. Fuentes-Pardo AP, Ruzzante DE. Whole-genome sequencing approaches for conservation biology: Advantages, limitations and practical recommendations. *Molecular Ecology*. 2017;26: 5369–5406. doi:10.1111/mec.14264
179. Stebbins RC. A field guide to western reptiles and amphibians. Houghton Mifflin Harcourt; 2003.

180. Bradford DF, Tabatabai F, Graber DM. Isolation of remaining populations of the native frog, *Rana muscosa*, by introduced fishes in Sequoia and Kings Canyon National Parks, California. *Conservation Biology*. 1993;7: 882–888.
181. Knapp RA, Matthews KR. Non-native fish introductions and the decline of the mountain yellow-legged frog from within protected areas. *Conservation Biology*. 2000;14: 428–438.
182. Vredenburg VT. Reversing introduced species effects: Experimental removal of introduced fish leads to rapid recovery of a declining frog. *PNAS*. 2004;101: 7646–7650. doi:10.1073/pnas.0402321101
183. Knapp RA. Effects of nonnative fish and habitat characteristics on lentic herpetofauna in Yosemite National Park, USA. *Biological Conservation*. 2005;121: 265–279. doi:10.1016/j.biocon.2004.05.003
184. Knapp RA, Boiano DM, Vredenburg VT. Removal of nonnative fish results in population expansion of a declining amphibian (mountain yellow-legged frog, *Rana muscosa*). *Biological Conservation*. 2007;135: 11–20.
185. Poorten TJ, Knapp RA, Rosenblum EB. Population genetic structure of the endangered Sierra Nevada yellow-legged frog (*Rana sierrae*) in Yosemite National Park based on multi-locus nuclear data from swab samples. *Conservation Genetics*. 2017;18: 731–744. doi:10.1007/s10592-016-0923-5
186. Hon T, Mars K, Young G, Tsai Y-C, Karalius JW, Landolin JM, et al. Highly accurate long-read HiFi sequencing data for five complex genomes. *bioRxiv*. 2020; 2020.05.04.077180. doi:10.1101/2020.05.04.077180
187. Magoč T, Salzberg SL. FLASH: fast length adjustment of short reads to improve genome assemblies. *Bioinformatics*. 2011;27: 2957–2963. doi:10.1093/bioinformatics/btr507
188. Li H. A statistical framework for SNP calling, mutation discovery, association mapping and population genetical parameter estimation from sequencing data. *Bioinformatics*. 2011;27: 2987–2993. doi:10.1093/bioinformatics/btr509
189. Alexander DH, Lange K. Enhancements to the ADMIXTURE algorithm for individual ancestry estimation. *BMC Bioinformatics*. 2011;12: 246. doi:10.1186/1471-2105-12-246
190. Weisrock DW, Hime PM, Nunziata SO, Jones KS, Murphy MO, Hotaling S, et al. Surmounting the large-genome “problem” for genomic data generation in salamanders. 2018.
191. Kimura M, Weiss GH. The stepping stone model of population structure and the decrease of genetic correlation with distance. *Genetics*. 1964;49: 561.
192. Shaffer HB, Fellers GM, Magee A, Voss SR. The genetics of amphibian declines: population substructure and molecular differentiation in the Yosemite Toad, *Bufo canorus* (Anura, Bufonidae) based on single-strand conformation polymorphism analysis (SSCP) and mitochondrial DNA sequence data. *Molecular Ecology*. 2000;9: 245–257. doi:10.1046/j.1365-294x.2000.00835.x
193. Rovito SM. Lineage divergence and speciation in the Web-toed Salamanders (Plethodontidae: Hydromantes) of the Sierra Nevada, California. *Molecular Ecology*. 2010;19: 4554–4571.
194. Maier PA. Evolutionary past, present, and future of the Yosemite toad (*Anaxyrus canorus*): a total evidence approach to delineating conservation units. San Diego State University; 2018.

195. Hoban S, Arntzen JA, Bruford MW, Godoy JA, Hoelzel AR, Segelbacher G, et al. Comparative evaluation of potential indicators and temporal sampling protocols for monitoring genetic erosion. *Evolutionary Applications*. 2014;7: 984–998. doi:<https://doi.org/10.1111/eva.12197>
196. Avise JC, Walker D, Johns GC. Speciation durations and Pleistocene effects on vertebrate phylogeography. *Proceedings of the Royal Society of London Series B: Biological Sciences*. 1998;265: 1707–1712.
197. Hewitt GM. Genetic consequences of climatic oscillations in the Quaternary. *Philosophical Transactions of the Royal Society of London Series B: Biological Sciences*. 2004;359: 183–195.
198. Rissler LJ, Hijmans RJ, Graham CH, Moritz C, Wake DB. Phylogeographic Lineages and Species Comparisons in Conservation Analyses: A Case Study of California Herpetofauna. *The American Naturalist*. 2006;167: 655–666. doi:10.1086/503332
199. Gillespie AR, Clark DH. Glaciations of the Sierra Nevada, California, USA. *Developments in Quaternary Sciences*. Elsevier; 2011. pp. 447–462.
200. Sherman CK, Morton ML. Population declines of Yosemite toads in the eastern Sierra Nevada of California. *Journal of Herpetology*. 1993; 186–198.
201. Drost CA, Fellers GM. Collapse of a regional frog fauna in the Yosemite area of the California Sierra Nevada, USA. *Conservation biology*. 1996;10: 414–425.
202. Manel S, Joost S, Epperson BK, Holderegger R, Storfer A, Rosenberg MS, et al. Perspectives on the use of landscape genetics to detect genetic adaptive variation in the field. *Molecular Ecology*. 2010;19: 3760–3772.
203. Joost S, Vuilleumier S, Jensen JD, Schoville S, Leempoel K, Stucki S, et al. Uncovering the genetic basis of adaptive change: on the intersection of landscape genomics and theoretical population genetics. *Molecular ecology*. 2013;22: 3659–3665.
204. Wenzel MA, Douglas A, James MC, Redpath SM, Pierrney SB. The role of parasite-driven selection in shaping landscape genomic structure in red grouse (*Lagopus lagopus scotica*). *Molecular Ecology*. 2016;25: 324–341. doi:<https://doi.org/10.1111/mec.13473>
205. Peek RA, O'Rourke SM, Miller MR. Flow regulation associated with decreased genetic health of a river-breeding frog species. *bioRxiv*. 2018; 316604.
206. Schoville SD, Tustall TS, Vredenburg VT, Backlin AR, Gallegos E, Wood DA, et al. Conservation genetics of evolutionary lineages of the endangered mountain yellow-legged frog, *Rana muscosa* (Amphibia: Ranidae), in southern California. *Biological Conservation*. 2011;144: 2031–2040.
207. Backlin AR, Hitchcock CJ, Gallegos EA, Yee JL, Fisher RN. The precarious persistence of the Endangered Sierra Madre yellow-legged frog *Rana muscosa* in southern California, USA. *Oryx*. 2015;49: 157–164.
208. Lawson DJ, van Dorp L, Falush D. A tutorial on how not to over-interpret STRUCTURE and ADMIXTURE bar plots. *Nature Communications*. 2018;9: 3258. doi:10.1038/s41467-018-05257-7